MEDDELELSER OM GRØNLAND
UDGIVNE AF
KOMMISSIONEN FOR VIDENSKABELIGE UNDERSØGELSER I GRØNLAND
BD. 165 · NR. 2

THE ISOTOPIC COMPOSITION OF NATURAL WATERS

WITH SPECIAL REFERENCE TO THE GREENLAND ICE CAP

BY

W. DANSGAARD

WITH 35 FIGURES IN THE TEXT
AND 8 TABLES

KØBENHAVN
C. A. REITZELS FORLAG
BIANCO LUNOS BOGTRYKKERI A/S
1961

CONTENTS

PREFACE

The present work was initiated in 1952 and carried out at the Biophysical Laboratory, University of Copenhagen, except for part of the experiment described in section 6.1., which was made at the Chemistry Department, Northwestern University, Illinois, in 1955.

The author wishes to express his indebtedness to the numerous people who have contributed to the completion of the work. First and foremost thanks are due to the late Prof., Dr. Phil. H. M. HANSEN, Biophysical Laboratory, University of Copenhagen, to his successor, Prof. of physics, Dr. Phil. J. KOCH, and to the leader of the Arctic In stitute Greenland Expedition, 1958, Prof., Dr. P. F. SCHOLANDER, SCRIPPS, California, for their ever ready support, careful establishment of the best possible working conditions and for many inspiring discussions. Furthermore, thanks are due to the head of the Greenland department, ESKE BRUN, for his active interest in the work and to Prof., Dr. Med. F. SCHØNHEYDER, Biokemisk Institut, Aarhus, and Prof. M. DOLE, Ph. D., Northwestern University, Evanston, who kindly placed their mass spectrometers at my disposal. I also extend my gratitude to Mag. A. WEIDICK, Mineralogisk Museum, Copenhagen, for his continued helpfulness concerning the glacier problems, and to Dr. Tech. B. BUCHMANN for reading the manuscript and making many valuable suggestions.

The collection of the numerous samples treated in this work has only been possible due to the courtesy of Dr. J. BENDER and Mr. R. H. RAGLE, U.S. S.I.P.R.E., Wilmette, Illinois, Dr. M. DOPORTO, Meteorological Service, Dublin, Eire, Prof. A. BAUER, Strasbourg, France, Dr. E. ERIKSSON, International Meteorological Institute, Stockholm, Dr. A. JOHANSSON, Kungl. Lantbrukshögskolan, Ultuna, Sweden, Dr. KOROLEFF, Havforskningsinstituttet, Helsinki, Finland, Prof. Dr. Phil. P. BRANDT REHBERG, University of Copenhagen, Mag. J. JENSEN, Statens Planteavls Laboratorium, Lyngby, Mag. J. AMBROSEN, Radiofysisk Laboratorium, Copenhagen, and to the Trade Commisioner in Jakobshavn, Greenland, H. JACOBI.

The chemical engineers E. JØRGENSEN and J. KJØLSETH have been of great help in making the many measurements and drawings.

Financial support was granted by Statens almindelige Videnskabsfond, Arctic Institute of North America and Rask-Ørsted Fondet.

Copenhagen, Sept. 1960. W. DANSGAARD.

1. INTRODUCTION

The isotopy of the elements was first considered by the English physicist W. CROOKES in 1888. He suggested that the atoms of a given element may exist in several modifications, each having a whole-number mass. About 1910 positive ray experiments combined with chemical analysis confirmed CROOKES' assumptions; various modifications of thorium and lead were shown to have identical chemical properties, but different masses. In 1911 THOMPSON demonstrated neon to be a mixture of two isotopes with the masses 20 and 22. With his mass spectograph from 1919 ASTON found 202 isotopes of 71 elements. Of the heavy isotopes dealt with in the present work, deuterium was discovered by UREY, BRICKWEDDE and MURPHY (1932) and oxygen eighteen by GIAQUE and JOHNSTON (1929). Most of the possible stable isotopes are now known.

The chemical properties of the isotopes of a given element are almost identical, because they depend mainly upon the number of orbital electrons, which, in turn, is determined by the electrical charge of the nucleus. However, slightly different thermodynamic properties of the isotopes have been shown to cause small differences in the chemical properties, but this effect is important only in the low mass range, and especially for the hydrogen isotopes. The electrolytic separation of the hydrogen isotopes in water is based on different thermodynamic properties and on a kinetic effect. In general, the light isotopic component will react relatively fast.

The isotopy of the elements also influences physical processes like diffusion, adsorption and, of special interest for the present work, evaporation and condensation.

The fractionation factor of two isotopes participating in a chemical or physical equilibrium process is the ratio between the occurrences of the isotopes in one compound or phase divided by the ratio between their occurrences in the other component or phase. In other words, if N_1 and N_1' are the numbers of the two isotopic atoms in one compound or phase, while N_2 and N_2' are their numbers in the other one, the fractionation factor is

$$\frac{N_1}{N_1'} / \frac{N_2}{N_2'}.$$

Disregarding processes with hydrogen, the fractionation factors amount at the highest to a few per cent above unity. The fractionation factors have been determined experimentally only in a few cases, but they have been calculated from thermodynamic considerations for many simple processes (cf. UREY, 1947).

Both physical and chemical methods have been developed for artificial separation of isotopes. Of special interest in this work, however, are the fractionation processes occurring in nature.

BRISCOE and ROBINSON (1926) first showed that the isotopic composition of the elements are not universal constants, but varies from one compound to the other. They also pointed out that the study of these variations could lead to a better understanding of many natural processes. The technical facilities necessary for the accomplishment of such studies were not available at that time, but the idea has later formed the basis for the development of a new scientific field, which RANKAMA (1954) calls isotope geology. In a wide sense this field covers several sides of geophysics and geochemistry. RANKAMA's book treats the various sides of isotope geology and the comprehensive literature, which had appeared by 1954.

The present work deals with the behaviour of deuterium and, particularly, oxygen eighteen in the hydrosphere. Several branches of research such as meteorology, glaciology, oceanography and hydrology will be touched, and some introductory remarks will be given in connection with each chapter.

2. MEASURING TECHNIQUE

2.1. **Introduction.**

The occurrences of the stable hydrogen isotopes in natural substances are related to each other approximately as

$$H^1 : H^2 = 999840 : 160 \text{ parts per million (ppm).}$$

The analogous figures for the stable oxygen isotopes are

$$O^{16} : O^{17} : O^{18} = 997600 : 400 : 2000 \text{ ppm.}$$

The isotopy of hydrogen and oxygen causes no less than nine isotopic components of water. They have all whole-number masses ranging from 18 for the lightest component ($H^1{}_2O^{16}$) to 22 for the heaviest one ($H^2{}_2O^{18}$). The occurrence of the components containing more than one heavy isotope is usually negligible, which reduces the number of important components to four: $H^1{}_2O^{16}$, $H^1H^2O^{16}$, $H^1{}_2O^{17}$ and $H^1{}_2O^{18}$.

In the present work the deuterium content of a sample will be denoted by

$$a_D = \frac{(D)}{(H) + (D)} \cdot 10^6 \quad (= \text{approx. } 160 \text{ ppm}),$$

(H) and (D) being the quantities of deuterium and hydrogen atoms in the sample. Analogously, the O^{18} content of a sample is denoted by

$$a_{18} = \frac{(O^{18})}{(O^{16}) + (O^{17}) + (O^{18})} \cdot 10^6 \quad (= \text{approx. } 2000 \text{ ppm}),$$

or just "a" in cases where this symbol can not be mixed up with a_D.

Until very recently no means have been available for measuring the absolute values of a_D and a_{18} with high precision. It is much easier to measure differences in isotopic composition between two samples. Fortunately, the greatest interest is attached to variations in isotopic composition, the measurement of which is, consequently, a common feature of all techniques hitherto applied in isotope geology.

Before world war II most isotope work on water was carried out as density measurements. Differences in the density of water samples after distillation were often attributed to different deuterium contents neglecting variations in the occurrences of the oxygen isotopes. Today, such work has hardly more than historical interest.

The first attempt of distinguishing between the hydrogen and the oxygen contributions to the density variations was presented by LEWIS and LUTEN (1933a), who gave two equations relating the deuterium and the O^{18} abundances with the variations in density and index of refraction. The influence of O^{17} was neglected. The same authors (1933b) equilibrated the water with excess of other materials containing either hydrogen or oxygen. By this treatment the contribution of one of the isotopic components was removed. Similar methods were used by RIESENFELD and CHANG (1936a).

WAHL and UREY (1935) electrolyzed the water, burned the oxygen with deuterium-free hydrogen and measured the density of the resulting water. A similar method was used by DOLE (1936) and other investigators.

During the past decade the mass spectrometer has been the dominating factor of the evolution. The history of mass spectrometry began with THOMSON's mass spectrograph (1911). Positive ions passed parallel electric and magnetic fields, and the ions having the same ratio between the charge, e, and the mass, M, blackened a photographic plate along a parabola characteristic for e/M. With this instrument the presence of isotopes could be demonstrated. Measurement of ion masses and the fractional occurrences of the isotopes became possible with the improved mass spectrograph designed by ASTON (1919), in which ions of equal e/M were focussed along a straight line. DEMPSTER's instrument from 1918 was particularly suitable for isotope ratio measurements. All ions were accelerated through the same voltage drop (V) and thereafter deflected 180° in a magnetic field (H). The radii of curvature of their paths were then given by

$$r = \frac{k}{H}\sqrt{V\frac{M}{e}} \qquad (1)$$

k being a constant. Thus a mass dispersion was obtained. This is the principle used in all modern mass spectrometers.

With NIER's design from 1947 a 60° deflection instrument became commercially available, which was able to give isotope abundances in the lower mass range with a relative accuracy of a few per mille or, used with extreme care, even 1 or 0.5 per mille of the natural heavy isotope occurrences. This latter accuracy is almost what was obtainable

in the very best but more complicated density measurements (cf. TEIS, 1946).

The mass spectrometric measuring accuracy was increased by a whole order of magnitude to $\pm 0.01\%$ by the improvements introduced to the NIER mass spectrometer by NEY and by MCKINNEY, MCCREA, EPSTEIN, ALLEN and UREY (1950). Of these improvements the use of a double inlet system with valves (p. 13) and of a vibrating reed electrometer (p. 16) has been transferred to the instrument used in the present work.

Admission of water or water vapour into the mass spectrometer has some bad consequences. It adhers easily to the inner parts of the vacuum system, which causes a quickly increasing background (p. 21) and, thereby, unstable working conditions.

As far as deuterium measurements are concerned the water is, therefore, always transformed into hydrogen and oxygen, and the measurement is carried out by comparing the two hydrogen components, H_2^1 and H^1H^2 (cp. BOTTER and NIEF, 1958).

In oxygen isotope work excess of water is isotopically exchanged with carbon dioxide, e.g.

$$H_2O^{18} + CO_2^{16} \rightleftharpoons H_2O^{16} + CO^{16}O^{18}.$$

After equilibration the O^{18} content of the CO_2 is equal to that of the water multiplied by a fractionation factor. The carbon dioxide is introduced into the mass spectrometer, and the measurement is carried out by comparing the isotopic components CO_2^{16} (mass 44) and $CO^{16}O^{18}$ (mass 46). This measurement is the basis for the present work. It will, therefore, be subjected to a detailed description in the following sections (2.2. to 2.10.).

2.2. Description of the mass spectrometer.

The mass spectrometer used in this work was built by Consolidated Engineering Corp. (type 21–201) on the basis of NIER's design (1947). On the following pages the instrument will be described in the subsections:

1. Inlet system.
2. Leak system.
3. Ion source.
4. Analyser tube.
5. Collector system.
6. Balance system.
7. Other electronic equipment.
8. Vacuum system.

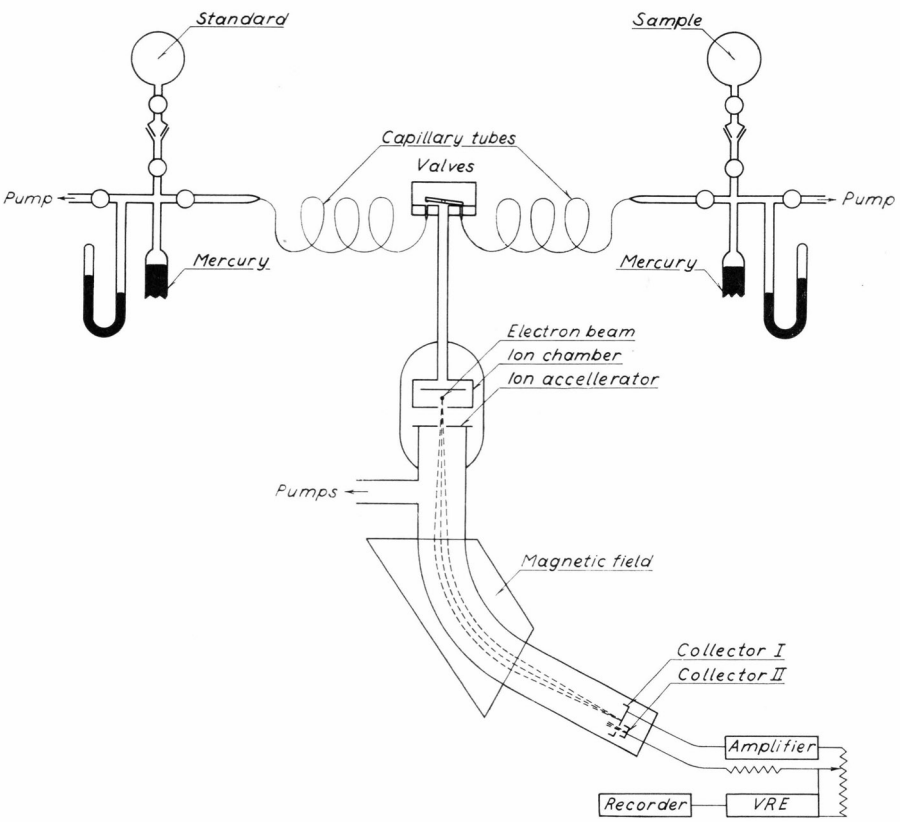

Fig. 1. Schematic drawing of the mass spectrometer with two symmetrical inlet systems. In the lower right side is shown the electrical measuring device.

1. **Inlet system.** As is seen from Fig. 1 the gas handling system consists of two symmetrical parts, one for the sample to be measured, the other for the standard gas. By raising or lowering the level of the mercury in the column the pressure of the gas in the left system is adjusted to a value (some 30 mm of mercury) giving the same intensity of the mass 44 ion beam ($\pm 1\%$) as the gas in the right system, when the latter gas is admitted to the ion source. The volume of each system is approx. 50 cm^3 under normal measuring conditions. After the measurement the inlet system is evacuated by a mechanical pump until the amplifier output has decreased to a value near the background (p. 21).

2. **Leak system.** Each of the gases to be compared is admitted to the ion source through a leak and a valve, the technical details of which appear from Fig. 2. Both valves are moved simultaneously by turning one handle so that one valve is open a time. Each leak is a copper capillary

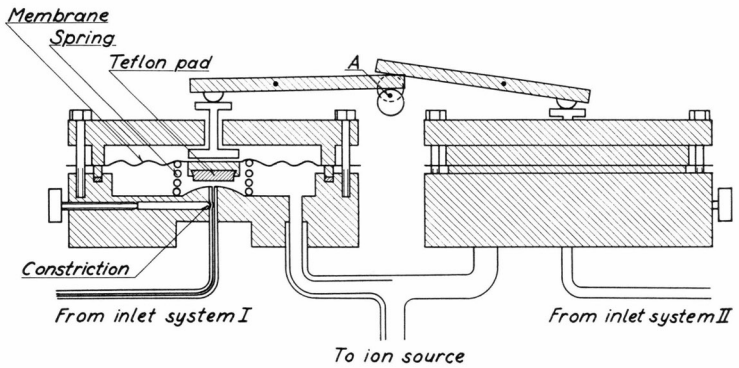

Fig. 2. The two valves with the capillary leaks. The right valve is closed. In the left one the spring lifts the membrane and, thereby, the teflon pad so that the left capillary is open for admittance to the ion source of the gas in inlet system I. The axis A is provided with a handle (not shown in the figure) and two eccentrics. By turning the handle 180° the teflon pad closes the capillary in the left valve at the same time as that in the right valve is opened.

tube (length 25 cm, inner diameter 0.18 mm) with a constriction 1.5 mm from its mouth in the valve. On the other side of the valve a wide copper tube (length 50 cm, inner diameter 4 mm) leads the gas into the ion source. The gas flow through the system is approx. 1 cm^3 per 24 hours measured at 0° C and 760 mm Hg.

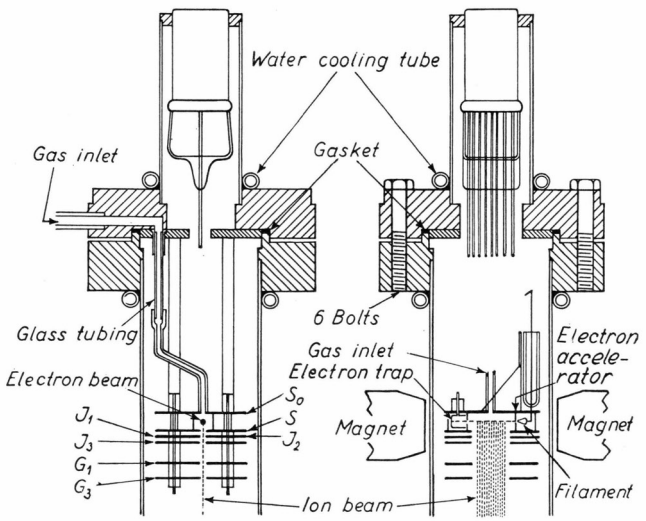

Fig. 3. Ion source.

3. **The ion source** has a tungsten filament (Fig. 3). The emitted electrons are accelerated through 100 volts, when entering the ion chamber through a slit. They leave the ion chamber through another slit and

are then collected in a trap. The total emission current is approx. 400 μ a, the trap current approx. 60 μ a. A weak magnetic field in the direction from trap to filament collimates the electrons in a narrow beam. Disregarding the earthed electrodes, G_1 and G_3, all the inner parts of the ion source operate at voltages of the order of 1200 volts. With the focussing magnet in a position giving maximum trap currents the potentials of the focussing electrodes J_1 and J_2 can be adjusted to give maximum

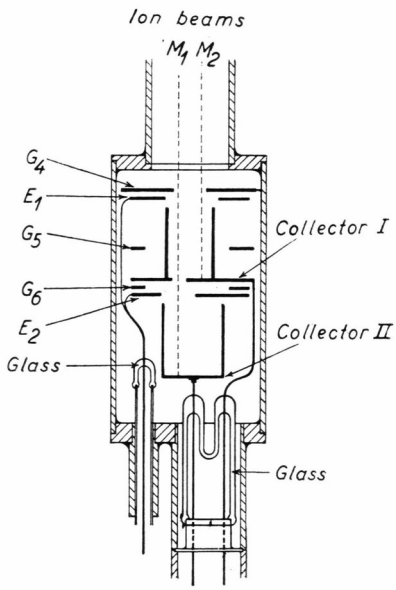

Fig. 4. Ion collectors.

intensity of the ion beam at the collector. The beam of positive, single charged ions leaving the ion source represents an electric current of the order of 10^{-9} amp.

4. **The analyser tube.** After being emitted from the ion source the ions enter the field from a truncated-sectortype magnet and their paths are bent about 60°. The radius of curvature is given by equation (1), p. 10. The ion accelerating voltage, V, is approx. 1200 volts, and the magnetic field strength, H, approx. 2600 oersteds. Single charged ions are always utilized in isotope abundance measurements. By adjusting H and/or V any mass can be deflected to hit the collector. The shape of the magnetic field causes a focussing effect on ions with the same mass and speed but emitted from the source in slightly different directions. In Fig. 1 the dashed curves indicate the paths of such ions. The ions following the left path spend longer time in the magnetic field and are thus deflected to a higher degree than those following the right path.

5. **The collector system** is shown in Fig. 4. Two beams with ions of different masses M_1 and M_2 ($M_1 > M_2$) enter from top. H and V are adjusted so that M_1 are focussed on the slit in the bottom of collector I and collected by collector II, whereas the intense beam of light ions falls on I. G_4, G_5 and G_6 are earthed shields. E_1 and E_2 are secondary electron suppressors operating at -45 volts. The charges arriving at

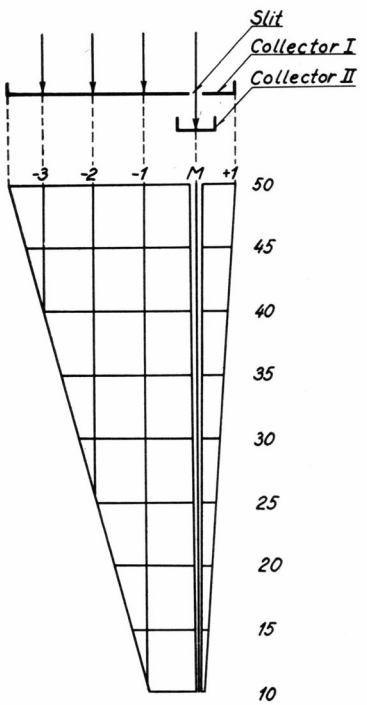

Fig. 5. The ions collected by collector I. When mass No. M is focussed on the slit, collector I is hit by those of No. M–1, M–2 etc. indicated in the figure.

the collectors are proportional to the number of ions removed from the ion source. The resulting currents, i_I and i_{II}, are led to the balance system. From equation (1) it appears that the difference between the radii of curvature of two adjacent masses depends upon the mass, and this is also true for the distance between their focussing points.

Fig. 5 shows the masses (M–1, M–2 . .) collected by collector I, when focussing mass No. M on collector II. When mass 46 is focussed on II, I collects the masses 45, 44 and 43. The double collector system as such is seen to be usable only for $M > 12$. If $M > 25$, more than one ion beam are collected by I.

6. **The balance system.** Collector I is connected to an amplifier with 100 % inverse feedback (Fig. 6). The overall voltage gain is thus

unity. The amplifier functions as an impedance transformer, the input and output resistances of which are 10^{10} ohms and less than one ohm, respectively. When an ion beam reaches collector I, a voltage appears at the output, which is numerically equal to the voltage drop (approx. -10 volts under the conditions described in section 2. 4.) caused by i_I passing the input resistor r_I. The $100\,^0/_0$ inverse feedback keeps the potential of collector I close to zero and makes the output proportional to i_I. This fact and the inner voltage gain being high explain why no linearity problems arise. The output is connected to a potentiometer,

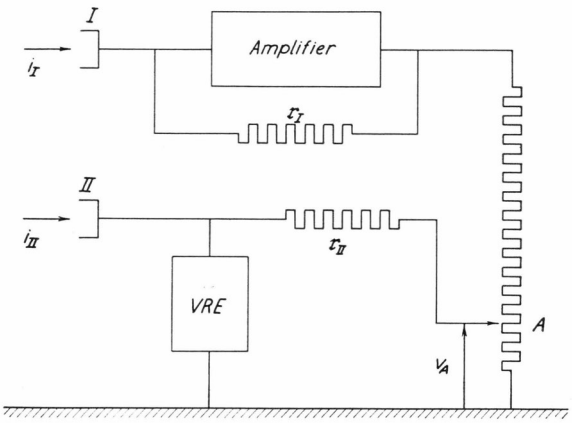

Fig. 6. Balance system for comparison between two ion currents, i_I and i_{II}. The vibrating reed electrometer is denoted by VRE.

the slide (A) of which is in turn connected to collector II via a high ohm resistor, $r_{II} = 10^{11}$ ohms. If A is adjusted so that its potential, V_A, is equal to the voltage drop developed by i_{II} passing r_{II}, the potential of collector II will be zero. This is indicated by a vibrating reed electrometer, VRE (maximum sensitivity 10 mV for full scale deflection, input resistance 10^{16} ohms). With point A grounded VRE measures i_{II}. The VRE replaces an originally installed amplifier II, similar to amplifier I mentioned above, and a galvanometer. This replacement was desirable, firstly, because the noise of amplifier II caused severe instability of the balance (the noise of amplifier I has much less influence due to the magnitude of i_I), and, secondly, because the use of a recorder became possible. The recorder sensitivity is 10 mV full scale deflection.

7. Other electronics.

The low voltage power supply gives a regulated 225 volts d.c. voltage to the amplifier and to the high voltage power supply, as well as regulated 6.3 volts a.c. voltage for the heaters of the tubes. The stability of the d.c. voltage is better than $0.1\,^0/_0$.

The emission regulator operates at the ion accelerating voltage. It feeds the filament of the ion source. The emission current controls the regulating unit.

The high voltage power supply gives up to 2000 volts d. c. ion accelerating voltage and also operates the Philips ionization gauge, which measures the pressure in the analyser tube. By using a heat insulated dry battery for the grid potential in the stabilizing triode instead of the originally installed constant voltage tube the noise was reduced by a factor of 5 to $\pm 0.01\,^0/_0$ outside the traffic rush hours. During long periods of time the average voltage varies less than $\pm 0.005\,^0/_0$.

8. **The high vacuum system** consists of a mechanical forepump and a 2" mercury diffusion pump. The pressure just above the dry ice cooled trap is approx. 10^{-6} mm Hg, with both valves closed, and $2\text{–}3 \cdot 10^{-6}$ mm Hg, when a sample is admitted to the ion source. Under this latter condition the pressure in the ion chamber is probably of the order of 10^{-4} mm Hg. In order to keep the background low the analyser tube is occasionally heated by electrical heaters and the trap is at the same time allowed to warm up to room temperature.

2. 3. **Preparation technique.**

The preparation technique for O^{18} analysis of water was described by Epstein and Mayeda (1953), Baertschi (1953) and by Dansgaard (1953 b).

The latter author uses 5 cm^3 of water, which is frozen in a flask with a total volume of 60 cm^3. The next step is evacuation of the flask to about 10^{-3} mm Hg. After melting, during which dissolved or trapped gases escape, refreezing and re-evacuation the flask is filled with tank CO_2 to a pressure of approx. 100 mm Hg. Thereupon the flask is shaken at 24° C the night over. Next day the CO_2 is removed from the flask and trapped by liquid air in a U-tube together with some water vapour. The CO_2 is then released by raising the temperature to −80° C and retrapped in a dry flask by liquid air. Finally, any trace of gaseous impurities are removed from the solid CO_2 by evacuation.

During the shaking isotopic equilibrium is established between the CO_2 and the water:

$$CO_2^{16} + H_2O^{18} \rightleftharpoons CO^{16}O^{18} + H_2O^{16}.$$

The time needed for equilibration is 2 hours, if the water is acid (cf. 2. 6. 7., p. 33). The fractionation factor, f, is 1.04 at 24° C (cf. 2. 6. 9.,

p. 34). After the equilibration, therefore, the O^{18} content of the CO_2 is equal to that of the water multiplied by f (in case of excess of water, cf. 2. 6. 8., p. 34), and the CO_2 can be used as a measuring object in the mass spectrometer.

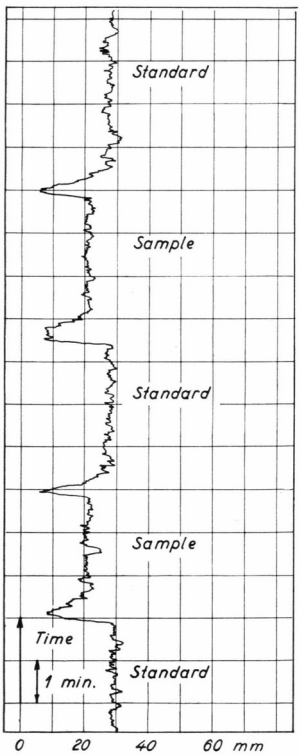

Fig. 7. Recording of the balance values for the standard and a sample. The sensitivity is 1.5 mm deflection for $R_s - R_{std.} = 1$ ppm or $\Delta a = 0.46$ ppm.

2. 4. **Comparison of the sample and the standard.**

The sample and the standard CO_2 are introduced into their respective inlet systems and in turn admitted to the ion source. Peak 46 is focussed on collector II. Collector I then collects the mass numbers 43, 44 and 45 (p. 15).

The sample pressures, P_r on the right and P_l on the left inlet system, are adjusted to give the same output (± 0.5 per cent), approx. 10 volts, on the amplifier. P_r and P_l are then some cm Hg, somewhat depending on the leak constriction in question. P_r and P_l differ less than 5 per cent from each other.

When the approximate balance value, $R_{std.}$, of the potentiometer (Fig. 6) has been found for the left system containing the standard, the VRE output is recorded during some minutes (Fig. 7). Then the

sample is admitted to the ion source by moving the valves, a new approximate balance value, R_s, is found, and after another couple of minutes the procedure is repeated. When the sensitivity has been found by determining the recorder deflection per unit of change of the balance value (1.5 mm for a change of R of 1 ppm, when the total output is 10 volts), the difference between the balance values can be determined:

$$\Delta R_m = R_s - R_{std}.$$

ΔR_m is to be corrected by the difference obtained with standard gas on both systems under similar conditions. The latter difference is caused by the leaks not being exactly equal. It has always been less than 1 ppm. The formula for calculation of Δa from ΔR_m is given in section 2. 7., p. 35.

2. 5. **Rational presentation of the results.**

The criterion for an appropriate way of presenting the results seems to the author to be that the final data are not influenced (beyond the limits given by the reproducibility) by instrumental errors caused by mass discrimination, background, imperfect resolving power, etc.

Several different functions have been used in isotope geology. A common feature is the consideration of the fact that determination of the true isotopic composition of a sample is extremely difficult, while measurement of differences in isotopic composition is relatively easy.

Some investigators record their data in terms of

$$r = \frac{(A)}{(B)}$$

(A) and (B) being the quantities of the isotopes A and B in the sample, or actually in terms of

$$\Delta r = r_{sample} - r_{standard},$$

considering the fact that they estimate the r-value of their standard. Experimentally,

$$\Delta R = R_s - R_{std}$$

is determined, R_s (for the sample) and R_{std} (for the standard) being the ratio between the peak corresponding to the ions containing one atom of the heavy isotope in question and the peak caused by the ions consisting of the light isotopes only. Thus, in work with deuterium

$$R = (HD)/(H_2),$$

with carbon thirteen

$$R = (C^{13}O_2^{16})/(C^{12}O_2^{16}),$$

and with oxygen eighteen

$$R = (C^{12}O^{16}O^{18})/(C^{12}O_2^{16}).$$

Δr is derived from ΔR after correction for possible fractionation caused by the preparation technique etc.

Another group of investigators use a function given as:

$$\delta = \frac{\Delta R}{R_{std}} \cdot 1000 \text{ per mille.}$$

ΔR and R_{std} usually having the same meanings as above.

The present author uses the Δa function given by

$$\Delta a = a_s - a_{std} \text{ ppm},$$

$$a = \frac{(A)}{(A)+(B)} \cdot 10^6 \text{ ppm}.$$

This function is generally used in the tracer technique. Δr and Δa do not differ essentially from each other, because

$$a = \frac{r}{1+r} \cdot 10^6 \text{ and } \Delta a = \frac{\Delta r}{1+2r_{std}} \cdot 10^6 \text{ ppm},$$

if $r_{std} \cong r_{sample}$. This is the case here, since the greatest measured deviation from the standard is $2^0/_0$ of a_{std}. The absolute value of $1+2r_{std}$ is known with a good precision, since $1 >> 2r_{std}$.

If the heavy isotope in question may occur in two atoms of the molecule (N^{15} in N_2, or O^{18} in CO_2), Δa is related to Δr as:

$$\Delta a = \frac{\Delta r}{2(1+r_{std})} \cdot 10^6 \text{ ppm}.$$

Δa is calculated by correcting the measured ΔR_m for instrumental and preparation effects (cf. 2. 7.). This gives ΔR, which is inserted in one of the equations

$$\Delta a = \frac{\Delta R}{1+2r_{std}} \cdot 10^6 \text{ and } \Delta a = \frac{\Delta R}{2(1+r_{std})} \cdot 10^6 \text{ ppm}.$$

2.6. The sources of error and their influence on the Δr, Δa and δ functions.

In this section the above mentioned calculation will be described in details and, at the same time, the influences of the different sources of error on the functions will be discussed with special reference to the measurement of small differences in O^{18} contents of water samples, i.e. at the highest $\pm 2\,^0/_0$ from a standard.

The sources of error, which will be taken into consideration, are those arising from

1. background,
2. incomplete resolving power,
3. the factor $c = r_I/r_{II}$,
4. mass discrimination,
5. inability to distinguish between different ions of equal mass,
6. pollution with atmospheric air,
7. incomplete equilibration,
8. lack of excess of water in the equilibrium process and
9. the fractionation factor, f, of the equilibrium process.

The correction for 1. and 2. will be shown to be additive terms to the measured R_m (pp. 22 and 24). Thus, if the sample and the standard are measured with the same mass 44 peak the errors will cancel when forming Δa and Δr, because these functions depend on differences in R_m between sample and standard. However, the δ function will be affected by these errors, because R_m for the standard occurs in the denominator of δ.

On the other hand, the errors 3. and 4. are corrected for by factors to the R_m. Therefore, these errors affect the Δa and Δr functions, whereas they cancel in δ.

2.6.1. Background.

Traces of residual gases and vapours in the analyser tube and the ion source are responsible for the background spectrum, which can be measured with both valves closed.

In what follows the background value and the total height of the peak caused by ions with mass A are called B_A and H_A. Thus,

$$M_A = H_A - B_A \tag{2}$$

is the contribution of the sample gas to the total peak height.

When measuring O^{18} content in CO_2, as described on p. 11, the ions with mass 43, 44 and 45 are collected by collector I, when mass 46 is focussed on collector II. Therefore, the balance value of the potentiometer is

$$R_m = \frac{H_{46}}{H_{45} + H_{44} + H_{43}} = \frac{H_{46}}{H_I}$$

disregarding the c factor (p. 25). H_I denotes the total output of the amplifier. What is needed for the further evaluation is, however,

$$R_m + k_B = \frac{M_{46}}{M_{45} + M_{44}},$$

k_B being the background correction.

The total differential of R_m is

$$dR_m = \frac{1}{H_I} dH_{46} - \frac{H_{46}}{H_I^2} dH_I = k_B .$$

Considering equation (2), dH_{46} is put equal to $-B_{46}$ and $dH_I = -B_I$, B_I ($= B_{45} + B_{44} + B_{43}$) being the background output of the amplifier. This gives the background correction:

$$k_B = -\frac{B_{46}}{H_I} + \frac{H_{46}}{H_I^2} B_I .$$

For the mass spectrometer used in this work a typical background correction is calculated in Table 1 to approx. -6 ppm or $-0.15\,^0/_0$ of R_m. Since k_B is an additive term it only affects the δ function, e.g. a δ value of $20.00\,^0/_{00}$ will come out as $20.03\,^0/_{00}$ if not corrected for background. However, this error is less than the reproducibility of difference measurements.

Table 1.

H_I mV	H_{46} mV	B_{43} mV	B_{44} mV	B_{45} mV	B_{46} mV	k_B ppm	R_m ppm
10000	40	5	10	0.5	0.12	-6	~ 4000

2. 6. 2. **Incomplete resolving power.**

Fig. 8 shows the part of the CO_2 mass spectrum, which includes the mass numbers 44 to 46. The spectrum has been obtained by measuring the ion current reaching collector II (cf. p. 16, l. 12 f. b.) as a function of the ion accelerating voltage.

The peaks are almost flat, which is due to the slit in collector I being wider than the individual ion beam at this very place. This is an important ion optical quality, as it reduces the requirements to the stability of the ion accelerating voltage. However, the ion optics is not free of abberations, which appears in the following facts: a) The sides of the peaks are not vertical. This is mainly due to the ion beams having finite widths. A finite change of the ion accelerating voltage is, therefore, required for moving the focus of the entire beam from collector I to

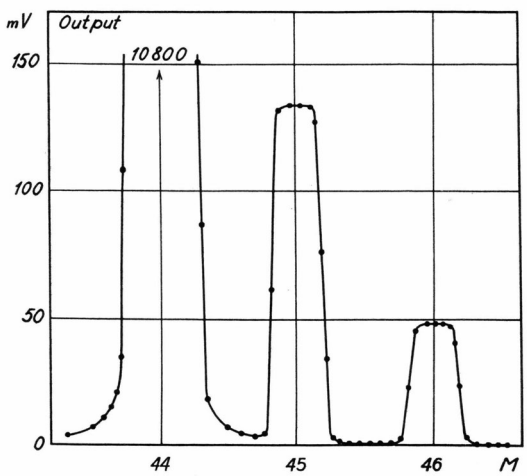

Fig. 8. Mass spectrum of CO_2 in the range from M = 44 to M = 46.

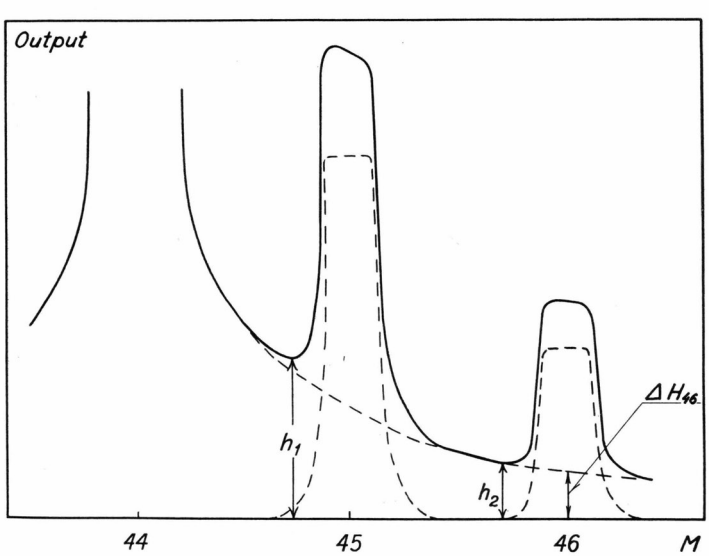

Fig. 9. The influence of the ion optical abberations on the mass spectrum (shown exaggerated).

the slit. b) The edges at the tops of the peaks are round and c) the basis of the peaks, especially the mass 44 peak, are indistinct (tail effect). These irregularities signify a non-uniform intensity in the beam caused by coulombic effects, slightly different initial ion energies, inhomogenities in the magnetic deflecting field etc. The tail of the mass 44 peak influences the neighbouring peaks and causes their tops not to be completely flat (shown exaggerated in Fig. 9).

The resolving power is usually defined as $M/\Delta M$. M is the highest mass, the peak of which can be completely separated from the neighbouring peak corresponding to mass M + 1. The resolving power of the mass spectrometer described here is 70, which is one order of magnitude less than that of modern commercial instruments. This is not important, however, as long as only mass range 44 to 46 is of interest.

In isotope work on CO_2 another definition of the resolving power is often used, namely

$$rp = \frac{h_1 + h_2}{2\,H_{44}} \cdot 100\,\%.$$

H_{44} is the 44 peak, while h_1 and h_2 are indicated in Fig. 9. In Table 2 rp is calculated for a typical case.

Table 2.

h_1 mV	h_2 mV	H_{44} mV	rp %
3.3	0.7	10000	0.02

In Fig. 9 the 44 tail is seen to make an additive contribution, ΔH_{46}, to the 46 peak. In the present instrument the contribution is usually of the order of 1 % of H_{46}, when H_{44} is approx. 10 volts. The effect cancel in Δa and Δr, whereas the relative error of δ values will be approx. 1 % if not corrected for. Correction should be made by using

$$R - \frac{\Delta H_{46}}{H_I}$$

instead of R.

Due to coulombic effects the 44 tail contribution to the 46 peak does not vary proportional to the 44 peak. This is one reason why the 44 beam intensity should be the same when measuring the sample and the standard.

2. 6. 3. **Different input resistors.**

The balance value, R_m, of the potentiometer (Fig. 6, p. 16) is related to the ion beams, i_{II} and i_I, to the two collectors as

$$i_{II}/i_I = c \cdot R_m, \qquad c = r_I/r_{II},$$

r_I and r_{II} being the input resistors.

NIER (1948) mentions that "the resistance value for the high resistors used for measuring the ion currents depends to a small degree upon the current passing through it. Thus the ratio of voltages impressed

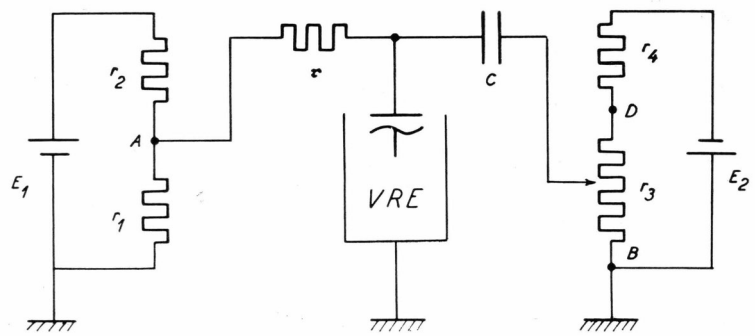

Fig. 10. Arrangement for measuring the ratio between the high input resistors.

on the amplifier may be in error by several per cent, if we are comparing two ion currents differing in magnitude by a factor of 100". This phenomenon is due to the high ohm resistors being semiconductors (cf. SHOCKLEY, 1951).

The influence of the current upon the resistance can be measured in the following way: In Fig. 10 the resistor in question, r, is connected on one side to the capacitor C and a vibrating reed electrometer, VRE, on the other side to point A of the potentiometer circuit ($E_1 - r_1 - r_2$) giving the left side of r the constant voltage V_A. The charge passing through r is tied up in C by manually moving the slide of the right potentiometer from B to D, and thereby changing the voltage of the right side of C from zero to V_D (negative) just fast enough to keep the voltage of the left side of C at zero, which is indicated by the VRE. If the total change takes τ sec, the current through r will be

$$i = \frac{V_D \cdot C}{\tau} = \frac{V_A}{r}$$

and thus

$$rC = \frac{V_A}{V_D} \cdot \tau.$$

Resistors r_1 to r_4 had well defined values, and the voltages E_1 and E_2 were measured with a high precision voltmeter. C was an air condenser in parallel connection with two trolitoul condensers. The total capacity was approx. 500 pf, the insulation better than 10^{15} ohms.

With r_I and r_{II} in turn substituting r, $r_I C$ and $r_{II} C$ were measured for values of V_A between 0.04 and 10 volts (corresponding to V_D values between -0.2 and -50 volts). From Fig. 11 $r_I C$ and $r_{II} C$ are seen to

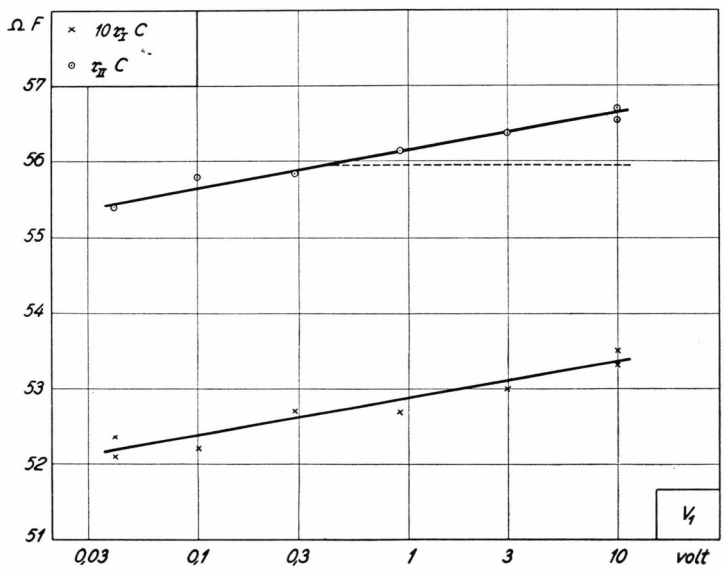

Fig. 11. $10\, r_I C$ and $r_{II} C$ as functions of the voltage drop across the resistors.

increase with V_A. The variation can not be ascribed to some kind of a dielectric effect in the capacitors, since a similar variation of $r_{II} C$ was found in another series of measurements with only the air condensor involved. Therefore, r must be responsible for the variation of rC. The temperature effect is negligible, the power dissipated in the resistor being of the orders of $2 \cdot 10^{-12}$ to 10^{-8} watt.

From Fig. 11, r_I/r_{II} is found to be 0.0941 with the same voltage drop across both resistors, but

$$c = r_I/r_{II} = 0.0954 \pm 0.0003,$$

when r_I and r_{II} are loaded with 10 and 0.4 volts, respectively, as is the case in O^{18} measurements on CO_2.

2. 6. 4. **Mass discrimination.**

Mass discrimination may arise in mainly four different ways in the mass spectrometer:

1. The light component may be depleted in the leak system because of differences in molecular velocities. This effect will change the composition of the reservoir gas with time.

2. The light molecules will escape easier from the ion source than the heavy ones. Consequently, the concentration of the light component will be depleted in relation to its occurrence in the gas admitted to the source.

3. Different ionization potentials for the components may cause some mass discrimination.

4. The isotopic ions utilized in the beam may be selected non-proportional to their concentrations in the source.

If the composition of the reservoir gas is known the total mass discrimination in the instrument can be found by comparison with the measured composition. This is possible with sufficient accuracy also for O^{18} isotopic work after r_I/r_{II} has been measured precisely (p. 26). The calculation is shown in Table 3 on the basis of a measurement on CO_2 from the $BaCO_3$ standard of the Svenska Riksmuseum.

Table 3.

$R^{46}_{45+44+43}$ uncorrected	43300 ppm
$c \cdot R^{46}_{45+44+43}$	4131 ppm
Correction for C^{13} and O^{17} (p. 32)	51 ppm
Correction for background (k_B, p. 22)	− 6 ppm
Correction for incomplete resolving power (rp, p. 24)	−47 ppm
R^{46}_{44} corrected	4129 ppm

The value 4129 ppm is 0.9 % higher than that given by CRAIG (1957) on the basis of NIER's measurement (1950). Practically the same value is found when the standard is admitted to the source from the other inlet system (cf. p. 19). Therefore the correction factor 0.991 for the total mass discrimination will be used below. It should be used when calculating Δr and Δa, whereas it cancels in the δ function.

As to the individual contributions to the mass discrimination mentioned above, Nos. 1 and 2 will be discussed on pp. 28–30. As to No. 3 (different ionization potentials for the isotopic components) no precise measurement of this effect have been published. "In isotopic studies it is *assumed* that the ionization potential and the probability curve are determined solely by the nuclear charge". (BARNARD, 1953). How-

ever, the order of magnitude of possible differences for the isotopic elements dealt with here may be almost the same as for the neon isotopes. Theoretical considerations indicate the ionization potential for Ne^{20} to be approx. $3 \cdot 10^{-4}$ % higher than that of Ne^{22} (RITZCHEL and SCHOBER, 1937). The corresponding difference for O^{16} and O^{18} should be half a per cent to be of any importance for the Δa values in this work. It is, therefore, considered negligible.

The importance of No. 4 (different probabilities for the isotopic ions to be utilized in the ion beam) is very difficult to tell. Usually, not even the sign can be estimated directly.

Mass discrimination in the leak system.

The ideal gas inlet and leak system should satisfy the following requirements (INGHRAM and HAYDEN, 1954):

a. The composition of the gas mixture in the ionization region of the source should be identical with that of the sample.

b. The concentration of the mixture being analyzed should not change with time.

c. In a gas mixture, a change in the amount of one substance should not affect the peak heights due to the others.

d. The gas flow rate should remain essentially constant during the analysis.

Two principally different types of leak have been used. The molecular leak, described by HONIG (1945), is a pinhole with a diameter much smaller than the mean free path in the sample reservoir. Since the flow through the hole as well as the flow out of the spectrometer is molecular, condition *a* is fulfilled. The same is the case with condition *c* because of the low pressure. However, a rather big hole is necessary for obtaining a sufficiently high pressure in the ion source, and so neither *b* (because of depletion of the light component) nor *d* is satisfied except in case of a very large reservoir.

The second type is the "viscous" leak (NIER, 1947). Fig. 12 is a schematic diagram showing the sample reservoir connected to the ion source by a tube (length L, diameter D) with a constriction, the geometry of which is not well defined. If the diameter of the constriction is of the same order as the mean free path or smaller a depletion of the light component occurs, which will be propagated by diffusion against the flow to a degree depending upon the flow rate. As time goes a stationary state is reached, in which the gas entering the ion source has a composi-

tion different from that of the sample. The flow is not purely viscous, neither is it purely molecular.

The idea behind the Nier leak is to use a capillary tube with a (viscous) flow fast enough to avoid or reduce the back diffusion. Thus, the composition of the gas flowing into the ion source is almost equal to that of the reservoir gas. Since, on the other hand, the flow out of the ion source is still molecular appreciable mass discrimination may occur. What is often more important, however, is that the time needed for reaching the stationary state is fairly short (Fig. 7). Thus, the Nier leak satisfies *b* and, for shorter periods of time, also *d*. What makes this leak important "is the fact that the ratio of any two peaks is characteristic

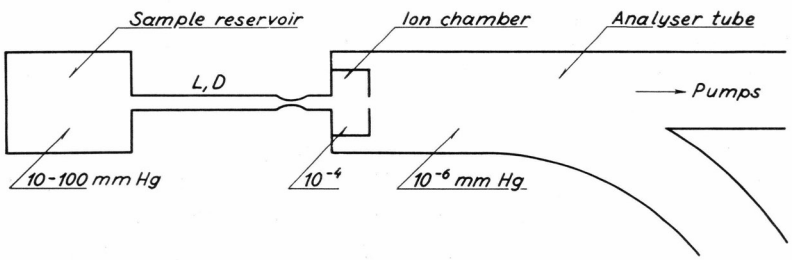

Fig. 12. Schematic drawing of reservoir, leak, ion source and analyser tube.

of the relative composition only. Thus it is the ideal leak to use for high precision in relative isotopic abundance and in any case where reference to a standard is made" (INGHRAM and HAYDEN, 1954).

Below the gas is supposed to be a mixture of the components A and B. Their partial pressures in the reservoir are denoted by P_A and P_B, in the ion chamber by p_A and p_B. The masses are called m_A and m_B and the ion currents i_A and i_B. Disregarding possible mass discrimination in the ion source we have for all kinds of leak

$$\frac{i_A}{i_B} = \frac{p_A}{p_B}.$$

The *molecular* flow rate out of the ion source is inversely proportional to the square root of the mass of the component in question. With a molecular leak this effect is compensated by the flow rate into the ion source having the same dependence upon the mass. Therefore,

$$\frac{i_A}{i_B} = \frac{p_A}{p_B} = \frac{P_A}{P_B}. \tag{3}$$

With a viscous leak, however,

$$\frac{i_A}{i_B} = \sqrt{\frac{m_A}{m_B}} \cdot \frac{P_A}{P_B}. \tag{4}$$

because the gas entering the ion source has the same composition as that in the reservoir.

Leak systems which are not strictly molecular nor viscous have been investigated by HALSTED and NIER (1950) and KISTEMAKER (1952). The mass discrimination can not be expressed by a simple equation in such cases, but the limits are given by equations (3) and (4). Thus, the mass discrimination in the leak system amounts at most to a factor, which for O^{18} measurements on CO_2 is

$$\sqrt{\frac{m_A}{m_B}} = \sqrt{\frac{46}{44}} = 1.022.$$

In contradistinction to the valves described by NEY and used in the MCKINNEY, MCCREA, EPSTEIN, ALLEN and UREY mass spectrometer (1950) the valves described on p. 13 stop the gas flow from one system when the gas from the other system is admitted to the ion source. This mode of operation excludes the possibility of any mixing between the two gases to be compared and, furthermore, no pumping system is required. On the other hand, some delay in the establishment of the state of equilibrium may be expected. However, Fig. 7 (p. 18) shows this not to be too bad.

2.6.5. The influence of C^{13} and O^{17}.

The measurement of O^{18} content in a CO_2 gas is complicated by the presence of the isotopes C^{13} and O^{17}, and also by the fact that collector I collects three different masses, namely 43, 44, and 45. The influence of C^{13} and O^{17} on the O^{18} measurement has been treated by CRAIG (1957) as far as the δ function is concerned.

What is needed for the determination of as well the Δr and Δa as the δ function is the ratio

$$R_{18} = \frac{(C^{12}O^{16}O^{18})}{(C^{12}O^{16}O^{16})}$$

the nominator and the denominator being the number of $C^{12}O^{16}O^{18}$ and $C^{12}O^{16}O^{16}$ ions collected per unit of time. However, the balance value R_m read on the potentiometer rather represents

$$R^{46}_{43+44+45} \simeq R^{46}_{44+45} = \frac{(46)}{(44)+(45)} = \frac{(C^{12}O^{16}O^{18})+(C^{13}O^{16}O^{17})+(C^{12}O^{17}O^{17})}{(C^{12}O^{16}O^{16})+(C^{12}O^{16}O^{17})+(C^{13}O^{16}O^{16})} \quad (5)$$

looking apart from instrumental effects such as background, c-factor etc.

In Table 4 (McCrea, 1950) is given the individual fractional occurrences of the ion beams of the corresponding masses presupposing (Nier, 1950) the true fractional occurrences of the isotopes to be

$$C^{12} : C^{13} = 98.90 : 1.10 \tag{6}$$

and

$$O^{16} : O^{17} : O^{18} = 99.757 : 0.039 : 0.204. \tag{7}$$

Table 4.

Mass	Ions	Individual fractional occurrence	Relative beam intensity
44	$C^{12}O_2^{16}$	0.9842	0.9842
45	$C^{13}O_2^{16}$	$1.095 \cdot 10^{-2}$	0.01172
	$C^{12}O^{16}O^{17}$	$7.7 \cdot 10^{-4}$	
46	$C^{12}O^{16}O^{18}$	$4.025 \cdot 10^{-3}$	0.00403
	$C^{13}O^{16}O^{17}$	$8.6 \cdot 10^{-6}$	
	$C^{12}O_2^{17}$	$1.5 \cdot 10^{-7}$	

After neglecting the $(C^{12}O_2^{17})$ term and reducing by $(C^{12}O_2^{16})$ Eq. (5) may be written

$$R_m = \frac{R_{18} + \dfrac{(C^{13}O^{16}O^{17})}{(C^{12}O^{16}O^{16})}}{1 + \dfrac{(C^{13}O_2^{16})}{(C^{12}O_2^{16})} + \dfrac{(C^{12}O^{16}O^{17})}{(C^{12}O_2^{16})}}$$

or, calling the two last terms of the denominator for R_{13} and R_{17} respectively,

$$R_m = \frac{R_{18} + R_{13} R_{17}}{1 + R_{13} + R_{17}}.$$

If the denominator is called D, the total differential may be written

$$\left.\begin{aligned} dR_m = {} & \frac{1}{D} dR_{18} - \frac{1}{D^2}(R_{18} + R_{13} R_{17} - D R_{17})\, dR_{13} \\ & - \frac{1}{D^2}(R_{18} + R_{13} R_{17} - D R_{13})\, dR_{17}. \end{aligned}\right\} \tag{8}$$

For small deviations from the isotopic composition indicated by Eqs. (6) and (7) the values in Table 4 may be inserted in Eq. (8), which then comes out as

$$dR_m = 0.988\, dR_{18} - 0.0032\, dR_{13} + 0.0070\, dR_{17}.$$

After solving the equation dR_{18} is put equal to ΔR and analogous for the other terms:

$$\Delta R = 1.012 \Delta R_m + 0.0032 \Delta R_{13} - 0.0071 \Delta R_{17}. \quad (9)$$

In this work differences in C^{13} and O^{17} content up to 2 and 1‰, respectively, may occur between the standard and a sample. Since R_{13} and R_{17} are approx. 11000 and 800 ppm this corresponds to $\Delta R_{13} = 220$ and $\Delta R_{17} = 8$ ppm. Thus, in the most unfavorable case, the two last terms of equation (9) make 0.7 and 0.06 ppm, respectively. The last term is always negligible, whereas the ΔR_{13} term is of the same order as the reproducibility.

CRAIG (1957) gives an equation for the correction of the δ function, which comes out as

$$\delta_c = 1.0014 \delta_m + 0.009 \delta (C^{13}) \quad (10)$$

after insertion of the values for the isotopic composition of the standard used in this work. δ_c and δ_m are the corrected and measured δ value for the CO_2 sample; $\delta (C^{13})$ is the δ value for the heavy carbon isotope in the sample relative to the standard. Formula (10) is valid for the use of standards with compositions deviating several per cent from that of the standard used here.

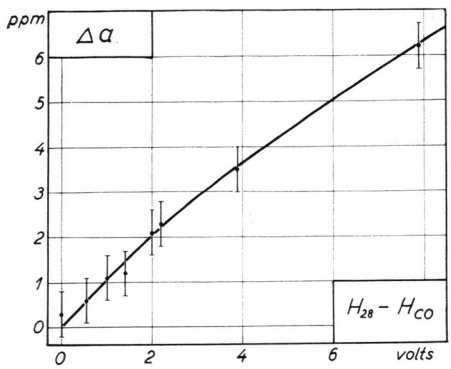

Fig. 13. The error due to pollution with air. The mass 44 peak is approx. 10 volts.

2.6.6. **Pollution with atmospheric air.**

If the sample is polluted with atmospheric air the R_m has shown to increase corresponding to a higher content of $CO^{16}O^{18}$. For quantitative reasons this can not be due to the addition of CO_2 from the air. The effect should rather be traced to a change in the mass discrimination and, furthermore, to a catalytic effect of the filament causing an ex-

change of oxygen isotopes between CO_2 and atmospheric oxygen, the latter being very high in O^{18} ($\Delta a \cong 90$ ppm).

The degree of pollution can be measured by the contribution (H_{N_2}) of N_2 to H_{28}. The rest of H_{28} (H_{CO}) is mainly due to CO^+.

Fig. 13 shows the deviation of the O^{18} content of standard CO_2 as a function of $H_{N_2} = H_{28} - H_{CO}$. All measurements were carried out with $H_{44} = 10$ volts. Under this condition $H_{CO} = 1.1$ volts.

The pollution can very easily be kept below a negligible degree corresponding to $H_{N_2} = 0.02$ volts.

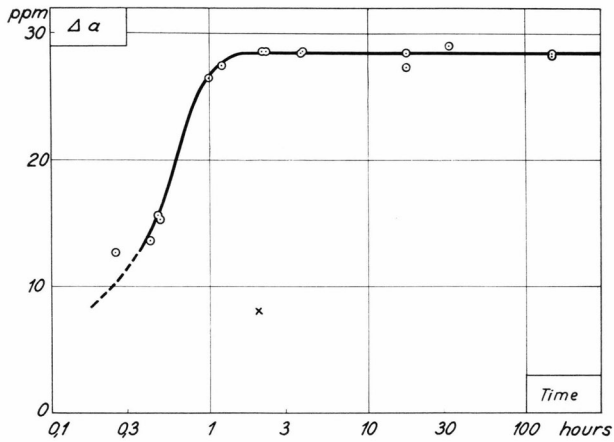

Fig. 14. Δa for CO_2 as a function of time of shaking with water. Equilibrium is established after 2 hours.

2. 6. 7. **Incomplete equilibration.**

The time needed for the equilibration process

$$CO_2^{16} + H_2O^{18} \rightleftharpoons CO^{16}O^{18} + H_2O^{16} \qquad (11)$$

to reach to a state of equilibrium depends upon the pH (Mills and Urey, 1940). The oxygen exchange between carbon dioxide and water is due to the reversible hydration, i.e. the left part of the process

$$CO_2 + H_2O \rightleftharpoons H_2CO_3 \rightleftharpoons H^+ + HCO_3^- \rightleftharpoons 2H^+ + CO_3^{--},$$

whereas no direct exchange takes place between the HCO_3^- or CO_3^{--} ion and the water. The solution should therefore be acid for fast equilibration. On the other hand, if the solution is acid further decrease in pH does not affect the rate of exchange.

Fig. 14 shows the O^{18} content in CO_2 which has been shaken with destilled water with pH = 5.5. Two hours shaking is seen to be sufficient for complete equilibration.

The cross at the time 2 hours indicates a measurement of a sample, which was treated like the other samples, except that it was not shaken. The exchange reaction is thus seen to be speeded up by shaking.

2. 6. 8. **Lack of excess of water in the exchange process.**

As just mentioned, water samples to be analysed for O^{18} are shaken with CO_2 for isotopic equilibration. If the gram atoms of oxygen admitted to the water in the form of tank CO_2 are not negligible compared to that in the water, the O^{18} content of the equilibrated CO_2 will be influenced by the initial isotopic composition of the tank CO_2.

CRAIG (1957) gives the following equation for the δ function:

$$\delta = \delta_m \frac{\varrho + f}{\varrho} - \frac{f}{\varrho} \delta_{(\text{tank } CO_2)} \text{ per mille,} \qquad (12)$$

where δ_m is the measured enrichment of the equilibrated CO_2 relative to the standard, and δ the corrected value. f is the fractionation factor of the equilibrium process (11), p. 33, and ϱ is the ratio of gram atoms of oxygen in the water sample to gram atoms of oxygen in the CO_2 introduced into the flask.

For the procedure described on p. 17 ϱ is approx. 400. For none of the tanks of CO_2 used till now δO^{18} has exceeded 2 per mille. Using these values and 1.04 for f at 24° C equation (12) comes out as

$$\delta = 1.0025\, \delta_m - 0.005 \text{ per mille.}$$

In measurements of O^{18} differences of at the highest $30^0/_{00}$ with an accurary of $0.25^0/_{00}$ (or 60 ppm with an accuracy of 0.5 ppm) the effect is at the highest $0.05^0/_{00}$ (0.1 ppm), i.e. negligible.

2. 6. 9. **The fractionation factor in the exchange process.**

When comparing a standard CO_2 with CO_2 in equilibrium with a water sample the fractionation factor, f, of the process

$$CO_2^{16} + H_2O^{18} \rightleftharpoons CO^{16}O^{18} + H_2O^{16}$$

should be taken into consideration. The O^{18} content of the water is equal to that of the equilibrated CO_2 divided by f and, accordingly, the O^{18} difference between two water samples is equal to the difference between the two equilibrated CO_2 gasses divided by f. Therefore, if the formula for the calculation of O^{18} differences in CO_2 is changed into

$$\Delta a = \frac{\Delta R}{2 f (1 + r_{std})} \cdot 10^6 \text{ ppm},$$

the Δa value for a water sample signifies the true deviation of the O^{18} content from a certain basic value equal to that of the standard divided by f. This basic value is usually of little importance. All what counts are the variations in isotopic composition from one sample to another.

BAERTSCHI (1953) compared his sample CO_2 with CO_2 in equilibrium with standard water. In this case f cancels in the δ formula, because it appears in both the nominator and the denominator. δ then signifies the per mille difference between the absolute O^{18} values of the waters. When using other standards than water the δ's do, naturally, not have the same meaning. It is often overlooked that in such cases variations in δ refer to CO_2 in equilibrium with the waters, but not to the waters themselves unless the δ's are divided by f.

The quantity f has not yet been measured precisely. The only experiment known to the author is that of WEBSTER, WAHL and UREY (1935), who found the value 1.047 at 0° C. However, UREY (1947) found by theoretical considerations 1.044 at 0° C and 1.039 at 25° C.

The variation of the f factor with temperature seems to be of the order of $2 \cdot 10^{-4}$ or 0.02 % per °C. Since the absolute O^{18} content of the samples is of the order of 2000 ppm a deviation of the exchange temperature of 1° C makes an error of about 0.4 ppm if not corrected for. However, since the fractionation factor and its temperature dependability are not very well known care was taken in the present work that the exchange reaction always went off at 24.0 ± 0.5° C.

2. 7. **Correction formula.**

Recognizing all the sources of error discussed above the Δa value for a sample should be calculated from the measured ΔR_m as follows:

Instrument reading	ΔR_m
Corrected for different input resistors ($c = r_I/r_{II}$, p. 26)	$c\,\Delta R_m$
Corrected for mass discrimination (d, p. 27)	$d \cdot c\,\Delta R_m$
Corrected for different C^{13} and O^{17} contents in standard and sample (looking apart from the c and d factors in the ΔR_{13} term and neglecting the ΔR_{17} term, p. 32):	$1.012\ cd\,\Delta R_m + 0.0032\,\Delta R_{13}$.

Corrected for fractionation in the equilibrium process:

$$\Delta R = \frac{1.012\ cd}{f} \Delta R_m + 0.0032\,\Delta R_{13}$$

From this the Δa comes out as (p. 20)

$$\Delta a = \frac{\frac{1.012\ cd}{f}\Delta R_m + 0.0032\,\Delta R_{13}}{2\,(1 + r_{std})} \cdot 10^6\,\text{ppm}. \qquad (13)$$

Insertion of the previous given values of c, d, f and r_{std} gives

$$\Delta a = (0.0459\,\Delta R_m + 0.0016\,\Delta R_{13}) \cdot 10^6\,\text{ppm}.$$

Δa values calculated from this formula mean the difference in ppm between the absolute O^{18} content of the water sample and a value equal to the absolute O^{18} content of the standard CO_2 divided by 1.04 (cf. p. 35).

2. 8. **Rational presentation of the results, II.**

On p. 19 it was stated that a suitable function should give the final data independent of instrumental effects. From this point of view all the functions Δr, Δa and δ are useable since sufficiently accurate corrections for instrumental errors can usually be attributed to all of them.

The preferable way of presenting the results seems to the author to depend on which kind of errors are the most pronounced for the particular mass spectrometer. If it is the additive errors, the Δa function should be preferred, and otherwise the δ function.

For the instrument used in this work the resolving power has varied rather much because of some contamination of the ion source. For this reason, and for keeping the continuity with the author's previous works, the Δa function will be preferred here.

2. 9. **Reproducibility.**

The nine measurements of distilled water shaken more than 2 hours (Fig. 14) are listed in Table 5. They provide a basis for an estimate on the overall reproducibility of the determination of small isotopic differences taking into account the uncertainties connected to the preparation as well as to the mass spectrometric measurement. The standard deviation of the individual measurement from the mean is 0.5 ppm. or $0.25\,‰$ of the absolute O^{18} content.

Table 5.

Time hours	Δ a ppm
2.15	28.6
2.28	28.6
3.85	28.5
3.87	28.6
17.5	27.4
17.5	28.5
32.5	29.1
149	28.4
149	28.3
	Mean: 28.44

2. 10. **The standard.**

As mentioned above (p. 35) it is not of great importance to know precisely the true values of the isotopic compositions of the samples dealt with in this work. For this reason, and also because of the difficulty connected with the measurement of absolute values, reference is always made to a standard gas.

Previously the author used CO_2 from a tank as a standard, called Danish standard, DS (DANSGAARD, 1953a, 1953b, 1954). However, using tank CO_2 involves the possibility of a steady increase in the O^{18} content of the remaining part of the standard because the gaseous phase is poorer in O^{18} than the liquid one. Nevertheless, repeated measurements on elder water samples have shown no significant drift in the composition of the DS during the three years it was used. In order to keep the continuity with the author's previous work the data given here are referred to the DS in the way described below. However, in the daily routine work, CO_2 in equilibrium with Copenhagen tap water (from June 1955) is used as a secondary standard. Such CO_2 is 22.9 ppm richer in O^{18} than the DS.

In order to obtain an approximate absolute value for the DS one must start with NIER's measurement (1950), 2039 ppm, for the O^{18} content in atmospheric oxygen (Table 6, line 1). On this basis CRAIG (1957) derived $2074._1$ ppm for the so-called PDB standard* (line 2). In the same work (p. 145) CRAIG claims the δ value of ocean water to be $-0.1\,‰$ relative to the PDB standard. However, this δ value is rather true for CO_2 in equilibrium with ocean water, which gives the difference put

* PDB is a Cretaceous belemnite, Belemnitella americana, from the Peedee formation of South Carolina (CRAIG, 1957).

Table 6.

Line	Sample	Δa ppm	a ppm
1	Atmospheric oxygen (NIER, 1950)		2039
2	PDB standard (CRAIG, 1957)		2074.1
3	CO_2 (ocean) – PDB	–0.2	
4	CO_2 (ocean)		2073.9
5	$a_{ocean} = CO_2$ (ocean)/f		1994.1
6	CO_2 (ocean) – DS	40.6	
7	DS		2033.3
8	CO_2 (Copenhagen tap) – DS	22.9	
9	CO_2 (Copenhagen tap)		2056.2
10	Copenhagen tap water		1977.0
11	DS/f		1955.0

down in Table 6 line 3, and the absolute value, 2073.9 ppm, for CO_2 in equilibrium with ocean water (line 4). Using the fractionation factor 1.04 for the equilibrium process ((11), p. 33) the absolute O^{18} content of ocean water becomes approx. 1994 ppm (line 5). CO_2 in equilibrium with ocean water has shown to be 40.6 ppm higher in O^{18} than the DS (line 6), which gives

$$a_{DS} = 2033.3 \text{ ppm.}$$

If the fractionation factor, f, in Formula (13), p. 36, were neglected the calculated Δa would indicate the absolute deviation from a_{DS} of the O^{18} content of CO_2 in equilibrium with the water in question, or

$$\Delta a = f \cdot a_w - 2033.3 \text{ ppm,}$$

a_w denoting the absolute O^{18} content of the water. The difference between the Δa values of two different waters would thus be

$$\Delta a_1 - \Delta a_2 = f \cdot (a_1 - a_2).$$

On the other hand, when using formula (13) with the factor f taken into consideration the Δa means

$$\Delta a = a_w - \frac{2033.3}{f} = a_w - 1955.0 \text{ ppm}$$

and the difference between the Δa values of two waters means

$$\Delta a_1 - \Delta a_2 = a_1 - a_2,$$

i.e. the difference between their absolute O^{18} contents.

Although the f factor is not too well known the latter method is preferred here, because only small Δa values occur and, therefore, only small absolute errors arise due to the uncertainty of f. Thus, Δa derived from formula (13) means the deviation of the absolute O^{18} content of the water from a basis value, which is approximately

$$2033/f = 1955 \text{ ppm}.$$

It should be born in mind that when the δ function is used in the literature in connection with O^{18} measurements on water, it often means the 46/44 ratio difference between CO_2 in equilibrium with the water and standard CO_2, i.e. actually

$$\delta = \frac{f \cdot R - R_{std}}{R_{std}},$$

R being the corrected 46/44 ratio for the sample CO_2, as it would be if f were equal to 1. The difference between the δ values for two water samples means

$$\delta_1 - \delta_2 = f\,(R_1 - R_2)/R_{std}.$$

The corresponding expression for the difference between two Δa values calculated from Eq. (13) is

$$\Delta a_1 - \Delta a_2 \simeq (R_1 - R_2)/2\,(1 + R_{std}).$$

The relation between the two functions is found by combining the two latter equations:

$$\Delta a_1 - \Delta a_2 = \frac{R_{std}}{2\,(1 + R_{std})} \cdot \frac{\delta_1 - \delta_2}{f} = \frac{a_{std}}{f}\,(\delta_1 - \delta_2).$$

For the PDB standard $a_{std} = 2074$ ppm, which gives

$$\Delta a_1 - \Delta a_2 = 1.994\,(\delta_1 - \delta_2) \text{ ppm},$$

when the δ values are expressed in per mille.

However, it is important to make clear that sometimes the δ values for waters given in the literature should be interpreted as relative differences of the O^{18} contents of the waters from that of ocean water. In other words, CO_2 in equilibrium with the water sample is compared with CO_2 in equilibrium with ocean water, which makes f cancel in the δ-formula. In this case the conversion formula given above changes into

$$\Delta a_1 - \Delta a_2 = 2.074\,(\delta_1 - \delta_2) \text{ ppm}.$$

Since Δa for ocean water is 39.1 ppm,

$$\Delta a = 2.074\,\delta + 39.1 \text{ ppm},$$

or

$$\delta = 0.482\,\Delta a - 18.1 \text{ per mille}.$$

3. ISOTOPIC FRACTIONATION OF WATER

Isotopic fractionation of water is attached to several processes in nature, e.g. biological activity and exchange with other materials. However, the fundamental reason for the considerable variations in the heavy isotope content of natural waters is the fact that the vapour pressure of H_2O^{16} ($p_{H_2O^{16}}$) is higher than those of HDO (p_{HDO}) and H_2O^{18} ($p_{H_2O^{18}}$). The vapour from a water reservoir is, therefore, poorer in D and O^{18} than the initial water, whereas the remaining water is enriched. Conversely, condensation from a limited amount of vapour gives an enriched condensate and a remaining vapour depleted in the heavy isotopes relative to the initial vapour.

3. 1. **Isothermal evaporation from a limited amount of water.**

In this section the changes of the concentrations of the heavy isotopic components in a two phase system will be considered in relation to an isothermal evaporation from initially q_0 grams of water. The vapour is assumed to be removed continuously from the system, and the process to go on so slowly that equilibrium virtually exists at the surface.

The following symbols will be used:

α: the fractionation factor $\left(\text{for D: } \alpha_D = \frac{p_{H_2O^{16}}}{p_{HDO^{16}}};\ \text{for } O^{18}\text{: } \alpha_{18} = \frac{p_{H_2O^{16}}}{p_{H_2O^{18}}}\right)$.

q_0: the total quantity of material in grams.

q: the quantity of material in the liquid phase.

μ: the molecular weight of the heavy components relative to that of the light one (for HDO: 19/18, for H_2O^{18}: 20/18).

A_w and A_v: the quantities in grams of a heavy component in the liquid and the gaseous phase.

a_w° and a_v°: the initial heavy isotope content (in ppm) in the liquid and the gaseous phase, respectively.

a_w and a_v: the heavy isotope contents of the liquid and the entire gaseous phase at an arbitrary stage of the process.

a'_w and a'_v: the heavy isotope contents of the amounts of liquid and vapour, respectively, resulting from an infinitesimal condensation or evaporation at an arbitrary stage of the process.

t: the temperature in °C.

T: the absolute temperature in ° K.

m: the saturation mixing ratio, i.e. the ratio between the mass of saturated water vapour and the mass of the dry air, with which the water vapour is associated*.

At an arbitrary stage of the evaporation process

$$A_w = \mu q a_w \cdot 10^{-6} \text{ grams.} \tag{14}$$

A further infinitesimal evaporation and removal of the vapour will change this quantity by

$$dA_w = \mu (q\, da_w + a_w\, dq) \cdot 10^{-6},$$

while the change of A_v will be

$$dA_v = -\mu a'_v\, dq \cdot 10^{-6},$$

which is equal to $-dA_w$.

Now, since H_2O^{16} and H_2O^{18} make an ideal solution,

$$a'_v = \frac{a_w}{\alpha}, \tag{15}$$

and we get

$$q da_w = a_w \left(\frac{1}{\alpha} - 1\right) dq. \tag{16}$$

Furthermore, by integration

$$a_w = a_w^\circ F_w^{\frac{1}{\alpha}-1}, \quad F_w = q/q_0. \tag{17}$$

This is Raleigh's formula for the process described, which is often called a Raleigh distillation. a_w increases as shown by the full curves in Fig. 15, when the process proceeds at 0° and 20° C.

Looking at the evaporation from ice the composition of the reservoir will not change due to the fixed localisation of the molecules in the cry-

* The values of m used in this work are taken from Smithsonian Meteorological Tables, 1951. They are corrected for the departure of the air-vapour mixture from the ideal gas laws.

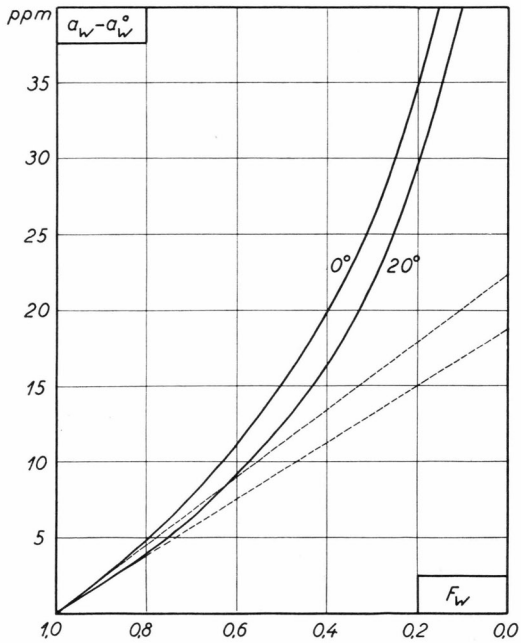

Fig. 15. Enrichment of the remaining fraction, F_W, of a water reservoir during a Raleigh evaporation (full curves) and during an evaporation in a closed two phase system (dashed curves).

stals. In this case $a_w = a'_v = a^\circ_w$ during the whole process. Table 7 shows some illustrative measurements on snow samples collected by A. BAUER at the same location on the Greenland ice cap. The enrichment due to evaporation is significant in the wet snow only.

Table 7.

Sample	Time of collection	Δ a in ppm
B1. Wet snow	59.6.21	−2.3
B2. Wet snow, same as B1	59.6.22	+2.5
B3. Dry snow	59.5.28	−0.5
B4. Dry snow, same as B3	59.5.29	−0.2

The only conceivable possibilities of fractionation of dry snow are direct exchange with the surrounding vapour and recrystalisation via sublimation. On its way from one crystal to another the vapour may be mixed up with the surrounding vapour. In most cases both of these effects are probably negligible.

Returning to evaporation from liquid we get a'_v from (15) and (17):

$$a'_v = \frac{a^\circ_w}{\alpha} F_w^{\frac{1}{\alpha}-1} . \qquad (18)$$

a_v can be obtained from the equation

$$A_v + A_w = \mu q_0 a_w^\circ \cdot 10^{-6}$$

the right side being the initial quantity of heavy component in the liquid. Using (14) and

$$A_v = \mu (q_0 - q)\ a_v \cdot 10^{-6}$$

we get

$$q_0 a_w^\circ = (q_0 - q)\ a_v + q a_w = (q_0 - q)\ a_v + q a_w^\circ F_w^{\frac{1}{\alpha}-1}$$

$$a_v = a_w^\circ \frac{1 - F_w^{\frac{1}{\alpha}}}{1 - F_w}. \tag{19}$$

The dotted lines in Fig. 15 reflect equilibrium processes, in which the vapour is not removed from the system. In such cases

$$a_w - a_w^\circ \to a_w^\circ \cdot \alpha \text{ for } F_w \to 0.$$

3. 2. **Isothermal condensation from a limited amount of vapour.**

Consider the reverse Raleigh process, i.e. isothermal condensation under equilibrium conditions from initially q_0 grams of vapour with a heavy isotope content of a_v° to $q_0 - q$ grams of vapour with heavy isotope content a_v.

The condensate is supposed to be removed from the gaseous phase. The formulae can be derived from (17), (18) and (19) by just changing the indices and using the reciprocal fractionation factor:

$$a_v = a_v^\circ F_v^{\alpha-1};\ F_v = \frac{q_0 - q}{q_0} = 1 - F_w. \tag{20}$$

$$a'_w = \alpha a_v^\circ F_v^{\alpha-1}. \tag{21}$$

$$a_w = a_v^\circ \frac{1 - F_v^\alpha}{1 - F_v} \tag{22}$$

If $a_v^\circ - a_v$ is plotted against F_v the curves will be close to the full curves shown in Fig. 15. Similarly, the dotted curves reflect $a_v^\circ - a_v$ as a function of F_v for a condensation process in a closed two phase system.

The Raleigh evaporation and the Raleigh condensation are not reversible as far as the quantitative isotopic conditions are concerned.

Thus a_w will be very high for the last part of the water in the first process, whereas a_w will be equal to αa_v° for the first small amount of water condensed in the latter process.

3. 3. The α factors.

The α factors, α_D for D and α_{18} for O^{18}, depend upon the temperature. LEWIS and CORNISH (1933) made the first determination of α_{18}.

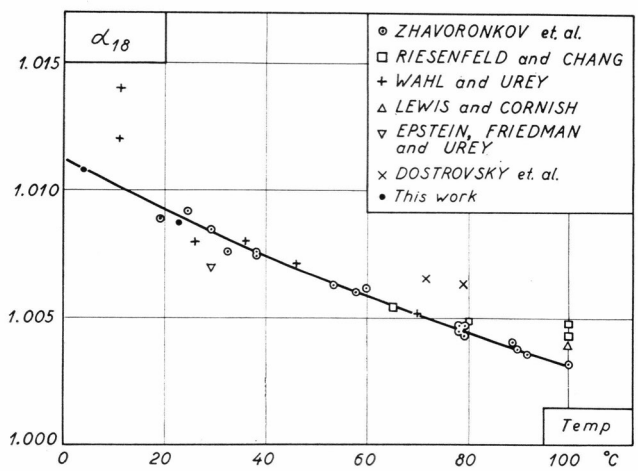

Fig. 16. The fractionation factor, α_{18}, as a function of the temperature. The curve is a graphical representation of Eq. (24).

Later RIESENFELD and CHANG (1936a) computed the following formulae on the basis of their own experiments and those of WAHL and UREY (1935):

$$\alpha_D = 0.86_2 \exp (130/RT), \qquad (23)$$
$$\alpha_{18} = 0.987 \exp (13/RT).$$

Later ZHAVORONKOV, UVAROV and SEVRYGOVA (1955) made an extensive study of α_{18} in the temperature range 15–100° C. Their formula for α_{18} is

$$\alpha_{18} = 0.9822 \exp (15.778/RT) \qquad (24)$$

or

$$\log \alpha_{18} = 3.449 \frac{1}{T} - 0.00781.$$

This correlation is shown graphically in Fig. 16 together with the measuring results of several authors.

The methods used have been equilibrium distillations at low pressures or Raleigh distillations. The trouble with the former one is to prevent

boiling, especially at low temperatures. As to the Raleigh distillation the possibility of non-equilibrium conditions at the liquid surface must be taken into consideration. CRAIG, BOATO and WHITE (1956) have pointed out that in case of violent evaporation the relatively high rate of reaction of H_2O^{16} causes the heavy isotope contents of the vapour to be lower than at equilibrium conditions.

The influence of non-equilibrium is demonstrated in the experiment described in the appendix (p. 96). The resulting α_{18} values are indicated by dots in Fig. 16. They are seen to support the formula of ZHAVORONKOV et al.

3. 4. **Non-isothermal processes.**

The formulae given in sections 3. 1. and 3. 2. are only strictly true for isothermal Raleigh processes because α depends upon the temperature. However, $\alpha_{18} - 1$ as well as $\alpha_D - 1$ vary only $1\,^0/_0$ per centigrade about the freezing point. Below is made a calculation in order to test whether usable approximations to the true values can be obtained for non-isothermal processes by using the same formulae with a constant α equal to its mean value in the temperature range in question.

In the most important formulae, (20) and (21), F_v is replaced by m/m_0:

$$a_v = a_v^\circ \left(\frac{m}{m_0}\right)^{\alpha-1} \tag{25}$$

$$a'_w = \alpha a_v^\circ \left(\frac{m}{m_0}\right)^{\alpha-1}, \tag{26}$$

where m and m_0 are the saturation mixing ratios at t and t_0 °C.

Table 8.

$a_v^\circ - a_v$ in ppm.

1	2	3	4	5	6	7
Process	t_0 °C	t °C	Formula (25)		Numerical integration	
			HDO	H_2O^{18}	HDO	H_2O^{18}
A	20	0	16.0	27.1	16.1	27.2
B	0	−20	22.3	38.3	22.4	38.1
C	0	−20	24.8	42.6	25.0	42.6
D	0	−20	17.7	29.7	17.9	29.7

We now consider some processes with condensation from a limited amount of saturated air due to cooling from t_0 to t °C. Formula (25) gives

$$a_v - a_v^\circ = a_v^\circ \left(\left(\frac{m}{m_0}\right)^{\alpha-1} - 1\right).$$

In Table 8, columns 4 and 5, the results are stated of a calculation of $a_v^\circ - a_v$ for HDO and H_2O^{18} using a constant α in 4 Raleigh condensation processes all starting with $a_{vD}^\circ = 145$ ppm and $a_{v18}^\circ = 1960$ ppm:

A. Isobaric cooling from 20 to 0° C.

B. Isobaric cooling from 0 to – 20° C, the vapour being in equilibrium with a plane surface of pure water.

C. Isobaric cooling from 0 to – 20 °C, the vapour being in equilibrium with a plane surface of pure ice.

D. Moist-adiabatic cooling from 0° C (p = 1000 mb) to – 20° C (p = 703 mb), the vapour being in equilibrium with a plane surface of pure water.

For a more strict evaluation, in which the variation of α is taken into consideration, we must go back to the differential equation (16) valid for the evaporation process. The corresponding equation for the condensation process is

$$q da_v = a_v (\alpha - 1)\, dq.$$

If q is replaced by the mixing ratio, m, i.e. if q is expressed in terms of grams water per kg dry air, we get

$$da_v = a_v \frac{\alpha - 1}{m} \frac{\partial m}{\partial t} dt. \tag{27}$$

Using the formulae (23) and (24) for α, a numerical integration in steps of 1° C gives the values of $a_v^\circ - a_v$ put down in columns 6 and 7 of Table 8. They are seen to be in good agreement with those calculated with constant α. Below formula (25) will be used in this way.

As to the fractionation of the condensate formula (26) cannot be used with constant factor α. However, changes in a_w' can be found with the same approximation as changes in a_v by using

$$a_w'(t) - a_w'(t_0) = \alpha(t)\, a_v - \alpha(t_0)\, a_v^\circ \tag{28}$$

and introducing (25) for a_v.

Figs. 17 and 18 show how a_w' decreases in the processes A–D as the condensation proceeds. The two vertical, dashed lines between the curves B and C in Fig. 18 refer to two isobaric processes starting at 0° C with the vapour in equilibrium with water (i.e. following curve B). When the temperature has reached – 10° (point b_1), respectively – 20° (point b_2), the vapour is supposed to turn to equilibrium with ice. This turn over causes a decrease of the vapour pressure, and the resulting

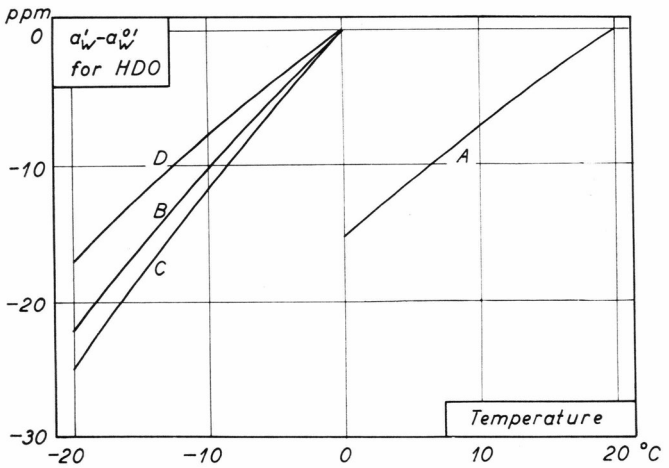

Fig. 17.

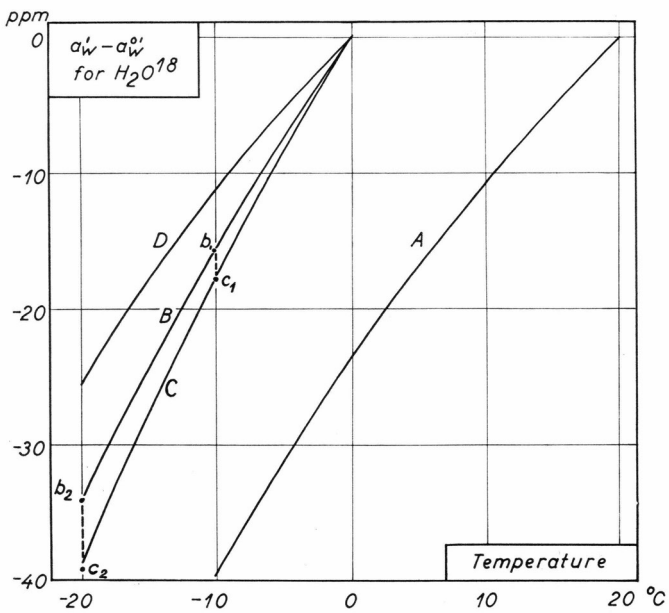

Fig. 18.

Deuterium and O^{18} enrichment of infinitesimal amounts of water condensed from a limited vapour reservoir in 4 cooling processes described in the text. The basis values for the enrichments are the heavy isotope contents, $a^{\circ\prime}_w$, of the first small amount of condensate.

condensation reduces a_v to such a degree that further condensation due to cooling makes a'_w change from the values indicated by the point c_1, respectively c_2, and follow curves very close to C. Therefore, in cases of equilibrium with ice, curves like C (if isobaric cooling) reflect the frac-

tionation no matter at which stage of the cooling the equilibrium turn over occurred.

In nature the precipitation from a cloud in equilibrium with water must be expected to be fractionated in accordance with curves like A, B or D, if no addition of new vapour occurs, and if the condensate leaves the cloud just after formation. In case the latter condition is not fullfilled, the observed fractionation will be less than calculated.

The transition of a cloud from equilibrium with water to equilibrium with ice hardly affects the isotopic composition of the precipitation to any observable degree; firstly, because the equilibrium turn over does not occur momentarily; secondly, because the condensate hardly leaves the cloud at the very moment of formation and, thirdly, because other more or less casual fractionating processes blur the picture.

The curves in Figs. 17 and 18 depend to some degree upon the initial values a°_{v18} and a°_{vD}. The chosen values are, however, typical for maritime air masses, which play an overwhelming role in the natural water cycle.

3. 5. Relative fractionation HDO – H_2O^{18}.

In Table 9 the slopes of the curves A to D in Figs. 17 and 18 are stated for the two limiting temperatures of the ranges. The ratio between the slopes, da'_{w18}/da'_{wD}, is seen in column 5. In all cases it is approximately 1.55, increasing with decreasing temperature. In the last column,

Table 9.

1	2	3	4	5	6
Process	t °C	$\frac{da'_w}{dt}$ in $\frac{ppm}{°C}$		$\frac{da'_{w18}}{da'_{wD}}$	$\frac{a'_{w18}-a^{0'}_{w18}}{a_{wD}-a^{0'}_{wD}}$
		HDO	H_2O^{18}		
A	20	0.66	0.98	1.48	1.48
	0	0.89	1.41	1.58	1.54
B	0	0.97	1.44	1.48	1.48
	−20	1.24	2.01	1.62	1.54
C	0	1.10	1.64	1.49	1.49
	−20	1.37	2.27	1.66	1.53
D	0	0.67	1.02	1.50	1.50
	−20	1.03	1.62	1.57	1.53

the ratio is stated between the enrichments in O^{18} and deuterium relative to the first small amount of water condensed from the vapour.

FRIEDMAN (1953) reports a linear correlation between his deuterium measurements and EPSTEIN and MAYEDA's O^{18} measurements on natural waters (1953). It appears from FRIEDMAN's data that the ratio between deviations of the δ-values (both in $^0/_0$) for O^{18} and deuterium is 0.124 ± 0.05. Multiplying this by the ratio between the absolute values of the standards (2074 ppm for the PDB (p. 38) and 148 ppm for the deuterium standard according to FRIEDMAN) gives

$$1.74 \pm 0.06 \text{ ppm } O^{18}/\text{ppm D},$$

which is high compared with Table 9, column 5. This may be due to 148 ppm being too low for FRIEDMAN's deuterium standard.

Recently DANSGAARD, NIEF and ROTH (1959) have measured the isotopic composition of a series of ice samples from a West Greenland iceberg. They find (cf. Fig. 30, p. 78)

$$1.53 \pm 0.08 \text{ ppm } O^{18}/\text{ppm D}$$

in good agreement with Table 9.

CRAIG, BOATO and WHITE (1956) mention a study of several hundred fresh water samples. The O^{18} concentration varied about $4^0/_0$, while the deuterium varied $30\ ^0/_0$. The linear correlation was reported to be good, but no details were given. However, as an interesting exception they found in acid hot spring waters less deuterium enrichment than O^{18} enrichment relative to the local surface water. They explain this as a result of a non-equilibrium distillation. A kinetic effect contributing to the fractionation will concentrate H_2O^{18} in the liquid to a higher degree than the lighter HDO.

4. HEAVY ISOTOPES IN NATURAL WATERS

As mentioned on p. 10, great efforts have been made for thirty years in order to map out and explain the distribution of the heavy stable isotopes in the water cycle in nature. KIMBALL (1949) has given a complete summary of the literature up to 1949 dealing with deuterium, and KIRSHENBAUM (1951) and INGERSON (1953) have reviewed the literature on the natural occurences of the hydrogen and the oxygen isotopes. Most work up to 1950 on determining heavy isotopes in water was based upon the density method. It is extremely difficult to obtain sufficient accuracy ($\pm 2 \cdot 10^{-7}$ g/cm^3) for measuring the small variations in question. The mere purification of the water without altering its isotopic composition is a painstaking problem. Only after the application of the mass spectrometer the results became sufficiently consistent.

4. 1. **Ocean water.**

GILFILLAN (1934) first demonstrated excess density of sea water over fresh water. The most extensive isotopic study of ocean water is that of EPSTEIN and MAYEDA (1953) covering 93 marine and 7 fresh water samples. Surface water shows to be a little enriched in O^{18} due to evaporation, whereas the deep water samples are a little depleted in O^{18} due to the polar bottom currents, the water of which has been mixed up with isotopically light fresh water from the ice fields. In ocean water which has not been directly contaminated with fresh water the O^{18} content varies only $\pm$ 1 ppm from the mean.

At the same time FRIEDMAN (1953) reported deuterium measurements on many of the same samples. As expected the same pattern showed up as for O^{18}. FRIEDMAN claimed the deuterium enrichments to be related to the O^{18} enrichments as the ratio between the vapour pressures of HDO and H_2O^{18} at 30° to 40° C.

For evident reasons, a possible gravitational fractionation should be looked for in stagnant water at great depths. Under such circumstances, sedimentation of the heavy components of water due to gravity should result in an exponential increase in heavy isotope content down-

wards, analogous to the situation for the components in the atmosphere (HAGELBERGER et al., 1951) and in solutions. DANSGAARD (1960) compared a group of samples from approx. 10,000 m depth in the Philipine Trench with another group of samples from 4000 m depth. No significant difference was observed in O^{18} within ± 0.2 ppm in spite of the fact that a difference of 100 ppm should be expected in case of equilibrium. On the other hand, the establishment of equilibrium was estimated to take a period of the order of magnitude of 10^8 years judging from FÜRTH's investigation of a similar problem (1938).

The result shows that the water masses in the Philipine Trench are not stagnant. Other investigators have drawn this same conclusion on the basis of measurements of other parameters.

The mean value of Δa for the ocean samples was 39.1 ppm.

4. 2. **Fresh water.**

Already in the thirties it was evident that the isotopic composition of fresh waters covered a much wider range than that of ocean waters.

FRIEDMAN (1953) measured the deuterium content in 19 North American rivers. Those draining the coastal regions (and especially the Southern ones) and the Mid West areas showed to be relatively high in deuterium due to the direct supply of water from maritime air masses and, probably for several rivers, considerable degree of evaporation. However, the rivers draining the Eastern slope of the Rocky Mountains are relatively poor in deuterium, because the water is partly derived from Pacific Ocean moisture, which has lost much of its heavy components in a Raleigh condensation during its passage over the mountains (KIRSHENBAUM, 1951).

DANSGAARD (1954) reported an investigation of 70 fresh water samples collected in climates ranging from tropical rainy climates to polar frost climate. In order to reduce errors due to casual evaporation the samples were collected from large reservoirs in which the water is continuously being replaced. Tap water was used in towns with ground water supply. In nature, river water was preferred to lake water, though river water is not ideal either (p. 56). Casual precipitation was not taken as representative for the local fresh water. The findings are grouped in Table 10, where the average values, $\Delta \bar{a}$, of the O^{18} occurrences are listed together with the lowest (Δa_{min}) and the highest (Δa_{max}) value within the various climatic types (the climatic classification is that given by KÖPPEN (1936)).

In the climates with a hot or dry season the composition of the fresh water depends on local conditions and on the season. However,

Table 10.

O^{18} content of ocean water and fresh waters.

		Number of samples	Δ ā ppm	Δa_{min} ppm	Δa_{max} ppm
Ocean water			39.1		
Fresh waters					
A	*Tropical rainy climates*	16	25	21	32
C	*Warm temperate rainy climates*				
Cwa	winter dry, summer hot	12	29	25	32
Cfa	no dry season, summer hot	4	34	28.5	42.5
Csa	summer dry and hot	4	26	25	26.5
Cfb	no dry season, summer warm	9	20.5	15.5	25
D	*Cool snow forest climate*				
Dfc	summer cool	1	16		
E	*Polar climates*				
ET	tundra climates*	6	8	5	10
EF	frost climate**	11	−18	−34.4	−6.2

* In excess of the 5 measurements reported in the 1954 paper the Upernavik sample referred to on p. 58 has been taken into consideration.

** The samples reported in the 1954 paper and averaging − 17 ppm were possibly not representative. This figure has here been replaced by the mean values of 11 icebergs given in Table VIII, column 6, p. 106.

from the climatic type Cfb and toward colder climates there is a general decrease in the O^{18} content of the fresh water. This corresponds with the model of the water cycle in nature given by EPSTEIN and MAYEDA (1953) who compared "the existing evaporation and condensation with that occurring in a several stage distillation column, where the amount of liquid in the reservoir flask is large compared to the liquid in the column. In order that several stage fractional distillations be accomplished, both evaporation and condensation (i.e., refluxing) must take place in the column. If condensate does not return to the reservoir flask, the resulting product will be of the same composition as the initial vapour that comes off the surface of the liquid in the flask (a single stage distillation). On the other hand, if the reservoir liquid both evaporates and receives back liquid condensed in the column, the composition of this condensate will be deficient in more volatile material relative to the initial vapour that came off the surface of the reservoir liquid and the remaining vapour will be more volatile. Continuous evaporation and condensation provides a mechanism for removing a fraction from the liquid reservoir that is more volatile than would be expected from a single evaporation step,

provided that the resulting distillation product is removed from the evaporation-condensation system."

DANSGAARD (1953) considered a simplified model of the water cycle consisting of mainly 3 processes:

1. Evaporation from a large reservoir (the oceans).
2. Cooling of the vapour, which causes condensation by processes like those called A, B, C, or D on p. 46.
3. Returning of the remaining vapour to the reservoir under (or with subsequent) heating.

Also, in a system like this, it would be possible to remove from the reservoir a fraction of liquid which is more volatile than the condensate in a simple single stage distillation, namely by reflux of the first part of the condensate and freezing of the last and most volatile part.

The vapour will be deficient in less volatile material relative to the first vapour given off from the surface. Speaking in the terms connected with the isotopic problem of the natural water cycle: Imagine we start with absolutely dry air, which takes up moisture from the ocean during process 1. After the cooling in process 2 the air still contains some (isotopically light) vapour. This is mixed up with ocean vapour during the following process 1 the mixture being poorer in O^{18} than after the first process 1. Each circulation causes further depletion until a state of equilibrium is reached with heavy isotope contents sufficiently low for the amount of heavy components given off in process 2 to be equal to that taken up in process 1.

The use of the EPSTEIN and MAYEDA model would undoubtedly be correct, but also difficult, for a calculation of the influences of the contributory processes determining the observed isotope distribution in the water cycle. One of the limitations of the simplified model is its neglecting the re-evaporation from the column. Nevertheless, the simple mechanism of Raleigh processes explains the actual findings rather well, as shown p. 62.

4. 3. **Atmospheric water vapour.**

The depletion in O^{18} in atmospheric vapour relative to vapour originating from a single evaporation was demonstrated (DANSGAARD, 1953b, 1954) by measurements on atmospheric vapour collected in Copenhagen in a freezing trap during 3 or 4 days periods from 1953, May 23, to 1954, May 21. The results are plotted in the lower section of Fig. 19. The mean of the year was $\Delta a = 4.7$ ppm compared with 21 ppm for pure ocean vapour.

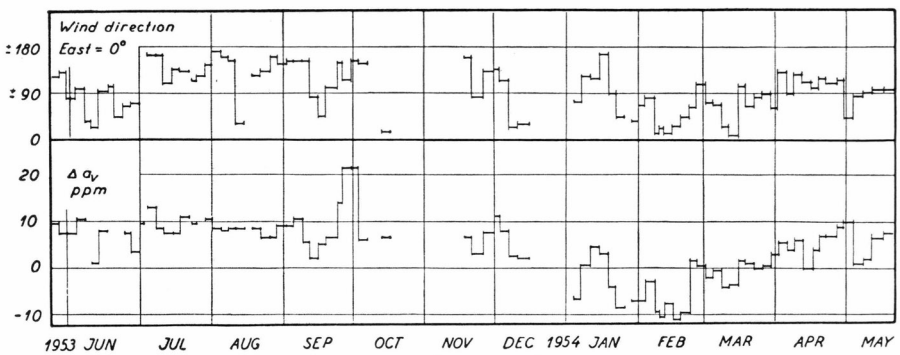

Fig. 19. Variation of the O^{18} content of atmospheric water vapour in Copenhagen, and its relation to the wind direction.

In spite of the fact that the weather in Denmark is governed mainly by maritime air masses, high values, such as 21 ppm (corresponding to equilibrium with ocean water), were found only in two periods about Oct. 1. As the weather conditions in the same periods were not unusual in other respects, the two high values may be erroneous (incomplete cooling of the trap?).

The deviation of the average wind direction from the East is shown in the upper part of Fig. 19. The correlation between the two curves just indicates that easterly winds in Denmark to a higher degree than westerly winds contain fresh water vapour or vapour which has been depleted in O^{18} by precipitative processes. Easterly winds occurred relatively frequently during the winter 1954; this is a contributory reason why the O^{18} content of the winter samples were relatively low. However, there is also indication for a seasonal variation of the O^{18} content due to other reasons; the samples from the period Jan. to Mar. are generally even lower in O^{18} than samples from outside this period collected in mainly easterly winds.

It is hardly possible to reach a more detailed interpretation of the individual observations, because the O^{18} content of atmospheric water vapour at a given location depends upon factors such as

a. the origin of the vapour,
b. the number and intensity of evaporation and condensation processes in the period before the arrival of the air mass to the location in question, and
c. the temperatures at which these processes take place.

4. 4. Precipitation.

The isopotic composition of precipitation depends upon

A. that of the precipitating vapour at the beginning of the condensation (a_v^0, p. 43),
B. the present mixing ratio in the air relative to its initial value (F_v, p. 43),
C. the degree of evaporation from the precipitation until it reaches the ground,
D. the degree to which the re-evaporated material re-enters the precipitating air mass and
E. the temperatures at which the evaporation and condensation processes take place.

The mean Δa for all precipitation released at a given locality gives some indication as to which stage of the natural water cycle the locality is to be traced. It is a tempting task to use the isotope data from numerous localities in order to put up a generally valid model for the water cycle in nature. The EPSTEIN and MAYEDA model probably constitutes the best qualitative approach, but as to the quantitative conditions hardly any simple model involves a solution of general validity.

4. 4. 1. Sampling technique.

When looking for possible correlations the technique for sampling of precipitation is very important. Firstly, seasonal variation of the heavy isotope contents should be taken into consideration (4. 4. 5.). Secondly, it should be noted that the isotopic composition of the individual rains or snows varies widely within the same season due to the complex dependability upon the many parameters mentioned above. Thus, in the winter 1954–55 the following values were obtained for Δa of the precipitation in Chicago: Late Nov. + 8, late Dec. + 24, late Jan. + 7, late Feb. + 31, late Mar. + 9 ppm (DANSGAARD, 1958).

Unless it is the aim to investigate the individual rains or snows, the samples should, therefore, represent the total amount of precipitation within wider periods of time adapted to the problem under investigation. Thus, if the total amounts of precipitation at various localities are to be compared, the samples should represent the precipitation for a whole number of years.

Due to evaporation, lake water has not the same composition as precipitation. The water in a lake at Ikerasak, Umanak District, Greenland, has $\Delta a = 21.4$ ppm, whereas the mean Δa for the precipitation in this region is approximately 5 ppm. CRAIG, MAYEDA and SUESS

(1958) have reported an enrichment of the same order for the water in Lake Neusiedler at Wien.

Disregarding possible enrichment due to evaporation, river water is representative for the precipitation in the area of drainage rather than for the precipitation at the place of collection.

Ground water seems better suited for representing the precipitation, although it is not ideal either. In Copenhagen the weighted mean of Δa for the precipitation during 3 years was 19.8 ppm, which is to be compared with the Δa values for Copenhagen tap (ground) water given in Table 11.

Table 11.

Δa for Copenhagen tap water (ppm).

	Measurement No.		Mean
	1	2	
Tapped 1955 June	21.9	21.7	21.8
— 1959 Oct.....	22.4	22.3	22.4
— 1959 Dec.	22.0	22.5	22.2
— 1960 Feb.	21.7	22.0	21.8
— 1960 Mar.	21.9	22.0	22.0
— 1960 May	22.1	21.7	21.9
			Mean: 22.0

It is worth noting that the tap water is subjected to only little isotopic seasonal variation, if any. Copenhagen tap water is only 2 ppm higher in O^{18} than the precipitation, which is interesting the more so as approximately 60% of the precipitation in Denmark re-evaporates. An evaporation of this order from a well stirred reservoir would cause an enrichment of the residue of some 11 to 20 ppm (cf. Fig. 15, p. 42). The fact that no considerable enrichment arises may be because most evaporation takes place from small reservoirs, which are not continuously blended with the main reservoir, e.g. complete drying up of puddles and complete evaporation of the water which reaches the surfaces of plants.

As a conclusion, it may be stated that precipitation collected during a long period of time should be preferred. In regions without severe evaporation ground water may serve as a sufficient substitute, whereas river water and, particularly, lake water should not be considered as representative for the precipitation.

4. 4. 2. **Geographical distribution of the isotopes and its relation to the air temperature.**

Table 10 reflects to some degree a correlation between the O^{18} content of fresh water and the air temperature as far as the cool and cold

climates are concerned. For the reasons mentioned above, however, a closer relation is to be expected between the annual means of the O^{18} content of the precipitation and the air temperature.

The problem now arises: What kind of mean values should be chosen? In the discussion given below $\Delta\underline{\bar{a}}_p$ denotes the mean of the O^{18} content of the precipitation fallen within the period of time τ, and weighted in accordance with the relative amounts given off by the individual storms, i.e.

$$\Delta\underline{\bar{a}}_p(\tau) = \frac{1}{Q}\int_0^Q \Delta a_p dQ,$$

where Δa_p is the O^{18} content of the infinitesimal amount of precipitation dQ, and Q is the total amount within a wide period of time, τ. Similarly, the weighted mean of the condensation temperature is defined as

$$\underline{\bar{t}}_c = \frac{1}{Q}\int_0^Q t_c dQ,$$

where t_c is the temperature at which dQ condenses. Furthermore, the following symbols will be used

t_a: the mean annual air temperature 2 m above ground level.

$\Delta\bar{a}_p$: the annual unweighted mean of the Δa values of the monthly amounts of precipitation or, in other words, the unweighted mean of the $\Delta\underline{\bar{a}}_p$ (τ = 1 month) values within a whole number of years.

Plotting of $\Delta\underline{\bar{a}}_p$ (year) against $\underline{\bar{t}}_c$ (year) for the various stations seems, a priori, to involve the best possibility for obtaining a correlation between the isotope distribution and a climatic parameter. However, $\underline{\bar{t}}_c$ is neither known for the ice cap stations referred to below, nor can it be deducted with sufficient accuracy for many of the coast stations, from which precipitation has been collected. A fact obtained by the ice cap stations is the temperature 10 m below the snow surface, where the temperature variations are supposed to be negligible (± 0.3°C, Benson, 1960). This temperature, t′, is for most of the ice cap equal to t_a*, for which reason t_a was chosen as the climatic parameter.

As to the possible isotopic parameters the unweighted $\Delta\bar{a}_p$ corresponds best to the unweighted t_a. $\Delta\bar{a}_p$ has, therefore, been chosen for the coast stations. It should be noted that the sampling technique used on the ice cap stations (random collection of snow from various depths

* t′ is close to t_a in regions with little or no melting (Koch and Wegener, 1930). However, in regions with considerable melting, e.g. caused by radiation, the seeping melt water may add heat to lower strata and, thus, make t′ higher than t_a.

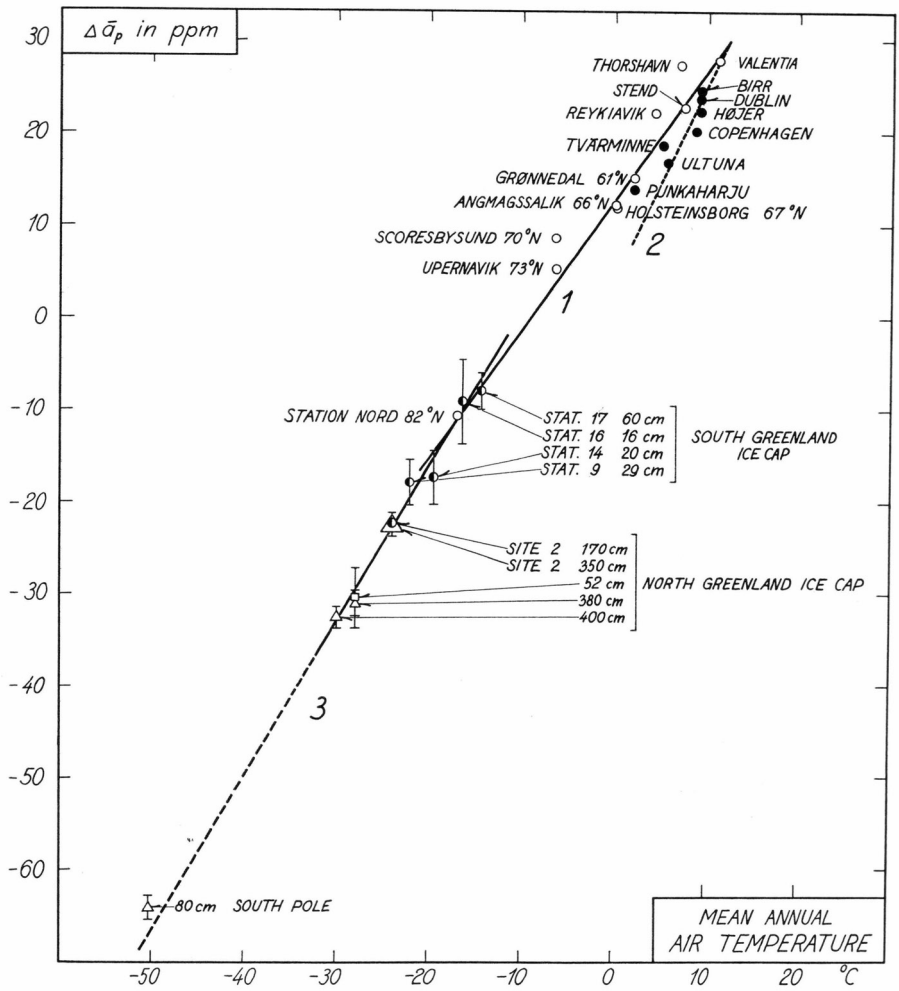

Fig. 20. Correlation between the annual means of the air temperature and the O^{18} content of the precipitation. The symbols are explained in the text p. 59.

The samples from Stend, (West Norway), Reykjavik (Iceland) and Ultuna (East Sweden) were supplied by the International Meteorological Institute, Stockholm, and Statens Lantbrukshögskola, Ultuna, Sweden; those from Valentia (West Ireland), Birr (Mid Ireland) and Dublin (East Ireland) by Meteorological Institute, Dublin; those from Tvärminne (South-west Finland) and Punkaharju (East Finland) by Havforskningsinstituttet, Helsinki; those from the Greenland coast stations Grønnedal, Angmagssalik, Holsteinborg, Scoresbysund and Station Nord by the Danish Forsvarets Forskningsråd and Radiofysisk Laboratorium, Copenhagen; those from Højer (East Denmark) by Statens Planteavlslaboratorium, Lyngby, while those from Upernavik and Copenhagen were collected by the present author. All the ice cap samples were collected by U.S. Snow, Ice and Permafrost Research Establishment (S.I.P.R.E.).

The 4 stations indicated by triangles were measured by EPSTEIN and BENSON (1959), and the square refers to a station measured by KULP et al. (1957).

at each location, or collection of a sample representing a thick layer of snow) rather leads to an isotopic composition corresponding to the weighted $\Delta \bar{a}_p$. Nevertheless, this parameter has been used as a representative for the ice cap stations for comparison with $\Delta \bar{a}_p$ for the other stations.

Fig. 20 shows the correlation between $\Delta \bar{a}_p$ and t_a. The stations are put into 3 groups:

1. 10 stations at sea-level and close to the ocean in the North Atlantic region are indicated by open dots.
2. 7 low altitude stations with more or less continental climate are indicated by filled dots.
3. 9 stations on the Greenland ice cap and 1 on the South Pole are indicated by half filled dots, triangles or by a square

Ad 1 and 2. The Upernavik sample was collected late July, 1958, from seeping water from moist soil. The $\Delta \bar{a}_p$ values for the other 16 stations in groups 1 and 2 are based on samples of monthly precipitation. The individual measurements are listed on Tables II, III and IV in the appendix (p. 99–101). For a given station the $\Delta \bar{a}_p$ was calculated as the unweighted mean of the Δa for the precipitation in each of the 12 months of the year. Each of these 12 monthly values were, in turn, calculated as the unweighted mean of the values of the available samples representing the month in question within different years, e.g. from Station Nord two April samples were available with the O^{18} contents -3.2 ppm for April 1958 and -9.5 ppm for April 1959. Thus, -6.4 ppm was used for April in forming the annual mean. On the other hand, no May samples were available from this same station. Therefore, May was represented by the mean of the values for the adjoining months (-6.4 ppm for April and -3.3 ppm for June).

Ad 3. The precipitation at each ice cap station was represented by a number of snow samples collected at different depths under the snow surface. The sum of the thickness of the snow layers involved is indicated in cm in Fig. 20.

In Table VI in the appendix some details are given on the 4 South Greenland ice cap stations indicated in Fig. 20 by half filled dots.

The Site 2 sample was part of a boring core, collected some 100 m below the snow surface. The mean annual air temperature, t′, at the South Greenland ice cap stations were measure by S.I.P.R.E. 10 m below the snow surface. For the North Greenland ice cap stations t′ was found from Fig. 29, p. 79, showing the temperature distribution on the ice cap (DIAMOND, 1958). t_a on the South Pole was taken from the S.C.A.R. Bull. No. 2 (1959).

Discussion on Fig. 20.

Apparantly the two parameters, $\Delta \bar{a}_p$ and t_a are related to each other in a rather simple way.

In the upper part of the figure, the 8 coast stations (except for Scoresbysund) on the border of the continent are very close to the full, heavy line, denoted by 1 (slope 1.33 ppm/° C). All the more or less continental stations in group 2 (filled dots) are below the line and the two Atlantic island stations, Thorshavn on the Faroes and Reykjavik in Iceland, are above the line.

The dashed line, denoted by 2 (slope 2.2 ppm/° C), indicates the isotopic variation with the temperature along the East and Northeast going path from Valentia, over Birr, Dublin, Højer and Copenhagen to Ultuna. This is roughly the track followed by most precipitative air in South and Mid Scandinavia.

The slopes of the lines 1 and 2 (1.33 and 2.2 ppm/° C) mainly reflect the H_2O^{18} depletion in the vapour in warm, moist maritime air masses, which on their way to either colder parts of the ocean (full line) or over the continent (dashed line) precipitate and at the same time exchange vapour with or take up new vapour from surface water. Ocean vapour is richer in O^{18} than vapour from fresh or brackish water, which is a contributory reason for the difference between the slopes of the lines. However, the temperature and the amounts of vapour taken up are also factors of importance. The values for the Finnish stations, Tvärminne and Punkaharju, are relatively high in spite of the fact that these stations are on the prolongation of the semi-continental path described above. The reason may be that the air takes up considerable amounts of new vapour when passing the Baltic sea. Another possible reason is that Finland gets a considerable amount of precipitation from North-West, i.e. from colder parts of the ocean.

The high values for Thorshavn and Reykjavik may be explained by these stations being far from extended areas with fresh water.

The systematism does not include sea-level stations with high mountains as a rain-shadow. This stands out clearly when comparing the Greenland stations Holsteinborg and Søndre Strømfjord (Table III (appendix), columns 2 and 3). These stations are both at sea level, are only 150 km apart and they have approximately the same mean annual temperature; however, they are separated from each other by high mountains. The means of Δa for the 6 monthly samples measured for both stations are 13.3 ppm for the coast station Holsteinborg and -0.1 ppm for Sdr. Strømfjord. It may serve as an explanation that when a moist air mass passes the mountains the foehn effect causes an increase in temperature at the same time as the H_2O^{18} content decreases due to loss of moisture on the upglide.

In Fig. 20 the Greenland ice cap stations apparently follow another line (No. 3) with the slope 1.70 ppm/° C. The ice cap precipitation is released under other conditions than that at the coastal stations. Firstly, the latter is released at approximately the same pressure, whereas the ice cap precipitation is partly due to lifting of air masses causing less fractionation per centigrade than isobaric cooling (cp. processes B an D, Fig. 18). Secondly, most of the year maritime air takes up new vapour from liquid water with approximately constant composition along the coast, whereas the air on the ice cap takes up new vapour, which is the poorer in O^{18} the higher the altitude of the locality in question. Thirdly, the latter evaporation is attached with fractionation determined by the ratio between the vapour pressures of the isotopic components, whereas little or no fractionation occurs by the evaporation of dry snow on the ice cap.

Any attempt to evaluate a theoretical explanation of the simple correlation between $\Delta \bar{a}_p$ and t_a is limited by the lack of knowledge as to the origin of the precipitative vapour, the influence of re-evaporated water or ice etc. (cf. pp. 54–55). However, it is worth noting that the simple Raleigh condensation curve for an isobaric cooling (curve A, Fig. 18) constitutes a fairly good approximation under the simple assumptions given below:

1. The condensation process starts with pure, saturated vapour in equilibrium with ocean water at 20°. The first small amount of precipitation given off will then have the same isotopic composition as the ocean water ($\Delta a = 39.1$ ppm).
2. The further condensation goes on under the conditions for a Raleigh process, i.e. immediate removal of the liquid phase and no supply of re-evaporated material.

In Fig. 21 the European and the Greenland stations have been transferred from Fig. 20 together with the corresponding part of the full, heavy line. The thin curve is curve A from Fig. 18 adjusted so that the first amount of water condensed at 20° C has $\Delta a = 39.1$ ppm. The same degree of approximation could be obtained by assuming the condensation to start at somewhat lower temperature and with an isotopically lighter mixture of ocean vapour and vapour left in the air mass from the preceeding cyclus.

At the lower temperatures the slope of the curve is considerably higher than that of the line. However, it should be born in mind that most of the stations defining the line in this region are high altitude stations, at which the precipitation is released partly by moist adiabatic processes like D (Fig. 18). If process A (full thin curve) is supposed to

change into moist adiabatic cooling at 0° C, respectively −10° C, the dashed curves in Fig. 21 show two possible fractionating processes on the Greenland ice cap. The consistency between the measured data and the simple Raleigh curves is surprisingly good considering the fact that re-evaporation from fresh water has been neglected. One reason may be

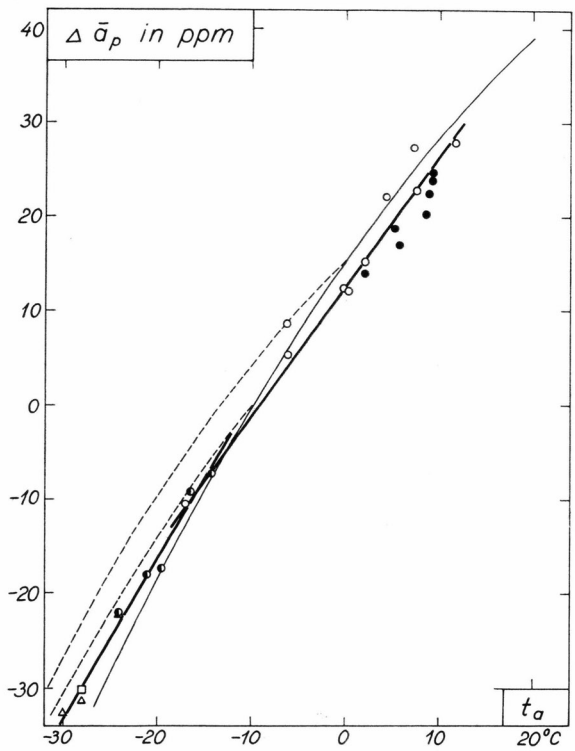

Fig. 21. The regularity in Fig. 20 shown as an approximation to Raleigh condensation processes. The full, thin curve is A from Fig. 18 (isobaric cooling). The dashed curves reflect the fractionation by adiabatic cooling (D from Fig. 18).

that only little of the re-evaporated material re-enters precipitating clouds, at least in the regions irvestigated here.

The correlation given by line 1 is expressed by the equation:

$$\Delta \bar{a}_p = 1.33\, t_a + 12.7 \text{ ppm}$$

valid for ocean coast stations at sea level and on the border of the continent in temperate and arctic climates. When using the δ function and the O^{18} content of ocean water as a reference value the correlation becomes

$$\delta \text{ (annual precipitation)} = 0.64_1\, t_a - 12.7 \text{ per mille.}$$

The corresponding expressions for line 3 are

$$\Delta \underline{\bar{a}}_p = 1.70\, t_a + 17.6 \text{ ppm},$$

$$\delta \text{ (annual precipitation)} = 0.82_0\, t_a - 10.4 \text{ per mille}.$$

The formulae for determination of t_a (or rather t′, cp. footnote on p. 57) on the basis of the measured O^{18} content of a representative snow or ice sample from the accumulation zone of the Greenland ice cap thus appear as

$$\left.\begin{aligned} t' &= 0.58_8\, \Delta \underline{\bar{a}}_p - 10.4\ ^\circ C \\ \text{or} \\ t' &= 1.22\, \delta \text{ (annual precipitation)} + 12.7\ ^\circ C. \end{aligned}\right\} \quad (29)$$

Recently, Picciotto, de Maere and Friedman (1960) have published measurements on precipitation from individual storms on the King Baudouin Base in the Antarctic showing the following correlation between the O^{18} content and the estimated condensation temperature, t, in the precipitating cloud:

$$t = 1.1\, \delta + 7.1\ ^\circ C. \quad (30)$$

In spite of the parameters not being entirely the same as those used in the present work, it is interesting that the isotopic temperature effect appears to be nearly the same (cp. the coefficients to δ in Eqs. (29) and (30)).

The mean deviation from line No. 3 of the 9 Greenland ice cap measurements (Fig. 20) is only 0.5°C. This regularity provides a method for determining the sites of formation of the icebergs emitted from West Greenland glaciers (Dansgaard, 1958). The details of an investigation of this kind will be given in section 5. 5. p. 84.

4. 4. 3. **Altitude effect.**

Considerable fractionation takes place when precipitation is given off under orographic conditions. Process D (p. 46, moist-adiabatic cooling) is an ideal case with immediate removal of the condensate and neither re-evaporation nor supply of heat. As to the O^{18} depletion, Table 9, column 4, shows a mean slope of curve D of 1.3 ppm/° C from 0° to −20° C. This gives an "ideal" altitude effect of −0.9 ppm/100 m using a lapse rate of −0.7°C per 100 m increasing altitude.

This effect accounts for the H_2O^{18} content in high altitude glaciers being very low (Dansgaard, 1953b). Epstein and Sharp (1959) reported the altitude effect in North Greenland to be −1.8 per mille/1000 ft., corresponding to −1.2 ppm/100 m. No further data were given.

If the slope of the line 3 (1.70 ppm/° C) is multiplied by the mean annual lapse rate in Greenland, −0.74° C/100 m (DIAMOND, 1958), the isotopic altitude effect

$$-1.26 \text{ ppm}/100 \text{ m}$$

is obtained in good agreement with EPSTEIN and SHARP's value.

In the mid section of Fig. 22, p. 65, a comparison is made between the Δa values for monthly precipitation (cf. p. 65) at the coast station Stend (near Bergen, Norway) and the mountain station Fanaråken (altitude 2100 m, 200 km NE of Stend). The altitude effect is evident but less than in Greenland. The difference between the mean annual temperatures for the two stations is 13.6° C, but the difference in O^{18} only 9.2 ppm judged from the 14 months in which samples are available from both stations (Table IV in the appendix, columns 3 and 4). This corresponds to a temperature effect of 0.7 ppm/° C, i.e. much less than the slopes of the lines in Fig. 20. Similarly the altitude effect is only −0.4 ppm/° 100 m. A possible reason may be found in the fact that the thickness of a precipitating cloud is much greater on the Norwegian West coast than in the Arctic. This causes the average lifting of a precipitating cloud in Norway to be relatively low, because only the bottom layers of the cloud are lifted corresponding to the elevation of the ground while the layers in 5 km height are hardly lifted at all. If this explanation is accepted, one should not expect always to find the same altitude effect in a given region by investigation of individual orographic rains. The variations of the height of the clouds will be reflected by varying altitude effect.

4. 4. 4. **Latitude effect in West Greenland.**

If the slope of line 1 in Fig. 20 (1.33 ppm/° C) is multiplied by the mean temperature gradient along the West Greenland coast (−0.70° C per degree latitude, cp. Fig. 29) one arrives at the isotopic latitude effect

$$-0.93 \text{ ppm}/^\circ \text{ lat.}$$

The H_2O^{18} contents of West Greenland icebergs also reflect a latitude effect of this order (cf. p. 94).

4. 4. 5. **Seasonal variation.**

RIESENFELD and CHANG's density measurements (1936b) first indicated winter precipitation to be isotopically lighter than summer precipitation. This was later shown to be true when speaking of total amounts of precipitation from extended periods within the season. As

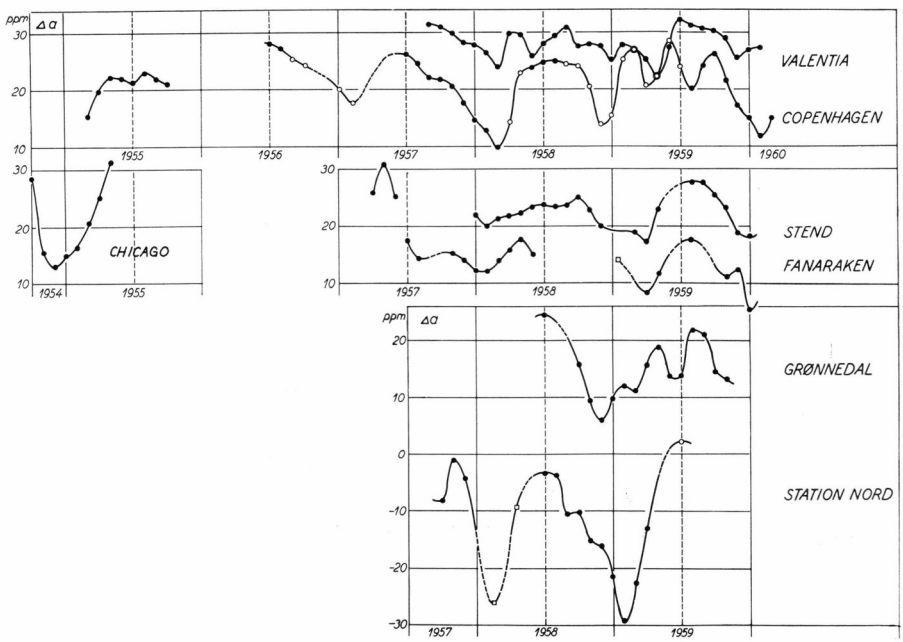

Fig. 22. Variation of the O^{18} content of the precipitation at 7 stations.

pointed out on page 55, however, the isotopic composition of the individual rains and snows varies widely within the same season, depending upon the pre-history of the precipitating vapour. In 1956, EPSTEIN reported winter snow falling on glaciers to be lighter in O^{18} than summer snow. O^{18} variations in ice were later used for glaciological studies (EPSTEIN and SHARP, 1959, EPSTEIN and BENSON, 1959).

The investigation of precipitation in Copenhagen gave no indication for a seasonal variation until a systematic collection of all precipitation was started in Feb., 1955. Unfortunately, the samples from two long periods in 1955–56 and in 1957 were spoiled by evaporation.

In Tables II, III and IV in the appendix the individual measurements are stated for a number of stations. For some of these stations the unweighted means of two months are plotted as dots in Fig. 22. Open circles are used in cases where the samples do not represent two calender months. Squares refer to precipitation in one month only.

The O^{18} content of the precipitation is seen to vary seasonally. As is the case for the air temperature, the O^{18} variations are relatively small (5–10 ppm) for stations with maritime climates like Valentia, Reykjavik and Thorshavn; somewhat higher (10–20 ppm) for stations with semi-continental climates like Copenhagen and Ultuna; and relatively high (20–30 ppm) for stations with continental and/or high arctic climates like Chicago and Station Nord.

The flutter, which characterizes the Copenhagen curve for the first 9 months of 1959, is probably due to the unusual climatic conditions prevailing in this period. Long spells of drought occurred in Feb.–Mar., May–June and Aug.–Sep. In the same months (except Aug.) the sparse precipitation was relatively high in O^{18} for the season, whereas it was relatively low in April and July with excess precipitation. This correlation may be ascribed to relatively high evaporation from the drops in rain with low intensity and falling through dry air. In April and July and the dry August most of the precipitation fell with high intensity and probably little loss and fractionation due to evaporation from the drops.

As another reason for the effect, one might think of relatively high evaporation from the collector in the dry months. This is unlikely, however, since the Copenhagen collector was emptied once a day and, furthermore, no increased effect was observed at the neighbouring station, Lyngby (Table II in the appendix), where the collector was emptied only once a month.

4. 4. 6. **Individual periods of precipitation.**

As pointed out above, one ought to take care in drawing conclusions from measurements on individual rains or snows. Such measurements are widely scattered owing to the influence of numerous meteorological parameters. Nevertheless, it is possible to deduct some common features for characteristic kinds of precipitation processes, and in special cases even to treat the phenomena quantitatively with some degree of success.

HARADA and TITANI (1935) found that the density of a rain of long duration decreased during the period. TEIS (1939) found that the density passed a minimum.

4. 4. 6. 1. ***Warm fronts.***

A warm front (AB in Fig. 23) is characterized by an inclined plane separating a moist, relatively warm air mass from the underlying cool, dry air.

DANSGAARD (1953) investigated the rain from a warm front, which passed Copenhagen on June 22, 1952. The upper part of Fig. 24 shows schematically the atmospheric conditions at the place of collection as a function of time. In the lower part, the sections of horizontal lines indicate the periods of time during which precipitation occurred. The showers preceeding the warm front showed a uniform O^{18} content of

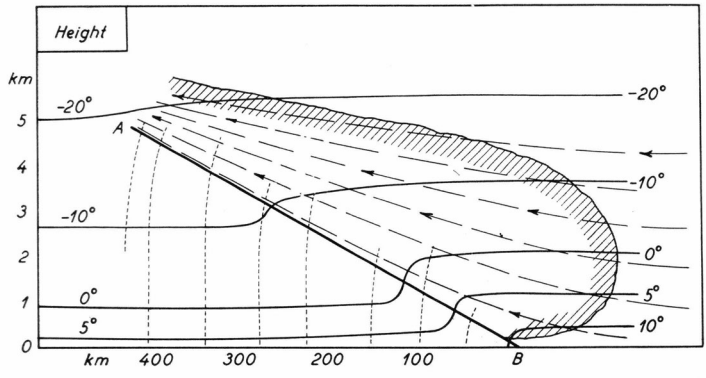

Fig. 23. Schematic drawing of a warm front. The arrows indicate moving air particles.

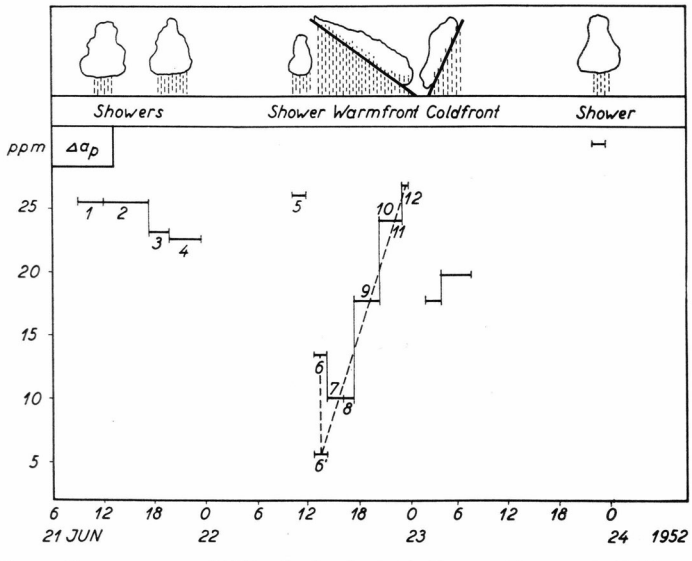

Fig. 24 (From DANSGAARD, 1953). Isotopic variation of the precipitation in Copenhagen during the passage of a front system. The weather situation is indicated in the upper part of the figure.

the rain, whereas the rain of the warm front showed a sudden decrease followed by an increase in O^{18}. These changes may be explained qualitatively in the following way: The first rain from the front fell at 12 o'clock on the 22nd. It came from the uppermost part of the front, in other words, from air, which had already lost a considerable amount of H_2O^{18} by condensation during the long ascent along the front. 7 hours later the rain was richer in O^{18} because it came from the middle section of

the front, where the air had lost less H_2O^{18}, and so forth. The O^{18} content of the rain changed 16 ppm during the passage of the warm front.

The very first warm front rain (sample 6) was not the lightest one; perhaps it was owing to this rain being exposed to vigorous evaporation during the relatively long fall through the relatively dry air. If this explanation is accepted, one may get a better value for the rain from the uppermost part of the front, at the time it was released from the cloud, by drawing a straight line through Nos. 12 and 7 and moving No. 6 downwards to intersection. This procedure gives a total change in O^{18} of 22 ppm.

If the condensation along the warm front is considered as a process of type D (condensation by moist-adiabatic cooling in equilibrium with water, p. 46), the procedure described on p. 46 can be used for calculation of the isotopic variation of the precipitation. At the basis of the cloud (200 m height) the pressure was approx. 1000 mb and the temperature 10° C, which for saturated air corresponds to a mixing ratio, m_0, of 7.76 g H_2O/kg air. At the top of the cloud (approx. 4000 m height), the pressure was approx. 615 mb and the temperature −14° C, which for saturated air corresponds to a mixing ratio, m, of 2.12 g H_2O/kg air. a_v^0 = 1960 ppm, m, m_0 and α = 1.0114 (the mean value of α in the temperature range +10 to −14° C) are inserted in equation (25) p. 45, which gives

$$a_v = 1960\ (2.12/7.76)^{0.0114} = 1931.5 \text{ ppm.}$$

With $\alpha = 1.0102_5$ and 1.0127_8 at +10 and −14° C, respectively, equation (28), p. 46, then gives

$$a_w^{0'} - a_w' = 24 \text{ ppm.}$$

This is more than both the directly measured (16 ppm) and the semi-empirically determined variation (22 ppm). However, it should be born in mind that the average cooling of the precipitating air is probably less than the temperature difference between the basis and the top of the cloud, because some of the precipitating air enters the cloud at higher levels than 200 m (Fig. 23). In such air the condensation starts at relatively low temperatures, and the moist-adiabatic cooling of this air is, therefore, less than for the air entering the cloud at lower levels. This is actually the same effect as mentioned in connection with the fractionation in orographic rain (p. 64). Another contributing reason for $a_w^{0'} - a_w'$ being less than calculated is that the condensate is not removed immediately from the vapour phase.

In a weak warm front the fractionation due to evaporation from the falling drops can easily overcompensate the lifting effect. This is demonstrated by the case described below:

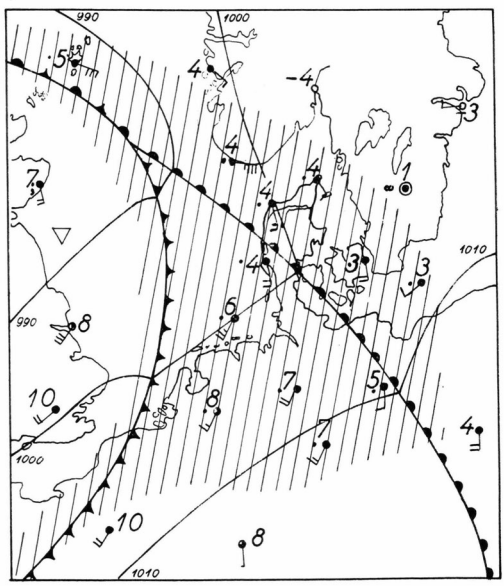

Fig. 25. Map on the weather situation in the North Sea region for 1957, Feb. 8, 0600 GMT. (From Daily Weather Report issued by the Danish Meteorological Institute).

On Feb. 8, 1957, a rather weak warm front approached Copenhagen from SW followed by a warm, stable, precipitating, tropical air mass (Fig. 25). The upper part of Fig. 26 gives the weather situation at the place of collection as a function of time; the middle section gives a record of the amount of precipitation; and the lower section the O^{18} content of the rain.

The reasons for the decrease of Δa at the beginning of the period could be that (1) the evaporation from the falling drops decreases with time as the cool air gets more and more humid, and (2) that mixing takes place between the warm and the underlaying cool air.

As to (2), the cool air contains vapour, which has not been depleted in H_2O^{18} during a condensation process, and would thus add isotopically heavy vapour to the upper part of the front. This effect is probable in connection with a cold front, as estimated by Epstein (1956), but most unlikely in cases with stable air like those described in the above.

The increasing O^{18} values after the passage of the warm front reflect the fractionation in the warm air during its horizontal passage through

the cloud. The air underwent an approximate isobaric cooling from 8 to 4°C at the ground and from 5 to 1°C in 500 m height. Using formulae (26) and (28) with $a_v^0 = 1960$ ppm

$$a'_w(t_o) - a'_w(t) = 6 \text{ ppm}$$

in reasonable agreement with the measured 8 ppm.

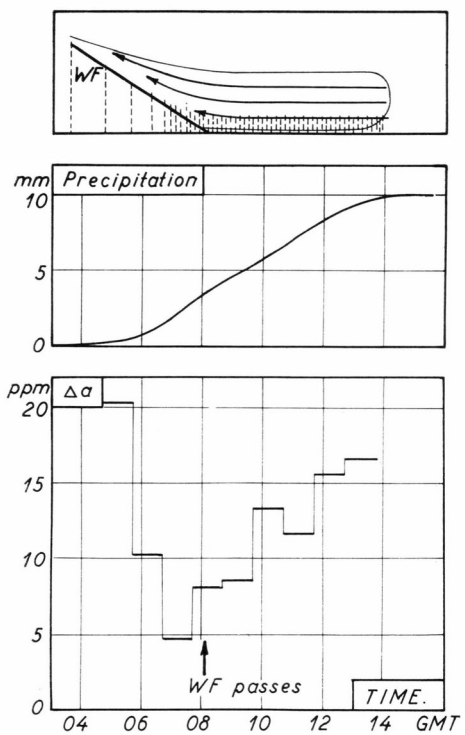

Fig. 26. Isotopic variation of the precipitation (lower section) fallen in Copenhagen during the passage of the front system shown in Fig. 25. The amount of precipitation is shown in the mid section. The upper section gives the weather situation at the place of collection.

4. 4. 6. 2. ***Showers.***

A shower is a phenomenon caused by instability in the atmosphere. Over land it most frequently occurs in the summer due to intense heating of the air close to the ground. If the air is sufficiently humid, the rise causes condensation of the vapour, whereby the latent heat of condensation is liberated. If the vertical temperature gradient in the resulting moist-adiabatic process is less than that in the surrounding air, the process will continue and a cumulus cloud is established.

When the falling drops leave the basis of the cloud they begin evaporating with intensities depending upon the relative speed, the

temperature and the humidity of the rising air. A part of a given drop may reach the ground as rain whereas the rest of it re-enters the cloud as vapour. Thus a cumulus cloud works in principle as part of a distillation column.

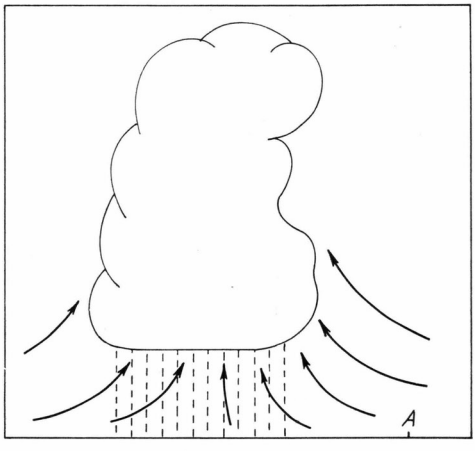

Fig. 27. Sketch of a cumulus could. The arrows indicate the movements of the air.

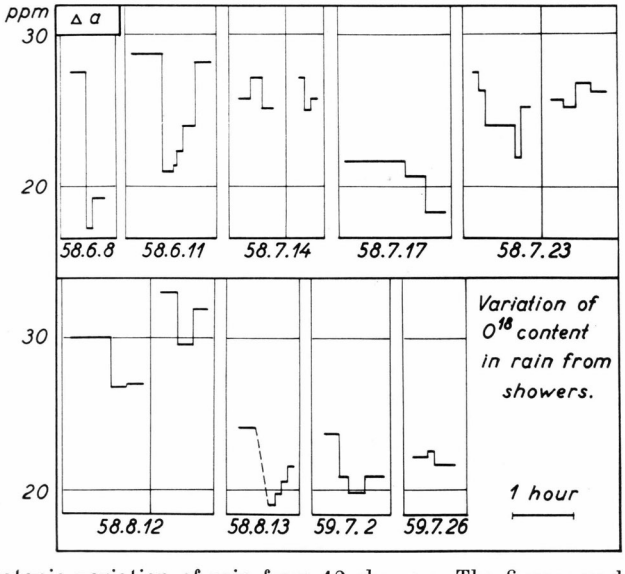

Fig. 28. Isotopic variation of rain from 12 showers. The figures under each section indicate the year, month and date of collection.

Fig. 27 is a sketch of a cumulus cloud, the arrows indicating the paths of the incoming air.

In Fig. 28 is shown some differentiated measurements on rain from 12 showers. In 9 cases, the heaviest rain was that falling in the beginning

of the period in question. In 7 cases, a significant increase in O^{18} content was observed at the end of the period.

An explanation may be found by imagining the cloud in Fig. 27 passing the collection place A from the left to the right. There are three contributory reasons for the first rain at A to be relatively heavy:

1. It originates mainly from the first stage of the condensation process in the air rising at the front of the cloud.
2. The drops fall through relatively dry air and are, therefore, subjected to considerable evaporation and enrichment in H_2O^{18}.
3. Owing to the great wind velocities, the evaporation from the falling drops takes place under non-equilibrium conditions, i.e. with high values of α.

There are two possible reasons for the low O^{18} content in rain from the middle of the cloud. Firstly, such rain mainly originates from higher levels, i.e. from vapour, which has already been depleted in H_2O^{18}. Secondly, the drops fall, even after having left the basis of the cloud, through air with high humidity; i.e. the evaporation and, therefore, the attached enrichment are small. A possible effect analogue to the fractionation taking place in distillation columns is thus overcompensated by the first of the above mentioned effects.

At the back of the cloud the conditions are similar to those at the front. Therefore, isotopically heavier rain is often given off from this part of the cloud. However, such rain is not as heavy as that from the front of the cloud because of less evaporation from the falling drops. This, in turn, may be owing to lower velocity and higher humidity of the air entering the cloud from behind.

A variation as described in the above could not be expected, naturally, if A is passed only by the peripherical part of the cloud.

Also the O^{18}-content of the total amount of rain given off at a given location from a passing shower highly depends on the distance from the path of the center of shower. In Table V in the appendix the two samples collected on July 26, 1959, represent the total amount of rain from the same shower collected at locations 9 km from each other and at the same altitude. The O^{18} difference is 4.7 ppm.

No close relation has been found between variations in the drop size and the O^{18}-content. However, this should not be taken as an evidence for the evaporation from the drops being of little importance, since the drop size is dependant on several other factors, such as the number of drops per unit of volume and the size distribution of the drops in the cloud.

Below is given an estimate of the depletion of liquid from a drop, which is necessary if the evaporation alone should account for the biggest

increase of the O^{18} content observed in rain from a shower (10.4 ppm, June 8, 1958). For α is used 1.02, taking into account the probable non-equilibrium conditions. a_w^0 is approx. 1970 ppm. Formula (17) p. 41 then gives:

$$a_w = 1970 + 10.4 = 1970 \cdot F_w^{-0.02}; \quad F_w = 0.76.$$

Thus an evaporation of only 24 % would account for the whole O^{18} variation in this extreme case. The actual evaporation is probably less because of the other contributory reasons for the O^{18} variation mentioned on p. 72.

Below it is shown that an evaporation of the above-mentioned order can easily occur. KINZER and GUNN (1951) have calculated the mass evaporation rate of freely falling drops:

$$\frac{dq}{dt} = 4\pi a D \left(1 + \frac{Ka}{S}\right) (\varrho_a - \varrho_b) \text{ g/sec},$$

where a is the radius of the drop, K is a dimensionless factor, S is the thickness of the transition shell outside the drop, D is the coefficient of

Table 12.
Evaporation from falling drops.

1	2	3	4	5	6	7	8	9	10
Drop diam. 2a cm	Rate of evaporation, dq/dt in ng/sec						q_0 μg	Terminal velocity m/sec	Fall before 100 % evap. m.
	Ambient temp. 0° C Relative humidity			Ambient temp. 20°C Relative humidity					
	90 %	70 %	50 %	90 %	70 %	50 %			
0.01	5.8	17	29	13	36	62	0.52	0.27	
0.03	33	98	170	76	220	380	14.0	1.17	
0.10	190	580	980	440	1300	2200	524	4.03	
0.30	1300	4000	5400	2900	8500	14000	14100	8.06	
	Time in sec for 20 % evaporation								
0.01	18	5.9	3.6	8.1	2.9	1.7			
0.03	86	29	17	37	13	7.4			
0.10	550	180	107	240	81	48			
0.30	2200	710	520	970	330	200			
	Fall in m before 20 % evaporation								
0.01	5	1.6	1.0	2.4	0.8	0.5			150
0.03	100	34	19	43	15	8.7			
0.10	220	74	43	97	33	19			42000
0.30	1800	570	420	780	270	160			

diffusion; ϱ_a is the saturated vapour density at the surface of the drop and ϱ_b is the vapour density of the environment.

The upper section of Table 12 gives dq/dt for various drop sizes and humidities at a total pressure of one atmosphere. In column 8 and 9 are recorded the mass, q_0, and the terminal velocity, v, of drops freely falling in air with pressure one atmosphere, temperature 20° C and humidity 50 % (after GUNN and KINZER, 1949).

On this basis, the approximate time and distance of fall before evaporation of 20 % of q_0 are calculated (middle and lower section of Table 12). The distance of fall before complete evaporation (at pressure 900 mb, temperature 5° C and humidity 90 %) is given in column 10 for two drop sizes (after FINDEISEN, 1939).

The distance of fall before 20 % evaporation is seen to vary from 10 to 200 m for drops of middle size. In actual cases with different drop sizes in the same air and, consequently, different velocities of fall the situation is complicated by collisions between the drops. However, the observed isotopic changes during showers may, evidently, be explained by evaporation from falling drops.

4. 4. 8. 3. ***Comparison between warm fronts and showers.***

The mechanism of the release of precipitation from a shower is to some degree analogous to that used in fractionation columns for artificial enrichment of O^{18} in water: Upward vapour passes downward liquid. This effect would give shower precipitation a tendency to average to a higher O^{18} content than warm front precipitation. However, since shower precipitation is often of high intensity, evaporation from falling drops having left the cloud probably constitutes an effect of the opposite tendency: Less percentage loss of water from the relatively big drops in showers corresponds to less enrichment. To this it may be added that the upward air in a shower is usually moist-adiabatically cooled to a higher degree than that in a warm front, which is another possible reason for shower rain to be isotopically lighter than warm front rain.

The shower activity over land is mainly a summer phenomenon. Sampling of warm front rain for comparison with showers should, therefore, only be carried out in the summer, owing to seasonal variation. This was not taken into consideration in the comparison reported by DANSGAARD (1954), which showed a higher mean value for showers than for warm fronts. The reason for the difference could be that the warm fronts were sampled all the year round, whereas the showers were sampled only in the summer and fall.

In Table V in the appendix measurements are stated on 11 warm fronts and 37 showers all sampled in the months of May to August. The means are 27.2 ± 1.2 and 24.9 ± 0.8 ppm. The difference is hardly significant.

4. 4. 6. 4. ***Cold fronts.***

A cold front appears when a cold air mass replaces a warm one. The cold air pushes its way under the warm air which is lifted up causing a formation of cumulus clouds. This event is much more violent than the warm front process. EPSTEIN (1956) has reported a detailed investigation of the precipitation given off during the passage of a cold front. Precipitation was collected in the Western part of the United States at several locations with different altitudes and distances from the coast. The rain got heavier in O^{18} as the cold air advanced from the north. The rain falling at high altitudes was relatively light in O^{18}. At a given location the O^{18} content of the rain in most cases passed a minimum shortly after the middle of the period. The isotopically heavy rain at the end of the period was ascribed to an increasing contribution of the vapour from the cold air mass to the precipitation.

5. INVESTIGATIONS ON GLACIER ICE

A glacier constitutes an enormous natural collector in which precipitation is accumulated layer by layer. During several decades glaciers have been the object of extended studies, not only because of their capacity as reservoirs of water power in many cases, but also because their physical and chemical properties reflect past and present climatic conditions.

In the preceeding chapter it has been pointed out that the variations in the heavy isotope content of water is very pronounced in the polar regions. Isotope investigations are, therefore, especially promising there.

Some of the possibilities for isotope studies on glacier ice were pointed out by DANSGAARD (1954, 1958) and EPSTEIN (1956). EPSTEIN and SHARP (1959) used especially the altitude effect for an investigation of the Malaspina and Saskatchewan glaciers, and EPSTEIN and BENSON (1959) showed the seasonal variation in O^{18} to be preserved in the Greenland ice for many hundred years. GONFIANTINI and PICCIOTTO's data (1959) from the King Baudouin base in the Antarctic indicated an O^{18} variation in snow of approx. 32 ppm, corresponding to an observed temperature variation of 20° C. The O^{18} measurements gave, furthermore, indications that the drift-snow does not come from very far South.

5. 1. **Main features of the geography and the glaciology of the Greenland ice cap.**

Next to the ice cap of Antarctic the Greenland ice cap is the largest glacier in the world. Fig. 29 is a map of Greenland. The dashed curves are contours of elevation. The ice cap covers 80 % of Greenland or an area of $1.7 \cdot 10^6$ km² and extends from 61° N to 82° N, a distance of 2300 km, while the width from West to East varies from 300 km in South to 800 km in the regions North of 70° N.

The altitude of the surface averages 2135 m (BAUER, 1954) and reaches 3200 m on the so-called northern dome. In North and Mid Greenland the ridge runs between the 38th and the 42nd degree of longitude leaving a 500 km long slope with increasing inclination down to

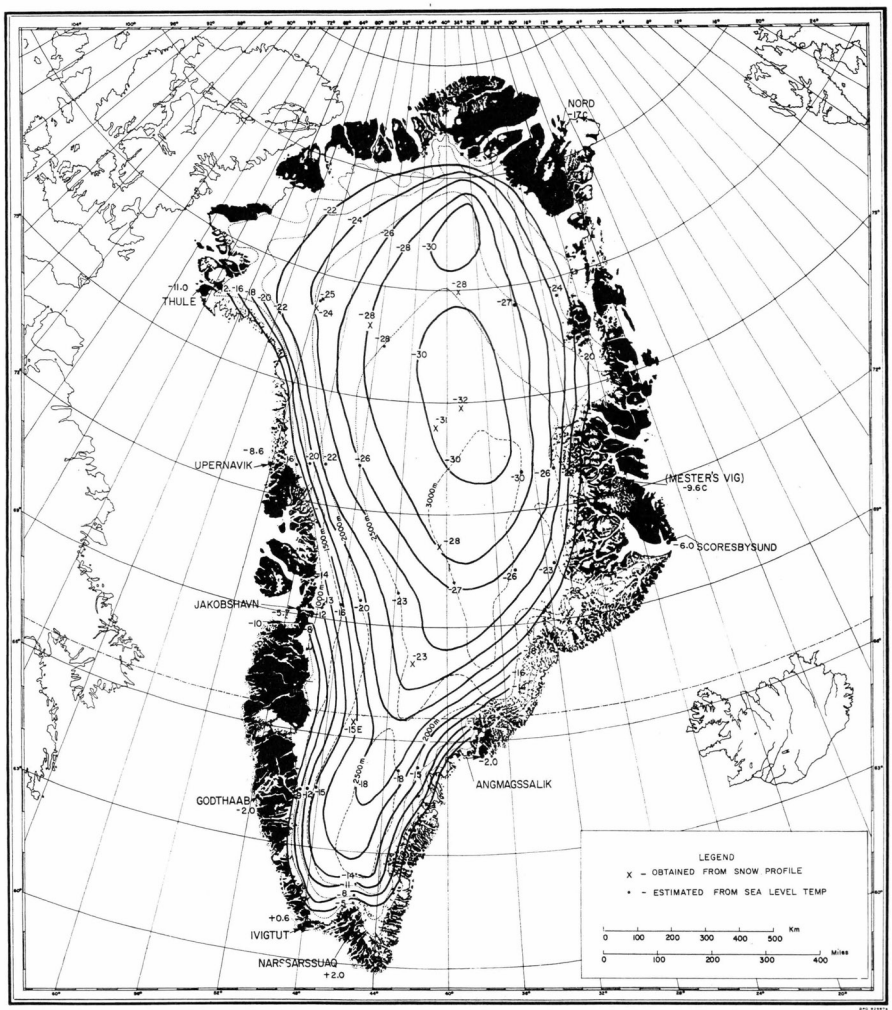

Fig. 29 (From DIAMOND, 1958). Map of Greenland made on the basis of a map issued by the Danish geodetic Institute, 1957. The thin curves on the ice cap are contours of elevation. The thick curves are drawn through locations with equal temperature 10 m below the surface.

the west coast. On the southern dome the altitude reaches 2800 m. The ridge runs towards SSW between the 42nd and the 45th degree of longitude leaving a western slope of 200 to 300 km length.

Disregarding the outlet glaciers, the western edge of the ice is located at elevations of 500 to 1000 m in South and Mid-Greenland, while in North Greenland the ice reaches the sea level over long distances, e.g. in the Melville Bay.

The thickness of the inland ice has been intensively studied, especially by the "Expeditions Polaires Francaises". From the data given by

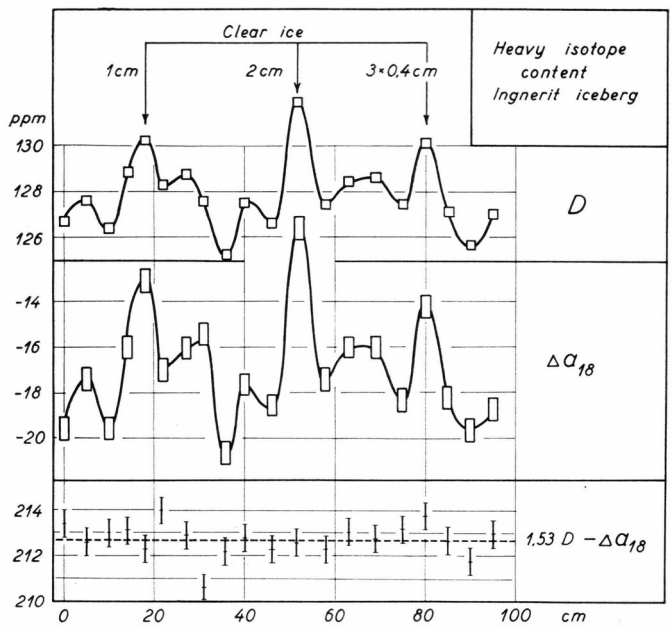

Fig. 30 (From DANSGAARD, NIEF and ROTH, 1959). Isotopic variation in an ice chunk extruded from the Ingnerit glacier, West Greenland. The samples were collected along a line perpendicular to parallel layers of clear ice.

HOLTSCHERER (1954), it appears that the ice is more than 3000 m thick over large areas in Central Greenland. 25 % of the bedrock is below the sea level (BAUER, 1954).

In West Greenland the elevation of the firn line (the limit between regions with accumulation and regions with ablation) varies from approx. 1200 m in the Melville Bay to approx. 1800 m in South (BAUER, 1954).

Thus a picture emerges of Greenland as a rocky bowl heaped with ice, which here and there overflows the rim due to continuous net supply of material. As a logical consequence of the model, the material balance of the ice cap arises as one of the most important problems of the Greenland glaciology. The accumulation and ablation at the surface, and the velocities and the paths of the ice flowing from the sites of formation to the coastal glaciers are all various sides of this main problem.

5. 2. **Isotopic stratification.**

EPSTEIN and BENSON (1959) demonstrated a periodical variation of the O^{18} content of the ice with depth at two sites in North Greenland. DANSGAARD, NIEF and ROTH (1959) investigated a West Greenland ice chunk, which was part of the ice later referred to as the Ingnerit ice

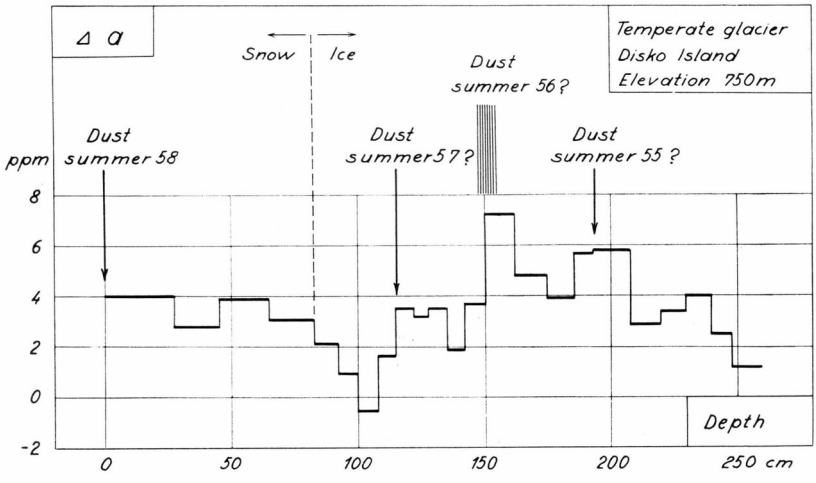

Fig. 31. O^{18} variation with depth in a temperate glacier on the Disko island, West Greenland.

(dating sample V, Table VII). If the clear ice layers (Fig. 30) are accepted as indications for part of the summer precipitation, the seasonal variations in deuterium as well as in O^{18} are shown to be preserved in the ice during several hundred years. The values of the clear ice layers are the highest, which most probably is owing to evaporation from the wet summer snow at the time of formation of the ice.

In temperate glaciers seeping melt water may blur the picture in some respects. If the water is not drained off, it will be mixed up with the snow and thus add water to these layers with an isotopic composition different from that of the snow. On the other hand, isotope analysis of the various layers during the melting season might be a useful tool for investigation of the material balance in such glaciers.

On August 4, 1958, samples were taken along a vertical line in a pit dug in a small, temperate glacier at Narssak, Disko Island, Greenland (69°53.5′ N, 52°58′ W, altitude 750 m). The distance between some distinct layers of dust (inclination 22°) were taken as indications for the net annual accumulation, as the dust is probably caught by the wet snow in the summer.

The O^{18} variations are shown in Fig. 31 as a function of depth. Relative maxima occur in all the dust layers. This may reflect the remains of the seasonal variation. If so, the melt water seems to have smoothed the variations so much that they can hardly be used for determination of the net accumulation. However, a more detailed sampling might give a more favorable picture.

The isotopic stratification of glacier snow and ice raises the problem whether the ice cap samples referred to in Fig. 20 are representative

for the mean annual O^{18} content of the precipitation at the locations of collection. The ideal reference sample should include all the material accumulated during a whole and high number of years. Such samples have not been available. However, it seems that the mean value of several samples might serve the purpose. In Table VI (appendix) some details are given on the South Greenland samples referred to in Fig. 20. They were collected by U.S. Snow, Ice and Permafrost Research Establishment in July-August, 1959. For each location the individual measurements are very scattered, even within the same season. The standard deviations are indicated in Fig. 20. The value of the SIPRE station Site 2 in North Greenland originates from a deep bore hole. The sample was taken 100 m below the surface and represents 1.77 m of ice or 3–4 years accumulation about 1800 A.D.

5. 3. **The movements of the ice.**

The mode of movement of glacier ice is still a matter of conjecture. During many years great efforts have been made in order to clearify the problem by laboratory experiments, theoretical considerations and field observations. The literature on these subjects has grown to such a degree that a covering review would exceed the frames of the present work. Reference is, therefore, made to reviews by SCHOUMSKY (1957), WORTH (1957), GLEN (1959) and, as regards the recent scientific activity on the Greenland ice cap, FRISTRUP (1959). At this place only a few lines will be given on some of the most important papers.

The old sliding hypothesis (first postulated by ALTMANN, 1751) attributed the movement of a glacier to sliding like a block over its bed (owing to gravity), often lubricated by melt water. Differential movements within the ice were not taken into consideration by this theory.

The granular theory (CHAMBERLIN, 1895, and others) supposes the individual grains to be the mechanical units of motion. The flow proceeds along the intergranular surfaces of least resistance under continuous recrystallisation and change of the size and relative positions of the grains.

The glide plane theory (PHILIPP, 1914, and others) ascribes the motion to slips along multitudinous glide planes. The ice is broken into blocks, which move like big, solid bodies (Block-Schollen flow). This theory explains the existence of high velocity gradients, and Block-Schollen flow has very recently been supposed to exist in the extremely fast streams of ice in West Greenland (BAUER, 1960a).

The extrusion theory (STREIFF-BECKER, 1938, DEMOREST, 1942) is based upon the assumption that hydrostatic pressure influences the

physical properties of ice so that the rate of flow increases with the depth under the ice surface. Flow rates increasing with depth have been observed by HAEFELI (1958) under the special topographic conditions prevailing at Jungfraujoch; however, extrusion flow can not exist in the Greenland ice cap, because an ice cap moving under such conditions could not be in statical equilibrium (NYE, 1952c).

The plastic theory (first put forward by FORBES, 1853) ascribes the ice movement to mechanical properties of ice analoguous to those of metals beyond the yield point. In the modern form of the theory (e.g. NYE, 1952a, 1957, 1958) the assumptions are made in agreement with the results obtained by laboratory experiments (GLEN, 1955, RIGSBY, 1957, STEINEMANN, 1958, and others). According to these experiments, ice behaves like an elastic material to small and brief stresses, whereas it yields under the influence of prolonged stresses. So far, no treshold value has been observed for the stress requisite to cause yielding. In 1955 GLEN found the following relation between the strain rate, $\dot{\varepsilon}$ year^{-1}, and the shear stress, σ bar:

$$\dot{\varepsilon} = k \cdot \sigma^n , \tag{30}$$

where k and n are constants; n is about 4 over the stress range 1–10 bars and at temperatures just below the melting point. The flow rate decreases with temperature. The value of n is equal to 1 for a purely viscous liquid, whereas the stress must exceed a certain value to cause flow of an ideally plastic material ($n \to \infty$). Ice is often called a quasi-viscous or a pseudoplastic material.

Hydrostatic pressure has no influence upon the flow law, but uniaxial compression perpendicular to the stress makes the strain rate increase (STEINEMANN, 1958).

In case of a big, flat ice mass like the Greenland ice cap laying on a practically horizontal bed, the pressure is high, whereas the flat shape causes small stresses originating from gravity. In other words, it is the flow law in the the low stress range, which is of interest here. Unfortunately, this range is difficult to investigate experimentally owing to the long periods of time involved.

Theoretical considerations based upon assumptions in accordance with the laboratory experiments have in many cases fully explained fenomena observed in natural ice masses (NYE 1952a, 1957, 1958, and others). However, NYE's attempt (1952b) to calculate the profile of the Greenland ice cap was only partly succesfull (BRUCE and BULL, 1955), possibly because the flow law is hardly as simple in the low stress range as indicated above. Thus, MEIER's thorough investigation of the Saskatchewan glacier (1960) pointed on the necessity of adding

another term in the flow law owing to grainboundary creep (JELLINEK and BRILL, 1956):

$$\dot{\varepsilon}_0 = k_1\sigma_0 + k_2\sigma_0^n \tag{31}$$

$\dot{\varepsilon}_0$ and σ_0 being the octaedral strain rate and shear stress ($k_1 = 0.018$ bar^{-1} year^{-1}, $k_2 = 0.13$ bar$^{-4,5}$ year^{-1}, $n = 4{,}5$). Accordingly, the ice would seem to be more viscous (i.e. higher $\dot{\varepsilon}$) at low stresses but more platic at high stresses than hitherto assumed. For $\sigma = 10^{-2}$ bar, (31) gives a value of $\dot{\varepsilon}$, which is five orders of magnitude higher than the $\dot{\varepsilon}$-value obtained with $k_1 = 0$. MEIER found, consequently, a remarkably fast decrease of the flow rate with increasing depth.

The knowledge of the physics of ice is still so limited and the stress systems in glaciers are often so complex that a simple "theory could only be made to cover all the known facts by straining both the facts and the theory" (BEILBY, 1921).

Measurements of the physical conditions prevailing in the Greenland ice cap are still rather sparse disregarding the outlet glaciers. This is owing to its inaccessibility and also to its enormous dimensions, which, e.g., makes the establishment of a geodetic profile very difficult, not speaking of the measurement of the flow rate far below the surface. The Expeditions Polaires Francaises (E.P.F.), 1948–55, the U.S. S.I.P.R.E. and the Expedition Glaciologique Internationale au Groenland (E.G.I.G.), 1957–60, have all given weighty contributions to the solution of many problems. E.G.I.G.'s geodetic measurements in 1959 will be repeated in a few years and then throw much light on the problem of the flow rate of the ice in the drainage area of the Jakobshavn glacier.

Several calculations have been made of the time needed for the ice to reach the coast. HESS (1904) stated that "eine einfache Rechnung belehrt uns, dass die Schneemengen, welche nahe an der von Nord nach Süd durch Grönland ziehenden Eisscheide anfallen, höchstens 2000 bis 3000 Jahre brauchen um als Bestandteile von Eisbergen in einen Fjord zu schwimmen". The age was obtained by simply dividing the total volume of the ice cap by the total annual accumulation. According to BAUER (1960b) the recent measuremens made by the E.P.F. give

$$\frac{2.35 \cdot 10^6 \text{ km}^3}{446 \text{ km}^3/\text{year}} = 5.300 \text{ years},$$

which is rather to be considered as an average value for the whole mass of ice assuming all ice to be replaced with the same frequency. Several authors have given strong indications for the existence of very fast ice streams (velocities up to 30 m per day) discharging into the glaciers at

Jakobshavn, Umanak and Upernavik. As regards the rates of flow the presence of ice streams allows the possibility that one piece of ice formed in an ice stream needs much shorter time for reaching the coast, than another piece of ice formed at the same distance from the coast but far from an ice stream. However, the westward movement in the marginal zone seems to be considerable even far from proper ice streams. Thus, by studying air photographs taken with an interval of 4 years WEIDICK (1960) observed displacements of moraines corresponding to approx. 25 m per year at the margin just South of Søndre Strømfjord air base.

The activity of the Jakobshavn glacier is enormous (650 m^3 per sec. BAUER, 1960), so its area of drainage must cover most of the ice cap in Mid Greenland. BAUER (1960a) considered it a circle section (radius 305 km) with the glacier outlet in the center. Under the assumptions of (1) material balance of the ice cap and (2) the velocity being independant on depth BAUER used data on accumulation and ablation and calculated the velocity distribution along a radial path giving 10, 25, 50, 100 and 200 m per year at the distances 55, 110, 150, 190 and 250 km, respectively, from the periphery.

HAEFELI (1960) calculated the horizontal component of the mean profile velocity, v_{xm}, along a SW going line towards Jakobshavn. He considered a 175 km wide and 525 km long drainage area. The rockbed was assumed to be horizontal. The value of v_{xm} was calculated to 10, 25, 50 and 100 m per year at the distances 60, 150, 260 and 400 km from ice divider.

As regards the vertical components of the paths of the ice, one consequense of HAEFELI's procedure is that the ice formed in Central Greenland would seem to sink down to great depths and only come to the surface again close to the outlet. If so, ice formed near the ice divider must be many thousand years old when it appears as icebergs (HAEFELI, 1960a, estimates up to 100,000 years) only because the annual accumulation is no more than a 0.1 per mille of the depth of the ice cap. On the other hand, in case of a more superficial flow on top of a large mass of relatively stagnant ice the discharged ice would be relatively young, whereas the ice close to the bed rock must be much more than 10,000 years old.

Methods for determination of the age and the origin of the icebergs would, naturally, be of great help for the investigation of the dynamics of the ice cap. In the sections 5.4 and 5.5 an attempt to evaluate such methods will be described.

5. 4. C^{14} dating of icebergs in West Greenland.

On the Arctic Institute Greenland Expedition 1958, 11 icebergs were sampled for C^{14} dating. The background, the sampling technique, the sources of error and the results of this investigation will be described in details by SCHOLANDER, DANSGAARD, NUTT, DE VRIES, COACHMAN and HEMMINGSEN (1961). The main points are given here, because this matter has a close connection to the next sections.

Glacier ice contains bubbles with atmospheric air trapped at the time of formation of the ice. C^{14} dating of the CO_2 content of the bubbles should thus give the age of the ice. 11 samples of ice (6–16 tons each sample) from 10 West Greenland glaciers were melted in evacuated containers, and the released gases passed through a CO_2 absorber.

In Table VII (appendix) some characteristics and measurements are given on the 11 dated ice samples. The data in columns 8 and 9 (volume of gas at NTP relative to that of the ice and the percentage content of CO_2 in the extracted air) are taken from SCHOLANDER, HEMMINGSEN, COACHMAN and NUTT (1960).

The datings are given in column 10. They range from close to zero to 3100 years ± 150 years. Only two of the 11 samples were older than 1000 years.

In several cases the air released from the ice had relatively high CO_2 contents compared with atmospheric air. However, even if all surplus of CO_2 were of recent date none of the investigated icebergs could be older than 4700 years and only 3 older than 2000 years.

5. 5. Determination of the region of formation of West Greenland icebergs.

The contours of elevation in Fig. 29 show the shape of the accumulation zone of the ice cap to be very smooth with only a slight inclination of the surface. This is reflected by the regular course of the curves through locations with the same mean annual air temperature. The heavy curves in Fig. 29 show the distribution of the temperature, t′, 10 m below the surface (cf. footnote p. 57).

The procedure by determining the region of formation of an iceberg is now quite simple:

1. the Δa value representing the O^{18} content of the iceberg is found,
2. the temperature t′ at the place of formation is found by using the correlation between $\Delta\bar{a}_p$ and t′ (Eq. 29, p. 63). The estimated accuracy is ± 1°C.

3. The possible region of formation is obtained from Fig. 29 as the strip of the ice cap limited by the $t' + 1$ and the $t' - 1°$ C curves.

If the distance, d, from the outlet of the glacier to the closest point of the t′ curve is measured, d should be considered as the minimum distance passed by the iceberg in question owing to a possible component of the path parallel to the isotherms.

5. 5. 1. **Sources of error.**

Due to the high solubility of CO_2 influx of even small amounts of melt water from the low altitude zones might change the C^{14} content of the ice considerably. As to the O^{18} content such influx also constitutes a source of error but of less importance. Thus, addition of as much as 5 % melt water from snow at a low altitude location ($t' \cong -10°$ C) to ice from high altitudes ($t' \cong -30°$ C) would cause an error of only 1° C on the estimated t′ value for the ice.

Other possible sources of error are deviations of the present climate and the shape and altitude of the ice cap from those at the times of formation of the icebergs. If the climate has become warmer or if the altitude of the ice cap has become lower since the time of formation of a given iceberg, the distance d would seem to be overestimated using the method described.

However, considerable error on the determination of d cannot arise owing to a general climatic change, i. e. a temperature change of the ice cap and, at the same time, a similar temperature change of the part of the ocean, which directly influences the climate on the ice cap. Such general climatic changes will, namely, not alter the geographical O^{18} distribution on the ice cap, because the heavy isotope distribution in the natural distillation column (p. 52) depends primarily upon the temperature *differences* in the column and only negligibly upon the absolute temperatures. Consequently, even though the obtained t′ values would be wrong, the use of them in the way described would still give the correct d values. Let us, for example, consider an iceberg with an O^{18} content n ppm below that of ocean water. Supposing that the O^{18} content of the ocean has remained constant, this corresponds to the same temperature difference, $\Delta t°$ C, in the natural distillation column at any time, regardless of possible overall temperature changes in the column. Furthermore, if we consider the shape of the ice cap at the latitude in question to have remained constant, Δt is a certain function of the distance from the West coast, again regardless of possible overall temperature changes.

Thus, only a change of the ice cap temperatures relative to that of the influencing part of the ocean could affect the distance determinations. Such relative change could be caused by variations in the altitude. A decrease in altitude of 250 m corresponds to an increase in relative temperature of approx. 2° C, which would cause an error of approx. 25 % on d, judging from the isotherms in Fig. 29, p. 77. However, recent investigations by WEIDICK (1961), argues strongly against considerable changes of the altitudes. In this connection it should be mentioned that if some ice is found with a representative Δa value well below −37 ppm (corresponding to $t' = t_a = -32°C$) such ice must originate from a period with lower relative temperatures (e.g. owing to higher altitudes of the ice cap) than at present since −32° C is the lowest mean annual air temperature on the ice cap today. Dating of such ice would, naturally, be very interesting.

If the correlation between $\Delta \bar{a}_p$ and t′ is used as described, the reference samples from the ice cap as well as the iceberg samples ought to include the accumulation of material from a whole number of years. Otherwise the seasonal variation might cause serious errors. However, such sampling technique is not applicable on icebergs, as no mean is available in the field for determination of the annual accumulation. The probable elimination of this source of error will be described in the next subsection.

Possible fractionation by evaporation from wet snow has no influence, as this effect is involved in the Δa values of the reference samples from the ice cap (Fig. 20).

Finally, the possibility of pollution with sea water should be considered. Sea water might seep into and freeze mainly as clear ice in cracks or crevasses in the ice at the glacier front. This was tested in one case: In Bredefjord some 100 small pieces of white ice were collected from the water just in front of the glacier and melted after wiping. The O^{18} content of the melt water mixture was −4.1 ppm. Another mixture of numerous small pieces of clear ice had $\Delta a = -4.0$ ppm showing that this kind of ice is refrozen melt water from the glacier; it does not originate from sea water, which has seeped into crevasses in the glacier ice.

5. 5. 2. **Sampling technique.**

The annual accumulation in North and Mid-Greenland is of the order of 20 to 60 cm of ice (BENSON, 1960). Sampling of blocks of ice with dimensions less than this has, therefore, hardly any significance. The greater the dimensions of the block the less will be the probable error.

The situation was ideal for the sampling of the amounts of ice used for dating. It was carried out by extracting some 50 cm^3 of the melt water from every second pot (each containing approx. 70 l of water). This gave a mixture of water, the isotopic composition of which was the true mean of that of several tons of ice. On top, this ice consisted of many blocks collected from various parts of a much larger amount of ice. The evaporation from the pots during the melting was of the order of magnitude of 0.02 $^0/_0$ and, thus, caused only negligible fractionation. Neither is the avoiding in some cases of broad stripes of clear ice considered as a serious source of error, because this ice hardly in any case amounted to 1 $^0/_0$ of the melted ice; furthermore, the isotopic composition of the clear ice layers does not deviate very much from the mean (Fig. 30, p. 78).

Other sampling methods are discussed in section 5. 7., pp. 91–94.

5. 5. 3. **Results of O^{18} analyses of the dated icebergs.**

In Table VIII (appendix) the following data are stated:

Column 1. The sample numbers.

Column 2 gives the number of amounts of ice involved in the particular sample. These amounts of ice might have different origins and different ages.

Column 3. Separate samples of melt water were prepared for O^{18} analysis so that they represented the amounts of ice melted in the number of pots indicated in column 3.

Column 4. The Δa values of the separate samples.

Column 5. The weighted mean Δa of the larger amount of ice indicated in column 2 for the dating samples II, III, IV, V and VIII.

Column 6. The weighted mean Δa of the entire dating sample.

Column 7. The temperature t′ at the site of formation found by using the Δa value of column 6 and the correlation between $\Delta\bar{a}_p$ and t′ given by equation (29), p. 63.

Column 8. The minimum distance between the region of formation and the outlet glacier. The uncertainty corresponds to $\pm$ 1°C on the determination of t′.

Column 9. The C^{14} dating transferred from Table VII (appendix) column 10.

Column 10. The minimum velocity found from columns 8 and 9.

Column 11. The Δa value in column 6 corrected for latitude effect (cf. p. 89).

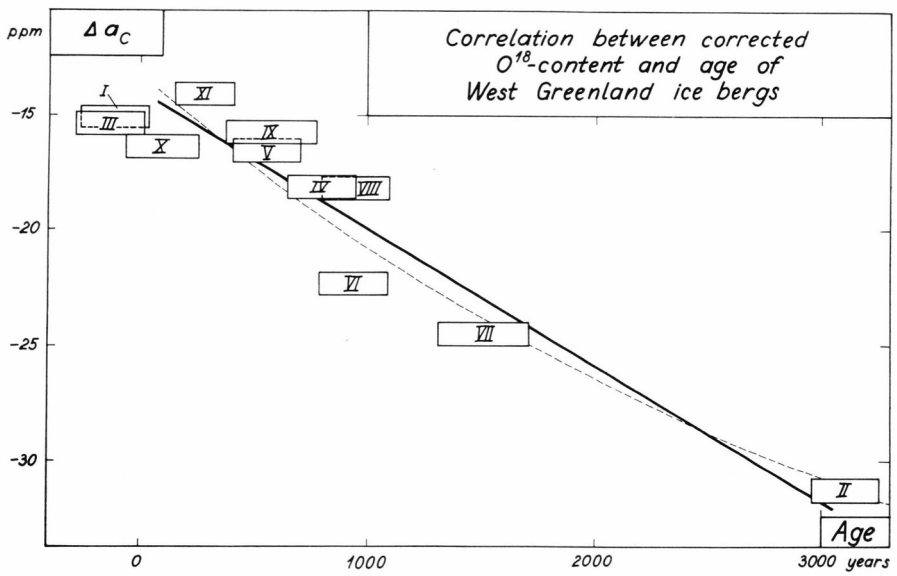

Fig. 32. The O^{18} content (corrected for latitude effect) of 11 icebergs as a function of the age determined by the C^{14} method.

Each of the dating samples Nos. I, II, III, VI, VII, and X was collected from the same iceberg. It appears from column 4 that they have all been homogeneous as far as the O^{18} content is concerned, except for the Upernavik ice (No. II). The extremely low O^{18} content indicates that this latter ice originates from a location very far from the coast. The significant O^{18} difference between the first and the last part of the ice (column 5) suggests a mixing of two very old, high altitude ice masses during their long and long lasting movement towards the coast.

The dating samples VIII and IX were rather homogeneous in O^{18} in spite of the fact that each of them were collected from more than one iceberg.

If two icebergs, formed at the same altitude but at sites n^0 latitude apart, flow westward with the same velocity, they will be approximately of the same age when extruded from the coastal glaciers. However, the O^{18} content of the northern iceberg will be $n \cdot 0.93$ ppm lower than that of the southern one, since the isotopic latitude effect in West Greenland is -0.93 ppm/^{0}lat. (cf. p. 64). Consequently, no direct correlation could be expected to exist between the O^{18} contents of the 11 dated icebergs and their ages. However, the latitude effect can be approximately eliminated from the O^{18} data by referring to the same latitude, e.g. 70° N. This is done by adding $(N - 70) \cdot 0.93$ ppm to the Δa value of each iceberg, if N is the latitude of the outlet glacier. Thus, the Δa_c values in Table VIII, Column 11, are obtained. The

two equally old icebergs mentioned in the beginning of this paragraph have, naturally, the same Δa_c.

In Fig. 32 the Δa_c values from column 11 are plotted against the ages. The vertical side of each rectangle indicates the estimated limit of error on the O^{18} measurement, whereas the horizontal side shows the statistical uncertainty on the C^{14} counting, i.e. the 67 % standard deviation.

The reason for the correlation is that the older icebergs usually originate from the regions with higher altitudes and, therefore, colder climate and lower O^{18} content in the precipitation. The very existence of a correlation (coefficient 0.8) between the two mutually independant C^{14} and O^{18} tests supports the general validity of the datings except for a systematic error.

5. 6. **Discussion of ice movements.**

As it appears from Table VIII (appendix), column 9, the ages of the sampled icebergs were between −130 and 3100 years ± approx. 150 year. These low figures are not caused by all the 11 icebergs being formed in the marginal zone of the inland ice, since column 8 shows the origin of the Upernavik ice to be 400–500 km from the coast. Its low age (3100 years) would seem to indicate a rather superficial flow. However, more data from high altitude ice are needed before a definite statement on this point can be made. Evidently, the 11 dated icebergs are so young that none of them could have sunk down to great depth in the ice cap.

Most of the icebergs originate from the marginal zone, though ice with no or few stripes of melt water was preferred. This could be owing firstly, to the fact that the net accumulation is relatively low in Central Greenland. Secondly, in two cases (samples I and III) the ice was collected from the upper parts of big, flat icebergs, which could hardly have turned round after the discharge from the glacier; the sampled ice may thus represent the youngest part of a large mass of ice, the deepest part of which is probably several hundred years older (SCHOLANDER et al., 1961).

Disregarding the dating samples I, III and X, for which the uncertainty of the C^{14} counting is more than 100 %, the mean velocities given in Table VIII, column 10, are strikingly consistent, ranging only from 110 to 270 m per year. The weighted mean is

$$154 \pm 15 \text{ m/year.}$$

The deviation from this mean is not significant for any of the eight dating samples irrespective of d varying between some 80 and 460 km.

A similar result would hardly have been obtained for 11 icebergs coming from one glacier with approx. circle-sector shaped drainage area, e.g. the Jakobshavn glacier. In such a glacier the flow rate must increase rapidly towards the outlet only because of the converging movement. On the other hand, in an imaginary glacier, draining a rectangular strip of the ice cap with no considerable converging movement, the velocity increase towards the outlet is probably much less. Since the drainage area of the Jakobshavn glacier covers an enormous area in Central Greenland, several of the other glaciers, from which dating samples were collected, must drain more oblong areas or areas not extending too far inland. This may be a contributary reason for the uniformity of the eight observed mean velocities.

Below, the measured mean velocities are put in relation to the considerations made by BAUER (1960) and by HAEFELI (1960), cf. p. 83. If one uses the velocity distribution calculated by BAUER, a numerical integration gives some 5000 (630) years as the time needed for an ice crystal to pass 80 (40) % of the assumed length, 305 km, of the drainage area of the Jakobshavn glacier. This corresponds to an approximate mean velocity of 50 (190) m per year.

A similar integration based on HAEFELI's calculated velocity distribution* gives approx. 8000 years for the movement through 80 % of the assumed length (525 km) of the drainage area, the relatively short time needed for the ice to move the last 125 km to the outlet being estimated to 600 years. The 8000 years corresponds to a mean velocity of the same order (50 m per year) as obtained above. The mean velocity for the movement through the last 40 % (210 km) of the assumed length of the drainage area can not be deduced directly from HAEFELI's data. Evidently, it must be considerably higher 50 m per year; but less than 200 m per year, since the first 100 km alone takes some 1100 years judging from HAEFELI's data.

Thus, it seems reasonable to conclude that the measured mean velocities are in substantial agreement with BAUER's and probably also with HAEFELI's considerations as regards icebergs, which are formed not too far from the coast; or in other words: as far as the region of the ice cap is concerned, where the flow of ice is determined by high shear stresses. On the other hand, there seems to be a serious disagreement as to the movement of ice formed far from the coast, i.e. in the low stress region; thus, the measured 150 m per year for the Upernavik iceberg is 3 times the velocity calculated from HAEFELI's data, though

* HAEFELI's v_{xm} values are used here as representative for the ice velocities at any depth. When disregarding the regions close to the margin and the ice close to the bottom this procedure hardly causes essential errors, because of the estimated slight velocity variation with depth resulting from the use of GLEN's law.

the conditions for the movement of this iceberg seem to be rather similar to those defining the problem, which was treated at the beginning of the previous paragraph.

As to the reasons for the discrepancy it should be pointed out that the O^{18} method for the determination of the distances leads to great absolute uncertainties on great distances owing to the small horizontal temperature gradients in Central Greenland. This is disadvantageous for the comparison between measured and calculated ages and, thereby, velocities; exact knowledge of sites of formation in Central Greenland is, namely, especially important for the calculation of the high ages, because of the small velocities in Central Greenland.

On the other hand, the calculation of flow rates at high altitudes, i.e. during the first and, by far, most time consuming part of the movements, is a critical point, because of the lack of knowledge of the location of the ice divider. Furthermore, at high altitudes the slope of the surface is small, which makes the shear stresses considerably less than 1 bar even at the bedrock; in other words, one has to do with the flow law in the poorly investigated low stress range. The possible existence of a first order term in the flow law is important, since its appearance in Eq. (31) makes $\dot{\varepsilon}$ increase by no less than 3 orders of magnitude for $\sigma_0 = 0.1$ bar. This would tend to increase the surface velocities relative to what would be expected from GLEN's law; the paths of the ice would seem to be more superficial than estimated by BAUER and by HAEFELI which, in turn, would tend to decrease the calculated ages (and especially the old ones) since BAUER and HAEFELI make the simplifying assumption (3) that the velocity is independant on the depth under the surface. Finally, it should be mentioned that possible rocky tresholds close to the outlet glaciers would seem to favour a relatively superficial flow. The existence of such a treshold may be doubtful at the Jakobshavn outlet, but absolutely probable at the outlets in the Umanak Bay, where 4 of the dating samples were collected.

5. 7. The possibility of secondary O^{18} dating of icebergs.

The correlation between the C^{14} datings and Δa_c (Fig. 32) seems to provide a method for O^{18} dating of icebergs. So far, such dating must, naturally, rely on the ages evaluated by SCHOLANDER et al. (1961) for the 11 icebergs I to XI. Obviously, much more work is desirable for establishing a solid basis for the correlation between the age and Δa_c. Such work includes, firstly, a primary dating of several icebergs by the C^{14} method and, if possible, by another independent method; secondly, an investigation of the scattering of the Δa_c values for icebergs of the

same age. This scattering is due not only to uncertainty on the C^{14} counting but also to the possibility that icebergs formed at the same isotherm have different ages, even in regions where the isotherms are practically parallel to the coast (cp. p. 83).

The line drawn in Fig. 32 is to be considered as a first approximation. Owing to the increasing temperature gradient on the ice cap towards the West coast (Fig. 29), the dashed curve in Fig. 32 might be a better approximation. This is also indicated by the necessarily increasing velocity of the ice when going westward. However, the straight line is considered a sufficiant approximation to the available measurements. On this basis, the method of the least squares gives the following equation for the correlation:

$$\text{Age} = -(162 \pm 9)\ \Delta a_c - (2260 \pm 170)\ \text{years},$$

which may also be written as

$$\text{Age} = -(162\ \Delta a_m + 140\ (N - 70) + 2260) \pm 300\ \text{years},$$

N being the latitude of the discharging glacier, and the $\pm$ values being standard deviations. In the evaluation of this equation, the ages of samples I and III have been put equal to zero. If the δ function is used with the O^{18} content of ocean water as a reference value, the equation comes out as

$$\text{Age} = -(336\delta + 140\ (N - 70) + 8590) \pm 300\ \text{years}.$$

The uncertainty connected to an O^{18} dating is twice as much as the best obtainable uncertainty with C^{14} dating of ice samples of about 10 tons. Nevertheless, considering the extremely difficult sampling technique connected to the latter method, the former one would constitute a promising aspect, if sampling of small amounts of ice could give a sufficiently representative sample for O^{18} analysis. Unfortunately, this problem was not investigated systematically during the expedition. However, the results reported below give some indication as to the probable errors, which will be introduced by three relatively simple sampling methods:

1st method: Melting of some 70 kg of ice (1 melting pot) and extraction of 50 cm^3 of the mixture.

2nd method: Sampling of one ice chunk (of the order of 1 m^3) by cutting off numerous pieces of ice from the entire surface and, as far as possible, from the interior of the chunk. After melting 50 cm^3 was extracted from the mixture (before cutting the ice the uttermost layer

was scraped off and discarded in order to prevent errors from contamination with sea water or from evaporation of melt water).

3rd method: Sampling of several chunks of the same mass of ice by the cutting technique described above.

Table 13.

Sample No.	Dating	Dimensions of chunk m	Pot No.	Characteristics of the ice	Δ a_m of dated ice ppm	Δ a of chunck or pot ppm
177	II		61		−34.4	−34.7
179	II		90		−34.4	−36.5
256	II		183		−34.4	−35.2
138	V_1		38		−19.9	−18.4
136	V_1		35		−19.9	−18.2
				Mean deviation	1.2 ppm	
264	I	3 · 2 · 2		As I	−19.8	−19.5
262	I	1.5 · 1 . 5 · 1.5		Thick double layers	−19.8	−16.8
180	II	0.7 · 1 · 1.8		As II	−34.4	−30.3
181	II	1.5 · 1 · 1		As II	−34.4	−36.7
140	IV_2	2 · 1.5 · 0.8		Many thick melt water layers	−17.0	−13.2
134	V_1	1.5 · 1.5 · 0.5		As V_1	−19.9	−31.4
135	V_1	1.2 · 0.8 · 0.8		As V_1	−19.9	−18.4
144–163	IV_2	77 cm perpendicular to the clear layers			−17.0	−16.9
12–43	$VIII_1$	109 cm perpendicular to the clear layers			−18.2	−17.2
				Mean deviation	3.1 ppm	
110	IV_1				−20.0	−21.5
64	VI				−22.7	−22.0
48	$VIII_2$				−16.9	−18.0
45	$VIII_1$				−18.2	−18.6
10	X				−15.7	−16.0
5	IX				−14.5	−13.6
				Mean deviation	0.8 ppm	

Parallel to the sampling described on p. 87 the three above mentioned sampling techniques were applied on some of the ice masses used for dating. Table 13 is divided into 3 sections each giving a comparison of the results obtained by one of the 3 simple methods and the mean Δ a value for the entire corresponding dating sample. In the first section 5 indivi-

dual pots of melt water are seen to deviate 1.2 ppm as a mean from the values of the corresponding large mass of ice.

The second section tells about 9 chunks of ice sampled according to method No. 2, except for the last two, which were sampled along 77 and 109 cm perpendicular to the stratification (Nos. 144 to 163 are the samples referred to in DANSGAARD, NIEF and ROTH, 1959, cf. p. 78). The mean deviation from the O^{18} values of the dating samples is as much as 3.1 ppm.

The last two chunks have approximately the same isotopic compositions as the corresponding dating samples, which was also to be expected, if the stratification is interpreted as being due to summer melting at the sites of formation. In case this interpretation is correct the samples 144–163 as well as 12–43 represent, namely, 3–4 years' accumulation, and the seasonal variations cancel when forming the mean.

The samples referred to in the lower section were collected by the third method. The mean deviation is only 0.8 ppm.

On the basis of the few data in Table 13 it must be concluded that the first or the third sampling method is to be preferred, if the melting of many tons of ice is not possible. However, sampling by cutting ice along a line perpendicular to the stratification may also do, if the stratification represents former horizontal layers of melted snow at the site of formation of the ice.

5. 8. **The latitude effect reflected by the icebergs.**

The isotopic latitude effect along the Greenland west coast was determined to -0.93 ppm/° lat. (p. 64). O^{18} measurements on 53 icebergs and chunks sampled on the expedition reflect an effect of the same order. In Fig. 33 they are put into 6 groups: 4 samples collected in Melville bay (at Kjær's glacier), 5 in the Upernavik icefjord, 20 in Umanak bay, 7 in Disko bay, 4 in Godthaabs fjord and 13 collected in Bredefjord. The figure shows the mean values plotted against the latitude. The line inserted has the above mentioned slope, -0.93 ppm/° lat. The standard deviations of the mean values indicated in the figure have nothing to do with the measuring accuracy and probably only little to do with the sampling technique. Thus, the great scattering in the Upernavik group is probably due to the 5 ice masses in question originating from widely different altitudes.

35 of the 53 samples referred to in Fig. 33 were collected by technique No. 2, described on p. 92. The individual sample is, therefore, not considered as representative for a large amount of ice; but taken together in groups, they reflect a latitude effect of approximately the same order as the calculated one, assuming the average altitudes of the origins of

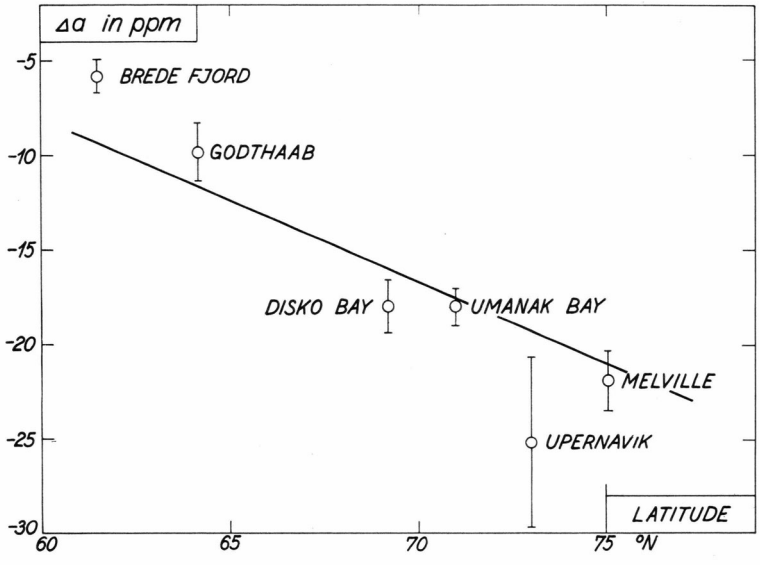

Fig. 33. The O^{18} content of 6 groups of icebergs as a function of the latitude of the outlet glaciers. The line has the slope -0.93 ppm/°lat. determined in section 4. 4. 4., p. 64.

the icebergs in the 6 groups to be almost the same (the ice discharged into Bredefjord probably originates from altitudes between 1900 and 2700 m compared to 1300–3200 m for the ice extruded from the Middle and North Greenland glaciers).

The Bredefjord icebergs are significantly higher in O^{18} than corresponding to the line. A possible reason for this is the fact that the climate in South Greenland is influenced by temperate, maritime air masses to a higher degree than the climate further North. As mentioned in subsection 4. 4. 3., p. 64, the isotopic altitude effect is relatively small in temperate, maritime climates (e.g. in Norway), i.e. the precipitation at high altitude stations is relatively high in O^{18}. Another contributing reason for the Bredefjord icebergs being rich in O^{18} would be an increasing evaporation from and, consequently, increasing O^{18} enrichment of wet snow in a southerly direction on the ice càp.

A priori, Fig. 33 indicates a latitude effect of -1.3 ppm/° lat. rather than -0.9 ppm/° lat. It might be tempting to apply this greater latitude effect when forming the Δa_c values for the dated icebergs (p. 89). Only the Δa_c values for samples Nos. I, II and XI would, thereby, be changed significantly, the line drawn in Fig. 32 would still constitute the best linear approximation to the correlation between Δa_c and the age, and none of the conclusions made on the basis of this figure would be affected.

6. APPENDIX

6. 1. **Experimental determination of α_{18}.**

In the experimental determination of α_{18} described below sources of error, such as boiling and kinetic effects (cp. p. 44), are eliminated.

Some few cm^3 of water were evaporated from a reservoir of approx. 400 cm^3. The vapour was collected in a freezing trap cooled by dry ice and acetone. If a_v^0 indicates the O^{18} content of the vapour and a_w that of the water reservoir (actually the mean value of the O^{18} contents of the water before and after the evaporation), then

$$\alpha_{18} = \frac{a_w}{a_v^0} = \frac{a_w - a_v^0}{a_v^0} + 1 . \tag{31}$$

Fig. 34 shows the evaporation chamber into which dry tank nitrogen entered from the left. The nitrogen then passed a double trap. The tube connecting the two individual traps was heated in order to re-evaporate escaping ice cristals (DE VRIES, 1957). When the collection was finished, the double trap was disconnected from the rest of the apparatus, and after evacuation the water was distilled into one of the traps, from which it was removed.

An error may arise if the collected ice has an O^{18} content, a_p, different from a_v^0 owing to escaping water vapour or ice crystals. Below is calcuated to which degree the nitrogen should be dried to make this error negligible.

Using a_p instead of a_w in Eq. (22), p. 43, we get

$$a_p - a_v^0 = a_v^0 \left(\frac{1 - F_v^\alpha}{1 - F_v} - 1 \right). \tag{32}$$

This equation is strictly valid only for an isothermal process. However, as shown in section 3. 4., p. 45, the equation for the condensation process,

$$a_v = a_v^0 \cdot F_v^{\alpha - 1}, \tag{20}$$

from which (32) is directly derived, is valid also for a non-isothermal process, if used with the mean value of α in the temperature range in question. Equation (32) gives

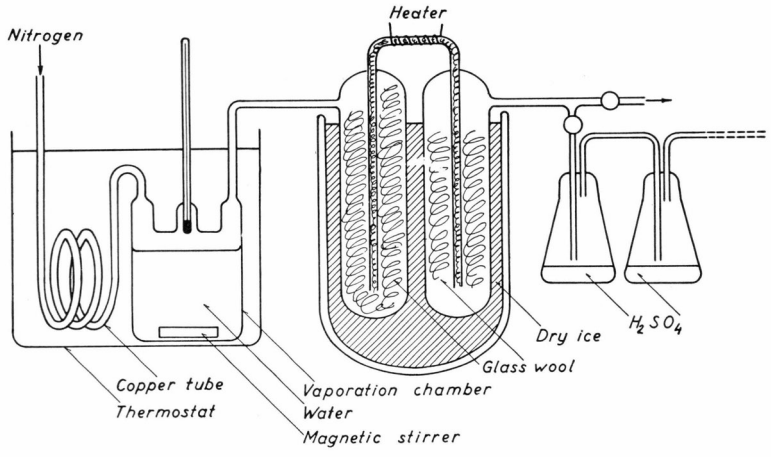

Fig. 34. Arrangement for evaporation of a small fraction of a limited amount of water, and collection of the vapour in two freezing traps. The flasks with H_2SO_4 shown to the right are for testing the drying efficiency of the traps.

$$F_v = 2 \cdot 10^{-3} \quad \text{for}$$

$$a_v^o = 1960 \text{ ppm}, \quad \alpha_{18} = 1.02 \quad \text{and} \quad a_p - a_v^o = 0.5 \text{ ppm}.$$

The latter figure is equal to the measuring accuracy. The value $F_v = 2 \cdot 10^{-3}$ shows that 2 per mille of the initial amount of water vapour may escape without causing considerable errors. If part of the water content in the nitrogen escapes as crystals, the requirement of the degree of drying is reduced. The crystals could, namely, originate from any part of the cooling process and their heavy isotope content would, therefore, hardly be extremely low.

In order to measure the drying efficiency of the double trap, the dried air was spread several times over the surface of 98.7% sulfuric acid (kindly made with special care for this purpose by Dansk Svovlsyre Fabrik, Ltd.). In some experiments with dry ice cooling nitrogen was led through the system with a flow rate of 6.8 mg air per sec. During 15 hours, 2.2 mg of water was absorbed by the acid corresponding to a mixing ratio, m, of 0.008 g H_2O per kg nitrogen, taking into consideration the water content in air in equilibrium with concentrated sulfuric acid (2.5 μg/l, MORLEY, 1885). In experiments with a flow rate of 50 cm³/sec, of which 8 cm³/sec was led through the acid containers, the same drying efficiency was found. This indicates that the remaining water in the nitrogen is due to vapour rather than to escaping ice crystals, because the latter effect should increase with the flow rate.

At 1000 mb the values of m are 18.1 and 5.1 g H_2O per kg air at 23° C and 4° C. The 0.008 g H_2O per kg nitrogen measured in the dried nitrogen thus corresponds to

$$F_v = 4 \cdot 10^{-4} \text{ at } 23^\circ \text{ C},$$
$$F_v = 1.6 \cdot 10^{-3} \text{ at } 4^\circ \text{ C},$$

which is satisfactory.

Table I column 6 shows incomplete humidifying in the chamber to occur at high flow rates only. The high values of α found under such circumstances could not be due to F_v being underestimated, since escape of considerable amounts of the last, isotopically light vapour would cause a decrease in the observed α values.

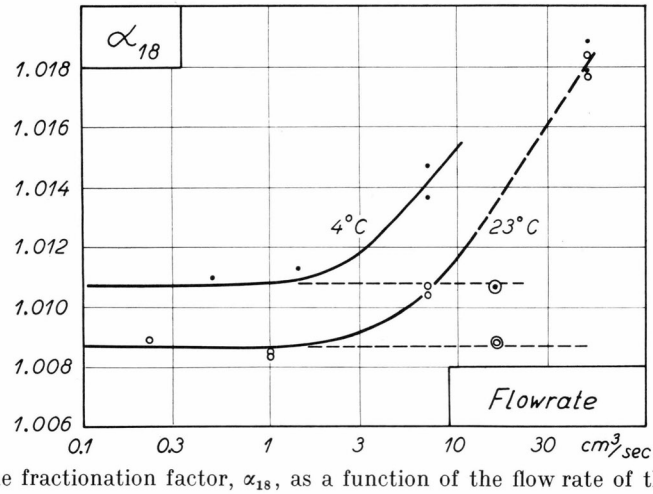

Fig. 35. The fractionation factor, α_{18}, as a function of the flow rate of the nitrogen passing the system shown in Fig. 34. A kinetic effect influences the results for flow rates higher 1 cm³/sec.

The results recorded in Table I are found by using $a_v^0 = 1960$ ppm in (31). They are plotted in Fig. 35 as a function of the flow rate. With the apparatus in question equilibrium is seen to be established at flow rates below 1 cm³/sec. at 23° C. At higher flow rates the relatively high rate of reaction of H_2O^{16} gains increasing influence. Evidently, the factors $\alpha - 1$ and $\frac{1}{\alpha} - 1$, which govern the Raleigh processes (Eqs. (17) and (20), pp. 41 and 43), can obtain numerical values at least double as high as the equilibrium values.

The double circles at the flow rate 16 cm³/sec. refer to the experiments Nos. 14 and 15 in which the nitrogen was led twice over a water surface before cooling. Repeated contact between vapour and liquid is seen to establish a fast isotopic exchange.

The α values 1.0087 at 23° C and 1.0108 at 4° C are plotted in Fig. 16 (p. 44) as dots. They are seen to support the results of ZHAVORONKOV et. al. (1955).

6. 2. **Tables.**

Table I.

Evaporation experiment (p. 98).

1	2	3	4	5	6	7	8	9	10
Exp. No.	Temp. °C	Flow rate cm^3/sec	Time hours	q* g	H** %	Δa_W ppm	Δa_v ppm	$\Delta a_W - \Delta a_v$ ppm	α_{18}
1	23	0.23	262	4.5	100	31.9	14.4	17.5	1.0089
2	23	1.0		3.5		32.6	16.0	16.6	1.0085
3	23	1.0		7.0		33.1	16.6	16.5	1.0084
4	23	7.0		10.2		29.8	8.9	20.9	1.0107
5	23	7.0	19.6	10.5	80	31.3	11.2	20.3	1.0104
6	23	50	2.5	5.5	50	32.2	−4.7	36.9	1.0184
7	23	50	2.4	5.0	50	34.6	0.2	34.4	1.0175
8	4	0.5	284	3.3	100	28.6	7.1	21.5	1.0110
9	4	1.4	96	3.0	100	29.8	7.6	22.2	1.0113
10	4	7.0	23.7	3.0	80			28.8	1.0147
11	4	7.0	23.7	3.0	80			26.9	1.0137
12	4	52	16.7	9.2	50	30.1	−7.0	37.1	1.0189
13	4	52	16.3	9.2	50	29.6	−5.5	35.1	1.0179
14	23	16	7.38	8.3	100	30.5	13.2	17.3	1.0088
15	4	16	16.0	5.7	100			20.9	1.0107

* q = the quantity of ice collected in the trap.

** H = the humidity at the outlet of the vaporation chamber, found by comparing q with the calculated amount of vapour in saturated air.

Table II.

Δa_p (ppm) of monthly precipitation in Copenhagen (Cop.) and Lyngby (Ly.) (pp. 59–66). P means the total amount (in mm) of precipitation in Copenhagen during the corresponding period of time.

	1955		1956		1957		1958			1959			1960		
	P	Cop.	P	Cop.	P	Cop.	P	Cop.	Ly.	P	Cop.	Ly.	P	Cop.	Ly.
Jan...					38	21.4[5]	45	12.6		44	20.8[12]	20.6	60	12.7	17.2
Feb...	8	12.2			30	13.6	106	12.7		4	29.4[13]		69	10.7	
Mar...	48	18.2					26	6.8		14	24.2[14]	23.4	44	19.2	
Apr...	29	20.8					128	21.5[7]		115	16.9[15]	17.3			
May..	48	23.1					48	23.7[8]	25.2	29	27.5[16]	23.7			
June .	36	20.4	54	26.7	12	26.0	32	23.4		11	29.4[17]	27.7			
July..	35	21.8	21	29.0	51	26.1	21	25.7	21.2	78	18.2	19.1			
Aug...	6	23.9	95	24.8	82	22.8	42	23.8	24.0	31	21.6	21.3			
Sep...	140	19.5	85	25.4[2]	80	21.0	57	24.8[9]	24.8	6	26.3				
Oct...	38	22.6[1]	56	22.7[3]	80	22.2	45	23.0[10]	23.4	37	25.7	23.6			
Nov. .					30	18.6	31	17.3[11]	21.8	19	17.0	22.1			
Dec...			59	18.2[4]	33	16.3	47	9.9	12.5	57	17.0	18.5			

[1] Oct. 1–18. [2] Sep. 1–Oct. 5. [3] Oct. 6–Nov. 11. [4] Dec. 9–Jan. 7. [5] Jan. 8–Feb. 12. Feb. 13–28. [7] Apr. 1–May 6. [8] May 7–31. [9] Sep. 1–Oct. 6. [10] Oct. 7–31. [11] Nov. 1–26. [12] Jan. 1–28. [13] Jan. 29–Feb. 25. [14] Feb. 26–Mar. 31. [15] Apr. 1–29. [16] Apr. 30–June 3. [17] June 4–30.

Table III.

Δa_p (ppm) of monthly samples of precipitation collected at Greenland stations (pp. 59–65).

	1	2	3	4	5	6	7
	Grønne-dal	Holsteins-borg	Søndre Strøm-fjord	Uma-nak	Ang-mags-salik	Scoresby-sund	Station Nord
1957, Sep.							−17.6
Oct.							+ 1.5
Nov.							− 3.7
Dec.							− 5.3
1958, Jan.					− 3.2		
Feb.					+16.7		−25.8
Mar.					+18.2	+ 9.7	
Apr.		+12.8			+10.1		− 9.3
May		+15.7			+14.6		
June	+26.6	+16.0			} +13.1		− 4.4
July	+21.9	+17.7					
Aug.		+ 9.4			+14.1	+ 6.7	− 5.0
Sep.	+18.3	+20.4		− 2.9	+13.7	+16.4	−15.8
Oct.	+12.8	+16.3	− 6.6		+ 5.8	+15.0	− 4.5
Nov.	+ 5.9	+15.1[3]			+10.7	+ 6.1	−25.8
Dec.	+ 8.0	+12.7[4]			+12.0	+13.1	− 7.2
1959, Jan.	+13.3	}			+ 6.4	− 4.0	−35.5
Feb.	+10.4	+ 2.5[5]	− 8.2	−11.8	+ 8.8	− 0.4	−22.3
Mar.	+11.9	+ 5.4[6]	−15.1	−15.0	+10.5	+11.9	−22.6
Apr.	+18.7	+14.3	− 2.9		+15.1	+11.6	− 3.2
May	+18.4	+15.2	+ 6.4	− 3.6	+20.5	+17.6	
June	+ 8.7	+13.8	+ 8.0		+17.7	+ 4.5	− 2.0
July	+18.5	+14.7	+ 9.3	+13.8	+17.3		+ 6.5
Aug.	+24.8			+20.8	+14.6		
Sep.	+17.0		+ 4.3	+19.4			
Oct.	+11.8	+ 8.1[8]		+17.8			
Nov.	+14.5		− 5.7[10]				
Dec.	+19.8[1]	+15.4[9]	} + 2.0[11]				
1960, Jan.	+13.0[2]						

[1] Dec. 4–Jan. 14. [2] Jan. 15–Feb. 15. [3] Nov. 5–Dec. 5. [4] Dec. 5–31. [5] Jan. 1–Feb. 23. [6] Feb. 23–Apr. 2. [7] Apr. 2–30. [8] Oct. 10–Nov. 2. [9] Nov. 12–Jan. 14. [10] Nov. 10–20. [11] Nov. 20–Jan. 27.

Table IV.

Δa_p (ppm) of samples of monthly precipitation collected at some European stations and in Chicago (pp. 59-65).

Period	1 Valentia	2 Thorshavn	3 Stend	4 Fanaråken	5 Reykjavik	6 Birr	7 Dublin	8 Højer	9 Lyngby	10 Ultuna	11 Tvärminne	12 Punkaharju	13 Chicago 1954-55
1957, Mar.			19.0										
Apr.			32.4										
May			28.7										
June			21.2	15.6									
July				18.9						28.5			
Aug.	31.7			9.2									
Sep.	30.6									16.3			33.8
Oct. .	30.9			15.5									22.8
Nov.	28.1			14.7									7.6
Dec.	27.8		23.3	13.2									18.4
1958, Jan.	27.4		20.4	12.3									11.3
Feb.	24.9		19.3	13.0									21.4
Mar.	21.9		23.0	17.4						12.5			19.9
Apr.	36.7		20.1	17.4	25.9					9.1			30.5
May	22.1		23.8	18.6		24.2	20.6	30.6	25.2	14.6	18.6	15.4	34.1
June	29.0		22.4	11.6	23.6	22.2	20.7			22.0	17.7	10.9	
July	26.5		24.6			25.3	29.3	26.8	21.2		22.5	17.2	
Aug.	31.9	27.4	21.9		21.1	23.4	25.0	25.7	24.0	22.0	21.9	24.6	
Sep.	29.3	23.4	25.0		29.2	27.1	27.7	25.9	24.8	20.5	27.6		
Oct.	25.4	28.5	24.6		22.4	27.4	22.5	25.7	23.4	22.5	20.6		
Nov.	29.9	28.7	20.6		27.1	27.0	25.8	20.0	21.8	15.7			
Dec.	24.8		19.0		23.2	23.0		22.3	12.5	7.6	16.0	5.0	
1959, Jan.	24.8	21.5		13.9		22.8	19.8	23.9	20.6		19.2	12.3	
Feb.	30.4	28.7	22.1		23.8	25.0	24.5				12.8	9.0	
Mar.	28.3	29.3	15.4	8.2	23.1	16.8	23.9	19.9	23.4	15.0	23.7	13.4	
Apr.	21.7	25.5	18.7	8.3	18.6	19.6	20.7	23.1	17.4	13.7	11.9	12.2	
May	22.7	27.0	26.7	14.7	26.8	25.8	28.3		23.7	25.4	23.1	20.8	
June	31.6	34.2			22.4	28.1	29.8	25.9	27.7		24.2	18.2	
July	32.1	30.7	26.3	18.5	18.3	28.6	23.0	27.7	19.1	25.2	14.0	18.2	
Aug.	29.9	28.3	28.7	16.2	22.9	29.7	30.3	27.1	21.3	20.2	27.9	12.5	
Sep.	30.8	31.6	26.3		22.1	33.4	31.3			17.6	14.2	14.2	
Oct.	29.2		24.2	6.9	22.4	18.6	19.6	27.1	23.6	19.4	20.8	16.5	
Nov.	28.4	23.8	21.1	15.4	14.8	22.1	20.8	20.5	22.1	16.3	15.1	15.8	
Dec.	23.4		15.2	9.5	16.9	16.6	18.4	25.4	18.5	14.9			
1960, Jan.	29.9	24.0	21.9	0.8	21.0	24.8	22.7	16.6	17.2	11.4			
Feb.	24.5	21.0				23.8	23.0						

Table V.

Measurements on individual warm fronts and showers (p. 74).

Warm fronts		Δa in ppm
Time of collection		
52. 6. 12	0700–2000	26
52. 6. 14	1540–1620	25
52. 6. 22	1100–2300	18.5
53. 5. 29	1500–1800	27
58. 5. 06	0300–1200	30.9
58. 5. 08	0920–1100	25.2
58. 5. 11	0000–1100	26.8
58. 7. 28	1300–2100	29.0
58. 8. 01–02	2000–0200	30.5
58. 8. 14	1300–1530	27.0
59. 6. 16–17	2000–0015	32.9
	mean:	27.2 ± 1.2
Showers		
52. 5. 29	0700–0800	25
52. 5. 29	0700–0800	26
52. 5. 30	0900–1400	27
52. 6. 08	0830–0900	29
52. 6. 09	0745–0800	29
52. 6. 16	1400–1500	26
52. 6. 20	1515–1545	25
52. 6. 21	1600–1720	24
52. 6. 23	2000–2100	30
52. 7. 13	1510–1715	23
58. 5. 09	0600–0630	18.5

Showers (cont.)		
Time of collection		Δa in ppm.
58. 5. 20	1800–1900	27.8
58. 5. 08	1715–1745	21.1
58. 6. 11	1030–1200	24.5
58. 6. 22	0900– ?	24.8
58. 6. 25	1000–1100	24.2
58. 7. 14	1415–1645	25.8
58. 7. 17	2100–2240	19.6
58. 7. 22	1800–2200	29.1
58. 7. 23	0915–1515	25.4
58. 7. 28	2100–2230	30.3
58. 7. 31	0430–0445	23.4
58. 8. 03	0420–0430	22.9
58. 8. 04	0000–0400	30.5
58. 8. 08–09	1200–1000	31.6
58. 8. 12	0920–1030	27.7
58. 8. 13	1200–1300	20.8
58. 8. 25	2100– ?	27.8
59. 6. 15	?	20.1
59. 6. 29	1700–1730	21.7
59. 7. 02	0930–1032	21.2
59. 7. 06	1240–1320	30.0
59. 7. 11	2010–2200	32.7
59. 7. 26	1600–1700	26.7
59. 7. 26	1600–1640	22.0
59. 7. 30	1615–1630	12.3
59. 7. 31	?	16.5
	mean:	24.9 ± 0.8

Table VI.

S. I. P. R. E. stations in South Greenland, (pp. 59 and 80).

No. 9. 64°29.6′ N, 44°37′W
Altitude 2746 m. t′ = −22.1° C
Accumulation: 30 cm H_2O

Sample No.	Depth cm	Season*		Δ a ppm
398	23–28	s	59	−14.8
399	51–55	w	58–59	−28.4
400	95–100	l s	58	−13.3
401	131–134	w	58–57	−19.0
402	162–166	s	57?	−11.3
403	190–193	s	57?	−20.0
		mean: −17.8 ± 2.5		

No. 14. 63°11.9′ N, 46°18′ W
Altitude 2604 m. t′ = −19.6° C
Accumulation: 56 cm H_2O

Sample No.	Depth cm	Season*		Δ a ppm
406	33–36	s	59	−21.4
407	78–81	w	59–58	−11.9
408	129–132	s	58	− 8.7
409	185–189	w	58–57	−24.6
410	216–220	s	57	−13.1
411	0–3	s	59	−24.5
		mean: −17.4 ± 2.9		

No. 16. 62°15′ N, 45°30′ W
Altitude 2440 m. t′ = −16.4° C
Accumulation: 72 cm H_2O

Sample No.	Depth cm	Season*		Δ a ppm
412	22–24	s	59	− 0.6
413	77–80	e s	59	−13.7
414	121–123	l w	59–58	−20.6
415	154–157	e w	59–58	+ 4.1
416	191–194	l s	58?	−14.1
		mean: −9.0 ± 4.6		

No. 17. 62°01′ N, 45°02′ W
Altitude 2440 m. t′ = −14.4° C
Accumulation: 86 cm H_2O

Sample No.	Depth cm	Season*		Δ a ppm
417	17–19	s	59	+ 3.5
418	85–88	e s	59	−23.7
419	167–170	w	59–58	−12.8
420	275–280	s	58	− 3.0
421	343–354	w	58–57	− 4.9
422	458–462	s	57?	−12.7
423	547–550	w	57–56?	− 3.8
424	620–624	s	56	− 3.8
425	702–706	w	56–55?	− 9.0
426	780–785	s	55	−12.3
427	860–864	w	55–54	−14.1
428	943–948	s	54	− 6.4
429	1058–1060	w	54–53?	+ 1.9
		mean: −7.8 ± 2.0		

* s: summer, w: winter, l: late, e: early.

Table VII. Data on 1

1	2	3	4	5
Sample	Place of collection	Number of loads, relative amounts	Amounts of melted ice (tons)	Stratification
I	A few km West of Kjær's glacier (75.0° N)	3 loads (25, 45 and 30%). From 3 places (100 and 300 m apart) of the same iceberg, 500 · 500 · 100 m^3.	11	Several stripes of clear ice.
II	In Upernavik icefjord (73.0° N).	1 load. All ice from one chunk (400 tons).	16	None.
III	At the mouth of Karrat icefjord (71.8° N).	2 loads (70 and 30%). All from one iceberg. 10^7 tons.	15	Several stripes of clear ice.
IV	Close to the Kangerdlukssuak glacier (71.4° N).	2 loads (80 and 20%).	10	
		1st load: One piece of ice covered by dust and 10 cm of loose ice.		50 cm layer of clear ice several other clear ice layers (not parallel).
		2nd load: 6 small chunks.		Few thin, non-parallel clear ice layers.
V	Close to the Ingnerit glacier (70.9° N).	2 loads (60 and 40%).	13	
		1st load: One piece of ice (10 tons), observed fall from the glacier.		Several irregular stripes of clear ice.
		2nd load: 10 pieces of ice.		Distinct stratification.
VI	In Qarajak icefjord av Ikerasak (70.3° N).	1 load. All ice from one block (800 tons).	12	A few, thin, parallel clear ice layers.
VII	Close to Kangilergata glacier (69.9° N).	1 load. All ice from one block, observed fall from the glacier.	11	Some thin, parallel clear ice layers. Two thick layers not parallel.
VIII	Close to Eqip glacier (69.8° N).	2 loads (75 and 25%).	8	
		1st load: One piece of ice.		Distinct stratification, parallel layers of white and clear ice. Algae in the clear ice.
		2nd load: A few pieces of ice.		Few, thin layers of clear ice.
IX	At the mouth of Jakobshavn icefjord (69.3° N).	2 loads.	6	
		1st load: One piece of ice. 2nd load: One piece of ice.		Distinct stratification.
X	At the mouth of Jakobshavn icefjord (69.2° N).	1 load: All ice from one block (800 tons).	8	
XI	Close to Bredefjord glacier (61.5° N).	Several pieces of ice. White and relatively homogenously looking chunks were preferred.	13	Numerous layers of clear ice.

nvestigated icebergs (p. 84).

6	7	8	9	10
Bubble shape, temperature	Consistency	Gas content in % (Number of measurements)	CO_2 content in % of the air (Number of measurements)	Age years
Cylindric, uniformly orientated, diam. 0.3–0.4 mm, length up to 4 mm.	Rather tough	3.8–6.3 (10)	0.06–0.17 (9)	−110 ± 150
Very small, needle shaped, same orientation and number per volume throughout the ice.	Extremely crackly	5.4–8.4 (13)	0.02–0.09 (13)	3100 ± 150
Very varying, in some pieces microscopic size. Not uniformly orientated.	Tough	2–9 (11)	0.02–0.20 (13)	−130 ± 150
				800 ± 150
Mainly long, cylindric. Round near the clear ice layers.		6.9–7.7 (2)	0.04–0.11 (6)	
Thin, well orientated.				
				560 ± 150
Long, not well orientated, round near the stripes.	Crackly	5.1–7.6 (6)	0.05–0.08 (6)	
Mostly rounded.		4.9–6.4 (5)	0.02–0.10 (5)	
Long, uniformly orientated −5° C in 1 m depth.	Crackly	7.7 (1)	0.04–0.10 (6)	940 ± 150
−5° C in 1–3 m depth.	Crackly		0.06–0.07 (4)	1510 ± 200
	Tough			950 ± 150
			0.09–0.11 (5)	
			0.07–0.09 (2)	
				575 ± 200
			0.21 (1)	
Long, thin, same orientation throughout the ice; −14° C in 2 m depth.	Crackly		0.08–0.26 (2)	100 ± 160
Some pieces had long, other round bubbles.	Tough	5.4–8.6 (9)	0.02–0.07 (9)	290 ± 130

Table VIII.

Determination of the sites of formation of 11 dated icebergs (p. 87).

1	2	3	4	5	6	7	8	9	10	11
Sample No.	Load No.	Pots No.	Δ a ppm	Δ a_m ppm	Δ a_m weighted mean ppm	t′ ° C	d 100 km	Age 100 years	v m/year	Δ a_c ppm
I	1	1– 40	−20.0		−19.8	−22.0	0.8 ± 0.2	−1.1 ± 1.5		−15.1
	2	41– 80	−19.9							
	2+3	81–120	−19.6							
	3	121–160	−19.6							
II	1	1– 40	−32.3	−32.7	−34.4	−30.6	4.6 ± 0.8	31.0 ± 1.5	150 ± 30	−31.6
		41– 80	−33.1							
		81–120	−32.6							
		121–160	−36.4	−36.3						
		161–230	−36.2							
III	1	1– 20	−18.2		−17.1	−20.5	0.6 ± 0.2	−1.3 ± 1.5		−15.4
		21– 40	−17.2							
		41– 60	−16.5							
		61– 80	−16.3	−17.0						
		81–100	−16.3							
		101–130	−17.4							
		131–150	−16.6							
	2	151–172	−17.4							
		173–190	−16.9	−17.2						
		191–211	−17.2							
IV	1	1– 17	−20.2		−19.4	−21.8	0.9 ± 0.2	8.0 ± 1.5	110 ± 30	−18.1
		18– 38	−20.2							
		39– 64	−20.2	−20.0						
		65– 90	−19.0							
		91–109	−20.4							
	2	110–134	−17.0	−17.0						
V	1	1– 40	−21.9	−19.9	−17.4	−20.6	0.9 ± 0.2	5.6 ± 1.5	160 ± 60	−16.6
		41– 80	−17.9							
	2	81–120	−15.3	−15.0						
		121–160	−14.7							
	3	161–190	−16.9	−16.9						
VI	1	1– 20	−22.2		−22.7	−23.8	1.9 ± 0.3	9.4 ± 1.5	200 ± 50	−22.4
		35– 50	−22.6							
		51– 70	−22.6							
		71– 90	−23.0							
		91–110	−21.9							
		111–130	−22.9							
		131–150	−22.5							

(continues)

Table VIII (cont.)

1	2	3	4	5	6	7	8	9	10	11
Sample No.	Load No.	Pots No.	Δa ppm	Δa_m ppm	Δa_m weighted mean ppm	t′ °C	d 100 km	Age 100 years	v m/year	Δa_e ppm
VII	1	1– 20	−24.2		−24.5	−24.8	2.6 ± 0.4	15.1 ± 2.0	170 ± 40	−24.(
		21– 40	−24.5							
		41– 60	−24.0							
		61– 80	−25.3							
		81–120	−24.2							
		140–155	−25.6							
VIII	1	1– 20	−18.0		−18.0	−21.0	1.5 ± 0.3	9.5 ± 1.5	160 ± 40	−18.:
		21– 40	−19.4	−18.2						
		41– 60	−18.2							
		61– 80	−18.2							
	2	81–110	−16.9	−16.9						
IX	1	1– 20	−15.6		−15.1	−19.3	1.4 ± 0.2	5.8 ± 2.0	240 ± 80	−15.:
		21– 40	−15.9							
	1+2	41– 60	−14.4							
	2	61– 80	−14.6							
X	1	1– 20	−16.0		−15.7	−19.6	1.5 ± 0.2	1.0 ± 1.6		−16.(
		21– 40	−14.9							
		41– 80	−16.0							
		81–120	−15.5							
XI	1	1– 70	− 7.1		− 6.2	−14.0	0.8 ± 0.2	2.9 ± 1.3	270 ± 140	−14.:
	2	71–120	− 6.2							
	3	121–190	− 5.5							

7. 1. SUMMARY

1., p. 7–8. **Introduction.**

Investigation of the stable isotopes in nature has acquired increasing importance in the past decade.

2., pp. 9–39. **Measuring technique.**

High precision measurements of the heavy isotope content in water are usually carried out with a mass spectrometer.

The way of presenting the results is discussed. Multiplicative instrumental errors cancel in the δ function giving relative differences between sample and standard, whereas additive errors cancel in the Δa function giving absolute differences (pp. 19–21).

A main point in the technique for measurement of O^{18} in water is the isotopic equilibration of the water with CO_2 (p. 17). CO_2 is used as a measuring object. The measuring technique is described (p. 18), and the sources of error are discussed (pp. 21–35). As to the last point, a method is described (p. 25) which allows a precise measurement of the ratio between the two high ohm resistors (10^{10}–$10^{11}\Omega$) under working conditions. It is concluded that both the above-mentioned functions are generally usable. If correction for some instrumental error is difficult the function should be chosen in which the error in question cancels.

The standard used in this work is described, and a conversion formula between δ and Δa is evaluated (pp. 37–39).

3., pp. 40–49. **Isotopic fractionation of water.**

Formulae are evaluated for the isotopic fractionation of water in isothermal evaporation and condensation processes. The fractionation factors, α (i.e. the ratio between the vapour pressures of the light and a heavy isotopic component of water), are given as functions of the temperature. An evaporation experiment (described in the appendix, p. 96) for determination of α for H_2O^{18} in the low temperature range confirms the formula given by ZAVORONKOV et al. (1955) (p. 44). Formulae for non-isothermal processes are evaluated p. 45. The ratio between the absolute enrichments of the heavy components, HDO and H_2O^{18}, is shown to be close to 1.5 (p. 48).

4., pp. 50–75. **Heavy isotopes in natural waters.**

Whereas ocean waters have rather uniform isotopic composition, the O^{18} content of fresh waters decreases with the temperature at the site of formation (p. 58).

A linear correlation is found (p. 62) between the annual means of the air temperature and the O^{18} content of the precipitation at ocean coast stations at sea level and with temperate or arctic climate. The O^{18} depletion is 1.33 ppm/° C. Another linear correlation is found between mainly the same parameters at Greenland ice cap stations with high altitudes. The O^{18} depletion is here 1.70 ppm/° C. The isotopic latitude effect along the West Greenland coast is -0.93 ppm/° lat. (p. 64).

The seasonal isotopic variation of the precipitation corresponds roughly to the seasonal variation in air temperature (p. 65). The isotopic variations during individual periods of rain are discussed (pp. 66–75).

5., pp. 76–95. **Investigations on glacier ice.**

Isotopic stratification in denterium and O^{18} is demonstrated in an iceberg and a temperate glacier (p. 78). The main lines are given of a determination of the age of 11 icebergs by the C^{14} method (described in detail by SCHOLANDER et al., 1961). 9 out of 11 icebergs were younger than 1000 years. The oldest one was 3100 ± 150 years.

A detailed description is given of a method for determining the sites of formation on the ice cap for each of the 11 icebergs: Firstly, the mean annual air temperature at the site of formation is found from the O^{18} measurement by using the linear correlation mentioned in section 4. Secondly, the site of formation and its distance from the outlet glacier is derived from the knowledge of the temperature distribution on the ice cap (p. 84). The distance passed by the 11 dated icebergs ranged from 60 ± 20 km to 460 ± 80 km.

The mean velocities ranged from 110 ± 30 m/year to 270 ± 140 m/year with the weighted mean 154 ± 15 m/year.

The results indicate a faster turnover for great parts of the ice cap than suggested by various theoretical considerations. None of the investigated icebergs could have sunk down to the deep strata of the inland ice (p. 89).

If the O^{18} contents of the 11 icebergs are corrected for latitude effect, they show a linear correlation with the ages which foreshadows the possibility of an iceberg dating on the basis of O^{18} measurements.

7. 2. РЕЗЮМЕ

1., стр. 7–8. **Введение.**

Изучение распределения стабильных изотопов в природе в последние годы приобретает все большее и большее значение для многих областей естественно-научного исследования.

2., стр. 9–39. **Техника измерения.**

Высокоточные измерения содержания в воде тяжелых изотопов производятся в наше время, обычно, массовым спектрометром.

Обсуждаются различные методы для указания массовых спектрометрических данных. Так называемой δ функцией указывается относительная дифференция между содержанием в образце и стандарте тяжелого изотопа. δ функция отличается тем, что мультипликативные инструментальные ошибки не сказываются на результате. Δ а функция, применяемая в настоящей работе, указывает на абсолютную дифференцию в частях на миллион между образцом и стандартом, причем исключаются аддитивные инструментальные ошибки.

Важным моментом при подготовке образцов для определения содержаний O^{18} в воде является обмен кислородных изотопов между образцом воды и CO_2. Когда этот процесс после минимум двухчасового встряхивания приходит к концу, то угледиоксид можно применять в качестве объекта измерения (стр. 17). Приводится детальное описание техники измерения (стр. 18), а также дискуссия об источниках ошибок (стр. 21–35). В этой связи упоминается метод точного измерения отношения между сопротивлениями в двух высоких омах (10^{10}–10^{11} Ω) при различных условиях работы (стр. 25). Что касается вопроса, какую из вышеуказанных функций следует предпочитать, делается вывод, что, обычно, можно применять обе эти функции. В случае, если имеются трудности с определением исправления той или иной инструментальной ошибки, то следует применять ту функцию, в которой исключается данная ошибка.

Описывается примененный в настоящей работе стандарт и выводится формула обращения между функциями δ и Δ а (стр. 37–39).

3., стр. 40–49. **Изотопическое фракционирование воды.**

Формулы выводятся для фракционирования при изотермических процессах испарения и конденсации. Фактор фракционирования α (= отношение между давлениями пара легкого изотопического компонента воды и одного из ее тяжелых изотопических компонентов) указывается как функция температуры. Опыт с испарением (описанный в приложении стр. 96) для определения α для H_2O^{18} при низких температурах подтверждает формулу, найденную экспериментальным путем **Жаворонковым** и др. (195[5] г.) (стр. 44). Выводятся формулы для неизотермических процессов (стр. 45). Отношение между абсолютными обогащениями компонентов HDO и H_2O^{18} является приблизительно 1,5 (стр. 48).

4., стр. 50–75. **Тяжелые изотопы в естественных водах.**

В то время как вода океанов имеет довольно однообразный изотопический состав, содержание O^{18} понижается в пресных водах в зависимости от температуры в месте образования (стр. 58).

Обнаруживается линеарная корреляция (стр. 62) между ежегодными средними значениями температуры воздуха и содержанием O^{18} в осадках на побережных станциях у океанов на уровне моря и в условиях от умеренного до арктического типов климата. Содержание O^{18} понижается на 1,33 части на миллион на градус Ц.

Другая линеарная зависимость, главным образом, обнаруживается между такими же параметрами станций на материковых льдах Гренландии. Содержание O^{18} понижается здесь на 1,70 части на миллион на градус Ц.

Что касается того же изотопа в осадках на материковых льдах Гренландии выводится изтопический эффект высоты, соответствующий $-1{,}26$ частям на миллион на 100 м разницы в высоте (стр. 64). Соответствующая вариация содержания O^{18} в осадках вдоль побережий Гренландии составляет $-0{,}93$ части на миллион на градус широты (стр. 64).

Сезонная вариация содержания O^{18} в осадках соответствует, в общих чертах, вариациям температуры (стр. 65). Даются примеры изотопических вариаций для периодов с фронтами теплоты и дождевыми ливнями (стр. 66–75).

5., стр. 76–95. **Исследования льда глетчеров.**

Указывается изотопическая стратификация в ледяной глыбе и температурированном глетчере (стр. 78).

Приводятся главные черты метода, примененного (стр. 84) при

C^{14} датировании 11 ледяных глыб. 9 ледяных глыб были менее 1000-летней давности, самая древняя 3100 ± 150 лет.

Те районы на материковых льдах, к которым относятся 11 датированных ледяных глыб, определяются следующим методом (стр. 84):

1: Исходя из содержания O^{18} в отдельной ледяной глыбе, находится ежегодняя средняя температура места образования при помощи указанной выше корреляции (стр. 63) между этими двумя параметрами.

2: На основании существующего в настоящее время распределения температуры на материковом льду место образования находится затем как район вокруг соответствующего изотерма. Растояния между местами образования и данными береговыми глетчерами вариируют от 60 ± 20 км до 460 ± 80 км.

Средние скорости, с которыми 8 из указанных 11 датированных ледяных глыб двигались с момента их образования, вариируют от 110 ± 30 м/год до 270 ± 140 м/год при взвешенном среднем значении в 154 ± 15 м/год.

Результаты указывают на быстрое перемещение материала на больших участках материкового льда, что касается центральных участков быстрее, чем это можно заключить из теоретических соображений. Ни одна из исследованных ледяных глыб не могла успеть опуститься глубоко в материковый лед на своем пути к побережью (стр. 89).

Если проверить содержания O^{18} в указанных 11 датированных ледяных глыбах в отношении географического эффекта широты, то они показывают линеарную зависимость от возраста, что указывает на возможность датирования ледяных глыб на базе измерений O^{18} (стр. 91).

7. 3. RESUMÉ

1., pp. 7–8. **Indledning.**

Undersøgelser af stabile isotopers fordeling i naturen har i de senere år fået en stigende betydning for adskillige naturvidenskabelige forskningsområder.

2., pp. 9–39. **Måleteknik.**

Præcisionsmålinger af de tunge isotopers forekomst i vand foretages nutildags sædvanligvis med et massespektrometer.

De forskellige metoder til angivelse af massespektrometriske data diskuteres. Ved den såkaldte δ funktion angives den relative differens mellem en tung isotops forekomst i en prøve og en standard. δ funktionen udmærker sig derved, at multiplikative instrumentelle fejl ikke indgår i resultatet. Δa funktionen, som anvendes i nærværende arbejde, angiver den absolute differens i ppm (parts per million) mellem prøve og standard, hvorved additive instrumentelle fejl udgår.

Et vigtigt punkt ved preparationen af prøver til bestemmelse af O^{18} forekomster i vand er udvekslingen af iltisotoper mellem vandprøven og CO_2. Når denne proces efter mindst to timers rystning er løbet til ende kan kuldioksyden anvendes som måleobjekt (p. 17). Der gives en detailleret beskrivelse af måletekniken (p. 18) og diskussion af fejlkilderne (pp. 21–35). Herunder omtales en metode til præcisionsmåling af forholdet mellem to højohmsmodstande (10^{10}–$10^{11}\Omega$) under forskellige driftsbetingelser (p. 25). Med hensyn til spørgsmålet om, hvilken af de ovennævnte funktioner, der er at foretrække, konkluderes det, at de begge sædvanligvis er anvendelige. I tilfælde af at korrektionen for en eller anden instrumentel fejl er vanskelig at bestemme, bør den funktion anvendes, i hvilken den pågældende fejl udgår.

Den i dette arbejde anvendte standard beskrives, og der udledes en omsætningsformel mellem δ og Δa funktionerne (pp. 37–39).

3., pp. 40–49. **Isotopisk fraktionering af vand.**

Formler udledes for fraktioneringen ved isoterme fordampnings- og kondensationsprocesser. Fraktioneringsfaktoren α (= forholdet mellem damptrykkene af vands lette isotopiske komponent og en af dets tunge

isotopiske komponenter) angives som funktion af temperaturen. Et fordampningsforsøg (beskrevet i appendix, p. 96) til bestemmelse af α for H_2O^{18} ved lave temperaturer bekræfter en formel fundet experimentelt af ZHAVORONKOV et al. (1955) (p. 44). Formler for ikke-isoterme processer udledes p. 45. Forholdet mellem de absolute berigelser af komponenterne HDO og H_2O^{18} er ca. 1,5 (p. 48).

4., p. 50–75. **Tunge isotoper i naturlige vandforekomster.**

Mens oceanvand har en ret ensartet isotopisk sammensætning, aftager O^{18} indholdet i ferskvandsforekomster med temperaturen på dannelsesstedet (p. 58).

Der påvises en lineær korrelation (p. 62) mellem de årlige middelværdier af lufttemperaturen og O^{18} indholdet i nedbør faldet ved oceankyststationer ved havets overflade og under forhold varierende fra tempererede til arktiske klimatyper. O^{18} indholdet aftager 1,33 ppm pr. ° C.

En anden lineær afhængighed påvises mellem i hovedsagen de samme parametre for stationer på Grønlands indlandsis. O^{18} indholdet aftager her 1,70 ppm pr. ° C.

For samme isotop i nedbøren på Grønlands indlandsis udledes en isotopisk højdeeffekt svarende til $-1{,}26$ ppm pr. 100 m højdeforskel (p. 64). Den tilsvarende variation af O^{18} indholdet i nedbøren langs Grønlands kyster er $-0{,}93$ ppm pr. breddegrad (p. 64).

Den sæsonmæssige variation af nedbørens O^{18} indhold svarer i store træk til temperaturvariationerne (p. 65). Eksempler gives på isotopiske variationer gennem perioder med varmefront- og bygeregn (p. 66–75).

5., p. 76–95. **Undersøgelser af gletscheris.**

Isotopisk stratifikation påvises i et isfjeld og en tempereret gletscher (p. 78).

Hovedtrækkene anføres (p. 84) af en metode, som er anvendt til C^{14} datering af 11 isfjelde. 9 isfjelde var yngre end 1000 år, det ældste 3100 ± 150 år.

De områder på indlandsisen, hvor de 11 daterede isfjelde stammer fra, bestemmes ved flg. metode (p. 84):

1. Ud fra det enkelte isfjelds O^{18} indhold findes dannelsesstedets årlige middeltemperatur ved hjælp af ovennævnte korrelation (p. 63) mellem disse to parametre.

2. På grundlag af den nuværende temperaturfordeling på indlandsisen findes dannelsesstedet derefter som området omkring den tilsvarende

isoterm. Afstandene mellem dannelsesstederne og de pågældende kystgletschere varierer fra 60 ± 20 km til 460 ± 80 km.

Middelhastighederne, hvormed 8 af de 11 daterede isfjelde har bevæget sig siden de dannedes, varierer fra 110 ± 30 m/år til 270 ± 140 m/år med en vægtet middelværdi af 154 ± 15 m/år.

Resultaterne tyder på en hurtig materialomsætning over store dele af indlandsisen, for de centrale deles vedkommende hurtigere end teoretiske overvejelser lader formode. Ingen af de undersøgte isfjelde kan have nået at synke dybt ned i indlandsisen på deres vej mod kysten (p. 89).

Hvis O^{18} indholdene for de 11 daterede isfjelde korrigeres for geografisk breddeeffekt udviser de en lineær afhængighed af alderen, hvilket peger på muligheden for isfjeldsdatering på basis af O^{18} målinger (p. 91).

8. REFERENCES

ALTMANN, J. G., 1751: Versuch einer Historischen und Physischen Beschriebung der Helvetischen Eisgebirge, Zürich.

ASTON, F. W., 1919: A Positive Ray Spectrograph. Phil. Mag. 38, p. 707–715.

BAERTSCHI, P., 1953: Über die Relativen Unterschiede im H_2O^{18} — Gehalt Natürlicher Wässer. Helvetica Chim. Acta, 36, 1352–1369.

BARNARD, G. P., 1953: Modern Mass Spectrometry. London, 326 p.

BAUER, A., 1954: Synthèse Glaciologique, Contribution à la Connaissance de l'Inlandsis du Groenland. Expéditions Polaires Françaises, p. 27–56.

— 1960a: Influence de la Dynamique des Fleuves de Glace sur Celle de l'Inlandsis du Groenland. UGGI-AIHS, Helsinki, Aug. 1960.

— 1960b: Personal communication.

BEILBY, G., 1921: Aggregation and Flow of Solids.

BENSON, C., 1960: Stratigraphic Studies in the Snow and Firn of the Greenland Ice Sheet. Geographical Symposium, Copenhagen.

BOTTER, R., and G. NIEF, 1958: Joint Conference on Mass Spectrometry, Sept. 1958, Pergamon Press.

BRISCO, H. V. A., and P. L. ROBINSON, 1926: The Constancy of Atomic Weights. Nature, 117, p. 377–378.

BRUCE, R. J. M. and C. BULL, 1955: Geophycical Work in North Greenland. Nature, 175, p. 892–893.

CHAMBERLIN, T. C., 1895: Recent Glacial Studies in Greenland. Bull. Geol. Soc. Amer., 6, 199–220.

CRAIG, H., 1957: Isotopic Standards for Carbon and Oxygen and Correction Factors for Mass Spectrometric Analysis of Carbon Dioxide. Geochim. et Cosmochim. Acta, 12, p. 133–149.

— G. BOATO and D. E. WHITE, 1956: Isotopic Geochemistry of Thermal Waters. Nat. Acad. Sci.. Nucl. Sci. Ser., Rep. No. 19, p. 29–36.

— T. MAYEDA and H. E. SUESS, 1958: Isotopische Zusammensetzung des Wassers des Neusiedler Sees bei Wien. Monatshefte für Chemie, 89, p. 173–174.

CROOKES, W., 1888: Elements and Meta-Elements. Journ. Chem. Soc., 53, p. 487–505.

DANSGAARD, W., 1953a: Comparative Measurements of Standards for Carbon Isotopes. Geochim. et Cosmochim. Acta., 3, p. 253–256.

— 1953b: The Abundance of O^{18} in Atmospheric Water and Water Vapour. Tellus, 5, p. 461–469.

— 1954: The O^{18} Abundance in Fresh Water. Geochim. et Cosmochim. Acta, 6, p. 241–260.

— 1958: Some Meteorological and Glaciological Problems Illustrated by Measurement of the Stable Oxygen Isotopes in Water (Danish). Fysisk Tidsskrift, nr. 2–3, p. 49–65.

DANSGAARD, W., 1960: The Content of Heavy Oxygen Isotope in the Water Masses of the Philipine Trench. Deep-Sea Research, 6, p. 346–350.
— G. NIEF and E. ROTH, 1960: Isotopic Distribution in a Greenland Iceberg. Nature, 185, p. 232.
DEMOREST, M., 1942: Glacier Regimens and Ice Movement within Glaciers. Am. Journ. Sci., 240, p. 31–66.
DEMPSTER, A. J., 1918: A New Method of Positive Ray Analysis. Phys. Rev., 11, p. 316–325.
DIAMOND, M., 1958: Air Temperature and Precipitation on the Greenland Ice Cap. U.S. S.I.P.R.E. Report No. 43.
DOLE, M., 1936: The Relative Atomic Weight of Oxygen in Water and Air. Journ. Chem. Phys., 4, p. 268–275.
DOSTROVSKY, I., D. R. LLEWELLYN and B. H. VROMEN, 1952: The Separation of Isotopes by Fractional Distillation. Journ. Chem. Soc., p. 3509–3517.
EPSTEIN, S., 1956: Variations of the O^{18}/O^{16} Ratios of Fresh Water and Ice. Nat. Acad. Sci., Nucl. Sci. Ser., Rep. No. 19, p. 20–25.
— I. FRIEDMAN and H. C. UREY, 1953: cf. EPSTEIN and MAYEDA (1953, p. 219).
— and T. MAYEDA, 1953: Variations of the O^{18} Content of Waters from Natural Sources. Geochim. et Cosmochim. Acta, 4, p. 213–224.
— and R. P. SHARP, 1959: Oxygen-Isotope Variations in the Malaspina and Saskatchewan Glaciers. Journ. Geol., 67, p. 88–102.
— and C. BENSON, 1959: Oxygen Isotope Studies. Trans. Am. Geophys. Union, 40, p. 81–84.
FINDEISEN, W., 1939: Gasverdampfen der Wolken und Regentropfen. Meteorol. Zeitschr. 56, p. 453–460.
FORBES, J. D., 1853: Norway and its Glaciers. Edinb.
FRIEDMAN, I., 1953: Deuterium Content of Natural Waters and other Substances. Geochim. et Cosmochim. Acta, 4, p. 89–103.
FRISTRUP, B., 1959: Recent Investigations of the Greenland Ice Cap. Geografisk Tidsskrift, 58, p. 1–29.
FÜRTH, R., 1938: Diffusion ohne Scheidewände. Handbuch d. phys. u. tech. Mekanik, 7.
GIAQUE, W. F. and H. L. JOHNSTON, 1929: An Isotope of Oxygen Mass 18. Interpretation of the Atmospheric Absorption Bands. Journ. Am. Chem. Soc., 51, p. 1436–1441.
GILFILLAN, E. S. Jr., 1934: The Isotopic Composition of Sea Water. Journ. Am. Chem. Soc., 56, p. 406–408.
GLEN, J. W., 1955: The Creep of Polycrystalline Ice, Roy. Soc. London Proc., Ser. A, 228, p. 519–538.
— 1959: The Mechanical Properties of Ice. Advances in Physics, 7, 254–265.
GONFIATINI, R. and E. PICCIOTTO, 1959: Oxygen Isotope Variations in Antarctic Snow Samples. Nature, 184, p. 1557–1558.
GUNN, R. and G. D. KINZER, 1949: The Therminal Velocity of Fall for Water Droplets in Stagnant Air. Journ. Meteorol., 6, p. 243–248.
HAEFELI, R., 1958: Druck- und Verformungsmessungen in Eisstollen, Compte Rendus et Rapports, 4, p. 492–499.
— 1960a: Glaziologische Einführung zur Frage der Bezeitigung Radioaktiver Abfallstoffe in den Eiskappen der Erde. Kolloquium der Hydrobiologischen Kommission und der Gletscherkommission der Schweitz. Naturforschenden Gesellschaft, Zürich, 22. Jan.
— 1960b: Zur Entwicklung der Schnee und Gletscherforschung, Wasser- und Energiewirtsshaft, Nr. 8–10.

HAGELBERGER, D. W., L. T. LOH, H. W. NEIL, M. H. NICHOLS and E. A. WENZEL: Does Diffusive Separation Exist in the Atmosphere Below 55 km? Phys. Rev., 82, p. 107–108. 1951.

HALSTED, R. E., and A. O. NIER, 1950: Gas Flow Through the Mass Spectrometer. Viscous Leak. Rev. Sci. Instr. 21, p. 1019–1021.

HARADA, M., and T. TITANI, 1935: Isotopic Composition of Rain and Snow water, Chem. Soc. Japan, 10, p. 206 and 263.

HESS, H., 1904: Die Gletscher, 426 p., Braunschweig.

HONIG, R. E., 1945: Gas Flow in the Mass Spectrometer. Journ. Appl. Phys., 16, p. 646–654.

INGERSON, E., 1953: Nonradiogenic Isotopes in Geology: A Review. Am. Bull. Geolog. Soc., 64, p. 301–374.

INGHRAM, M. G., and R. J. HAYDEN, 1954: Mass Spectroscopy, Nucl. Sci. Ser., Rep. No. 14, Nat. Acad. of Sci., Washington D.C.

JELLINEK, H. H. G., and R. BRILL, 1956: Viscoelastic Properties of Ice. Journ. Appl. Phys., 27, p. 1198–1209.

KIRSCHENBAUM, J., 1951: Physical Properties and Analysis of Heavy Water, New York, 438 p.

KIMBALL, A. H., 1949: Bibliography of Research on Heavy Hydrogen Compounds. McGraw-Hill Book Co., Inc., New York, 350 p.

KINZER, G. D., and R. GUNN, 1951: The Evaporation Temperature and Thermal Relaxation Time of Freely Falling Water Droplets. Journ. Meteorol., 8, p. 71–83.

KISTEMAKER, J., 1952: The Influence of Fractionizing and Viscosity Effects in Mass Spectrometric Gas Handling Systems. Physica, 13, p. 163–176.

KOCH, J. P., and A. WEGENER, 1930: Wissenschaftlischen Ergebnisse der Dänischen Expedition nach Dronning Louises Land und Quer über das Inlandeis von Nordgrönland, 1912–1913: Medd. om Grønland, vol. 75.

KULP, J. L., B. J. GILETTI and G. P. ERICKSON, 1957: Isotopic Studies on the Greenland Continental Glacier. Lamont Geol. Observatory, Columbia Univ., Oct. 1957.

KÖPPEN, W., 1936: Das Geographische System der Klimate. Handbuch der Klimatologie, Vol. 1 C, Berlin.

LEWIS, G. N., and R. CORNISH, 1933: Separation of the Isotopic Forms of Water by Fractional Distillation. Journ. Am. Chem. Soc., 55, p. 2616–2617.

LEWIS, G. N., and D. B. LUTEN, 1933a: The Refractive Index of H_2O^{18} and the Complete Isotopic Analysis of Water. Ibid. 55, p. 5061–5062.

— 1933b: A Simple Type of Isotopic Reaction. Ibid., 55, p. 3502–3503.

MCCREA, J. M., 1950: On the Isotopic Chem. of Carbonates and a Paleotemperature Scale. Journ. Chem. Phys., 18, p. 849–857.

MCKINNEY, C. R., J. M. MCCREA, S. EPSTEIN, H. A. ALLEN and H. C. UREY, 1950: Improvements in Mass Spectrometers for Measurement of Small Differences in Isotope Abundance Ratios. Rev. Sci. Instr., 21, p. 724–730

MEIER, M. F., 1960: Mode of Flow of Saskatchewan Glaciers. U.S. Geol. Survey, Prof. Paper 351.

MILLS, G. A., and H. C. UREY, 1940: The Kinetics of Isotopic Exchange Between Carbon Dioxide, Bicarbonate Ion, Carbonate Ion and Water. Journ. Am. Chem. Soc., 62, p. 1019–1026.

MORLEY, E. W., 1885: The Amount of Moisture, which Sulphuric Acid Leaves in a Gas. Am. Journ. Sci., 30, p. 140–146.

NIER, A. O., 1947: A Mass Spectrometer for Isotope and Gas Analysis. Rev. Sci. Instr., 18, p. 398–411.

Nier, A. O., 1948: Preparation and Measurements of Isotopic Tracers, Symposium.
— 1950: A Redetermination of the Relative Abundances of the Isotopes of Carbon, Nitrogen, Oxygen, Argon and Potassium. Phys. Rev., 77, p. 789–793.
Nye, J. F., 1952 a: The Mechanics of Glacier Flow. Journ. of Glaciol. 2, p. 82–93.
— 1952b: A Method of Calculating the Thicknesses of the Ice-sheets, Nature, 169, 529–530.
— 1952 c: Extrusion Flow, Journ. of Glaciol., 2, p. 52–53.
— 1957: The Distribution of Stress and Velocity in Glaciers and Ice-sheets. Roy. Soc., London Proc., Ser. A, Vol. 39, p. 113–133.
— 1958: A Theory of Wave Formation in Glaciers. Symposium of Chamonix, Ass. Int. d'Hydrol. Sci., No. 47, p. 139–154.
Philipp, H., 1914: Die Ergebnisse der Filchnerschen Vorexpedition nach Spitsbergen 1910. Petermanns Mitt., ErgH, 179.
Picciotto, E., X. de Maere and I. Friedman, 1960: Isotopic Composition and Temperature of Formation of Antarctic Snows. Nature, 187, p. 857–859.
Rankama, K., 1954: Isotope Geology, 535 p., London.
Riesenfeld, E. H., and T. L. Chang, 1936a: Dampfdruck, Seidepunkt und Verdampfungswärme von HDO und H_2O^{18}. Zs. Physikal. Chem., 33, p. 127–132.
— 1936b: Über den Gehalt an HDO und H_2O^{18} in Regen und Schnee. Dent. Chem. Ges., Ber., 69, p. 1305–1307.
Rigsby, G. P., 1957: Effect of Hydrostatic Pressure on Velocity of Shear Deformation of Single Crystals of Ice. U.S. S.I.P.R.E. Report No. 32.
Ritzchel, R., and H. Schober, 1937: Isotopieverschiebung im Neonspektrum. Phys. Zs., 38, p. 6–9.
S.C.A.R. Bulletin No. 2, 1959: The Polar Record, 9, p. 475–487.
Scholander, P. F., W. Dansgaard, D. C. Nutt, H. de Vries, L. K. Coachman and E. Hemmingsen, 1961: Radio-Carbon Dating and Oxygen-Eighteen Analysis of Greenland Icebergs. Medd. om Grønland, 165, No. 1.
Scholander, P. F., E. Hemmingsen, L. K. Coachman and D. C. Nutt, 1960: Composition of Gas Bubbles in Greenland Icebergs. In Press.
Schoumsky, P. A., 1957: Principes de Glaciologie Structurale. Centre d'Etudes et de Documentation Paléontologiques, No. 26.
Shockley, W., 1951: Electrons and Voles in Semiconductors, van Nordstrand, New York.
Steinemann, S., 1958: Experimentelle Untersuchungen zur Plastizität von Eis. Beitr. zur Geol. der Schweitz, Hydrologie, No. 10.
Streif-Becker, R., 1938: Zur Dynamik des Firneises. Zs. f. Gletscherkunde, 26, p. 1–21.
Teis, R. V., 1939: Isotopic Composition of Rain Water, Akad. Nauk. USSR, 23, p. 674.
— 1946: Isotopic Composition of Mineral Waters. Akad. Nauk. USSR, Doklady, 53, p. 135–137.
Thomson, J. J., 1911: Rays of Positive Electricity. Phil. Mag., 21, p. 225–249.
Urey, H. C., 1947: The Thermodynamic Properties of Isotopic Substances. Journ. Chem. Soc., p. 562–581.
— F. G. Brickwedde and G. M. Murphy, 1932: A Hydrogen Isotope of Mass 2 and its Concentration. Phys. Rev., 40, p. 1–15.
Vries, H. de, 1957: The Removal of Radon from CO_2 for Use in C^{14} Age Measurements. Appl. Sci. Res., Sect. 3, 6, p. 461–470.

WAHL, M. H. and H. C. UREY, 1935: The Vapour Pressure of the Isotopic Forms of Water. Journ. Chem. Phys., 3, p. 411–414.

WEBSTER, L. A., M. H. WAHL and H. C. UREY, 1935: The Fractionation of the Oxygen Isotopes in an Exchange Reaction. J. Chem. Phys., 3, p. 129–130.

WEIDICK, A., 1960: Personal communication.

— 1961: Glacier Fluctuations in Holocene Time in Julianehaab District, Southwest Greenland. I.N.Q.U.A. Congress, Warszawa.

WORTH, C., 1957: The Quaternary Era, p. 99–131. Arnold Publ. London.

ZHAVARONKOF, UVAROF and SEVRYUGOVA, 1955: Primenenie Mechenykh. Atomov v Anal. Khim. Akad. Nauk. USSR, p. 223–233.

Færdig fra trykkeriet den 27. juni 1961.